Amanda Gomes Marcelino Perez

PREPARATION, MODULATION, ENCAPSULATION AND CONTROLLED RELEASE OF PLATELET-RICH PLASMA FOR APPLICATION IN REGENERATIVE THERAPY

PREPARAÇÃO, MODULAÇÃO, ENCAPSULAÇÃO E LIBERAÇÃO CONTROLADA DE PLASMA RICO EM PLAQUETAS PARA APLICAÇÃO EM TERAPIA REGENERATIVA

Campinas, 2013

UNIVERSIDADE ESTADUAL DE CAMPINAS
FACULDADE DE ENGENHARIA QUÍMICA

Amanda Gomes Marcelino Perez

PREPARATION, MODULATION, ENCAPSULATION AND CONTROLLED RELEASE OF PLATELET-RICH PLASMA FOR APPLICATION IN REGENERATIVE THERAPY

PREPARAÇÃO, MODULAÇÃO, ENCAPSULAÇÃO E LIBERAÇÃO CONTROLADA DE PLASMA RICO EM PLAQUETAS PARA APLICAÇÃO EM TERAPIA REGENERATIVA

Thesis presented to the School of Chemical Engineering of the University of Campinas in partial fulfillment of the requirements for the degree of Doctor in Chemical Engineering

Tese apresentada à Faculdade de Engenharia Química da Universidade Estadual de Campinas como parte dos requisitos exigidos para obtenção do título de Doutora em Engenharia Química.

Orientadora: Profa. Dra. Maria Helena Andrade Santana

Co-Orientador: Prof. Dr. William Dias Belangero

ESTE EXEMPLAR CORRESPONDE À VERSÃO FINAL DA TESE DEFENDIDA PELA ALUNA AMANDA GOMES MARCELINO PEREZ E ORIENTADA PELA PROF^{A}. DR^{A}. MARIA HELENA ANDRADE SANTANA.

Assinatura do orientador

Campinas, 2013

Ficha catalográfica
Universidade Estadual de Campinas
Biblioteca da Área de Engenharia e Arquitetura
Rose Meire da Silva - CRB 8/5974

P415p

Perez, Amanda Gomes Marcelino, 1979-
Preparação, modulação, encapsulação e liberação controlada de plasma rico em plaquetas para aplicação em terapia regenerativa / Amanda Gomes Marcelino Perez. – Campinas, SP : [s.n.], 2013.

Orientador: Maria Helena Andrade Santana.
Coorientador: William Dias Belangero.
Tese (doutorado) – Universidade Estadual de Campinas, Faculdade de Engenharia Química.

1. Plasma rico em plaquetas. 2. Centrifugação. 3. Biomateriais. 4. Fator de crescimento. 5. Engenharia tecidual. I. Santana, Maria Helena Andrade,1951-. II. Belangero, William Dias,1952-. III. Universidade Estadual de Campinas. Faculdade de Engenharia Química. IV. Título.

Informações para Biblioteca Digital

Título em outro idioma: Preparation, modulation, encapsulation and controlled release of platelet rich plasma for aplication in regenerative therapy
Palavras-chave em inglês:
Platelet rich plasma
Centrifugation
Biomaterials
Growth factor
Tissue engineering
Área de concentração: Desenvolvimento de Processos Biotecnológicos
Titulação: Doutora em Engenharia Química
Banca examinadora:
Maria Helena Andrade Santana [Orientador]
Sônia Maria Malmonge
Maria Vitória Lopes Brada Bentley
Ângela Cristina Malheiros Luzo
Rubens Maciel Filho
Data de defesa: 19-08-2013
Programa de Pós-Graduação: Engenharia Química

Tese de Doutorado defendida por Amanda Gomes Marcelino Perez e aprovada em 19 de Agosto de 2013 pela banca examinadora constituída pelos doutores:

Profa. Dra. Maria Helena Andrade Santana

Profa. Dra. Maria Vitória Lopes Brada Bentley

Profa. Dra. Sonia Maria Malmonge

Profa. Dra. Angela Cristina Malheiros Luzo

Prof.Dr. Rubens Maciel Filho

ABSTRACT

Platelet Rich Plasma (PRP) is an autologous, no immunogenic therapy, which is able to stimulate and accelerate tissue regeneration. The PRP quality is essential for success in clinical applications. Despite the widely use of PRP therapy in different areas of medicine, the preparation conditions described in literature are dispersed and, together with the autologous nature of PRP and the absence of characterization, turn difficult the interpretation of literature data and comparison of clinical results. Therefore, professional and researchers claim for the standardization of PRP preparation as the basis for clinical studies. However, the standardization of PRP preparations requires basic science studies, which are still scarce. As described in literature, due to the autologous nature of PRP, the challenge is not to study PRP, but the development of these studies. Aiming to overcoming these challenges, we developed a strategy to analyze, the integration of the steps in PRP preparation, to turn feasible the design of the formulations properties a function of the preparation conditions, with a reduced number of experiments. This strategy was applied to P-PRP, a type of PRP rich in platelets and poor in leukocytes. The analysis of the results allowed selecting three architectures of fibrin gels, derived from the activation of intact platelets, as representative of a wide range of conditions for platelet activation. These gels were characterized with respect to rheological properties, GFs release, clotting time and the ability to sustain the growth of human adipose-derived mesenchymal stem cell (hADSCs). In a second phase, the studies contemplated the incorporation of PRP in hyaluronic acid gels aiming protection, sustained release of growth factors and the ability to sustain the growth of hADSCs .The obtained results contribute to standardization of the P-PRP, as well as open new opportunities to the use the natural fibrin scaffolds in combination with hyaluronic acid.

RESUMO

O plasma rico em plaquetas (PRP) é um tratamento autólogo, portanto não imunogênico, capaz de estimular e acelerar a regeneração tecidual. A qualidade do PRP preparado é fundamental para o sucesso da sua aplicação clínica. Apesar do intenso uso desta terapia em diversas áreas da medicina, as condições de preparação reportadas na literatura são muito dispersas e, juntamente com a natureza autóloga do produto e com a falta de caracterização dos diferentes PRPs, dificultam a interpretação dos dados da literatura e a comparação de resultados clínicos. Portanto, profissionais e estudiosos reivindicam a padronização do PRP como base para os estudos clínicos. Entretanto, a padronização do PRP exige estudos de ciência básica, os quais ainda são muito escassos. Tal como citado na literatura, devido à natureza autóloga do PRP o problema não é necessariamente estudar o PRP, mas antes o desenvolvimento desses estudos. Buscando contemplar estes aspectos, neste trabalho desenvolveu-se inicialmente uma estratégia de estudo para análise integrada das etapas do processo de preparação do PRP, de modo a tornar factível o delineamento das propriedades das formulações em função das condições de preparação, com um número reduzido de experimentos. Essa estratégia foi aplicada ao P-PRP, um PRP rico em plaquetas e pobre em leucócitos. A análise dos resultados permitiu selecionar três arquiteturas de géis de fibrina, derivados da ativação de plaquetas íntegras, como representativos de uma ampla gama de condições de ativação das plaquetas. Esses géis foram caracterizados quanto às propriedades reológicas, à liberação dos seus fatores de crescimento (FCS), o tempo de gelificação e à capacidade de sustentação do crescimento de células mesenquimais derivadas no tecido adiposo humano (hADSCs). Em uma segunda etapa, os estudos envolveram a incorporação do PRP em géis de ácido hialurônico visando proteção e liberação gradual dos seus FCs e seu desempenho como *scaffolds* no cultivo de hADSCs . Os resultados obtidos contribuem para a padronização do P-PRP, e também abrem novas possibilidades para utilização dos scaffolds naturais de fibrina em combinação com ácido hialurônico.

SUMÁRIO

AGRADECIMENTOS

À Universidade Estadual de Campinas, ao Departamento de Engenharia de Materiais e Bioprocessos e ao Programa de Pós-Graduação da Faculdade de Engenharia Química pela oportunidade concedida.

À Fundação de Amparo à Pesquisa do Estado de São Paulo (FAPESP) pelo apoio financeiro.

À Profa. Dra. Maria Helena Andrade Santana pela orientação, compreensão, oportunidade e confiança durante esses sete anos de trabalho.

Ao Prof. Dr. William Dias Belangero pela co-orientação e pela disponibilização do Laboratório de Biomateriais em Ortopedia.

À pós-doutoranda Ana Amélia Rodrigues, pela amizade, dedicação e comprometimento.

Ao aluno de iniciação científica Rafael Lichy pela imensa colaboração com este trabalho.

Ao Dr. José Fábio Lana (iMOR) por nos instigar a estudar esse assunto.

Ao Professor Dr. Edvaldo Sabadini do Departamento de Físico-Química do Instituto de Química da Unicamp pela utilização do reômetro.

À Dra. Angela Luzo pela disponibilização de seu laboratório para o isolamento e caracterização das células mesenquimais.

Aos queridos amigos que fiz no LDPB em todos esses anos: Aline Furtado Aline Mara, Amós Carneiro, Carolina Camerim, Felipe Ferrari, Fernanda Lopes, Gabriela, Júllia, Leandra Santos, Leandro, Luciana Lima, Marcos Rossan, Mariana Beatriz, Marina Vieira, Vieira, Pablo, Rafael Zômpero Rafaela Bicudo, Reinaldo Bastos, Renata Miliani, Rhelvis Oliveira, Silas Biroli, Sofia Galdames, Tiago Balbino, André Casimiro, Beatriz Zanchetta e Edgar Silveira, Caroline Sipoli, Micaela Vitor,

Patrícia Severino e Viviane Ferre. A todos vocês agradeço por tornarem o meu dia-dia mais agradável.

À Andréa Shimojo pela amizade e pela colaboração na interpretação dos estudos reológicos deste trabalho.

Ao Gilson Júnior, técnico do LDBP, pela amizade e pela colaboração com os ensaios.

Aos doadores que se dispuseram a doar sangue para este projeto.

Às pessoas mais importantes da minha vida, meus pais Antônio Carlos e Maria das Graças, aos meus irmãos Raquel e Renato, minha sobrinha Carolina, minha cunhada Kellen, meu marido Ivan e ao meu filho Mateus que está a caminho, por todo amor e incentivo.

A Deus por me dar a oportunidade de concluir mais esta etapa da minha vida.

LISTA DE FIGURAS

LISTA DE TABELAS

Lista de Abreviações da Revisão Bibliográfica

AH	Ácido Hialurônico
BC	*Buffy coat* ou camada leucocitária
FC	Fator de Crescimento
MGC	Megacariócito
PRP	Plasma Rico em Plaquetas
PPRP	Plasma Rico em Plaquetas Puro
L-PRP	Plasma Rico em Plaquetas e em Leucócitos
P-PRF	Plasma Rico em Fibrina Puro
L-PRF	Plasma Rico em Fibrina e em Leucócitos
PRGF	Plasma Rico em Fator de Crescimento
PRMF	Plasma Rico em Matriz de Fibrina
MEV	Microscopia Eletrônica de Varredura
PDGF	Fator de Crescimento Derivado de Plaquetas
TGF	Fator de Crescimento Transformador
fvW	Fator de Von Willebrand

Capítulo 1. INTRODUÇÃO

1.1 Organização da tese em capítulos

A apresentação desta tese está dividida em capítulos, conforme descrito a seguir.

O Capítulo 1 contempla uma introdução geral do trabalho contextualizando sobre o plasma rico em plaquetas, as principais lacunas presente na literatura e a abordagem de estudo utilizada neste trabalho. Neste capítulo são apresentados também os principais objetivos e contribuições deste trabalho.

O Capítulo 2 apresenta a Revisão Bibliográfica da literatura, abordando os diferentes aspectos no estudo do PRP.

Os Resultados obtidos nesta tese estão divididos na forma de cinco artigos científicos, todos submetidos periódicos internacionais, apresentados nos Capítulos de 3 a 7. Assim, os itens introdução, metodologia, resultados, discussão e conclusões de cada etapa constam em cada artigo nos seus respectivos capítulos.

O Capítulo 3 apresenta o artigo *"Relevant Aspects of Centrifugation Step in the Preparation of Platelet-Rich Plasma"* já submetido para o periódico *Journal of Blood Transfusion (Hindawi Publishing Corporation)*, ressalta os aspectos relevantes envolvidos na etapa de centrifugação da preparação PRP e analisa as suas implicações na composição final do produto.

O Capítulo 4 apresenta o artigo "Prediction and Modulation of Platelet Recovery by Discontinuous Centrifugation of Whole Blood for the Preparation of Pure Platelet-Rich Plasma", já publicado pelo periódico *Bioresearch Open Acces (Mary Ann Liebert)*, volume 4(2), p.307-314, apresenta o delineamento de um modelo fenomenológico do comportamento do sistema para recuperação e concentração de plaquetas a partir do sangue total.

O Capítulo 5 traz o *artigo "Fibrin Network Architectures in Pure Platelet-Rich Plasma as Characterized by Fiber Radius and Correlated with Clotting Time"*, submetido ao periódico *Journal of Materials Science – Materials in Medicine (Springer)*, estuda a ativação do PRP através de um delineamento central composto rotacional (DCCR) e análise de superfície de resposta resultando em uma estratégia valiosa para predizer e correlacionar o raio das fibras de fibrinas e o tempo de coagulação.

O artigo apresentado no Capítulo 6, *"Assessment of the Effects of the Architectures of Fibrin Scaffolds on the Quality of Pure Platelet-Rich Plasma"*, submetido ao periódico *Journal of Tissue Engineering and Regenerative Medicine (Wiley)*, apresenta o estudo de scaffolds de fibrina com diferentes arquiteturas, obtidos a partir da ativação com diferentes proporções de agonistas e a influência dessas arquiteturas na liberação dos fatores de crescimento, no crescimento celular in vitro e no comportamento reológico.

O Capítulo 7, *"Impact of Hyaluronic Acid Microparticles on the Quality of a Cell-Seeded Fibrin Scaffold derived from Pure Platelet-Rich Plasma"* apresenta artigo a ser submetido ao periódico *Stem Cells and Development (Mary Ann Liebert)* e trata da formação de scaffolds de fibrina e ácido hialurônico através da incorporação de partículas de ácido hialurônico quimicamente reticuladas com divinilsulfona ao P-PRP, e seus efeitos na liberação controlada dos fatores de crescimento, no crescimento celular in vitro a influência de micropartículas de AH nas propriedades reológicas de géis de fibrina preparados a partir do P-PRP.

Finalmente, o Capítulo 8 apresenta as conclusões finais e as sugestões para trabalhos futuros.

1.2 O Plasma Rico em Plaquetas

A capacidade de modular o processo de cicatrização e acelerar a recuperação pós-cirúrgica é um assunto de intensa investigação científica. Geralmente, o processo de reparação tecidual compreende uma complexa cascata de eventos

biológicos, controlados por numerosas citocinas e fatores de crescimento (Anitua, Sanchez *et al.*, 2007; Cole, Seroyer *et al.*, 2010). Desse modo, a medicina regenerativa tem sido destacada como uma forma de estimular e acelerar a regeneração tecidual. O sangue humano possui aproximadamente 150.000 a 400.000 plaquetas/µL. O Plasma Rico em Plaquetas (PRP) é um concentrado autólogo de plaquetas humanas em um pequeno volume de plasma, onde a concentração de plaquetas pode ser de 1,5 a 7 vezes superior à concentração no sangue. Ele surge como um tratamento autólogo, não imunogênica, capaz de induzir reparo cicatricial do osso e partes moles (Cole, Seroyer *et al.*, 2010).

Os estudos do Plasma Rico em Plaquetas aplicado à cicatrização tecidual e regeneração óssea tiveram seu início na década de 90 (Everts, Devilee *et al.*, 2006). Desde então inúmeras publicações mostram o bom desempenho da aplicação clínica do PRP nas mais diferentes áreas da medicina e odontologia, tais como ortopedia (Dallari, Savarino *et al.*, 2007), cirurgia plástica (Cervelli, Gentile *et al.*, 2009), cirurgia buco-maxilofacial(Gentile, Bottini *et al.*, 2010) e no tratamento de feridas crônicas (Rozman e Bolta, 2007; Hammond, Hinton *et al.*, 2009).

As plaquetas apesar de serem fragmentos celulares derivados de megacariócitos (MGC) da medula óssea, apresentam um grande número de estruturas como glicogênio, lisossomos e, principalmente, dois tipos de grânulos, aqueles conhecidos como grânulos densos (ricos em ADP, ATP, serotonina e cálcio) e os α-grânulos (ricos em fatores coagulantes, fatores de crescimento, e proteínas que medeiam a adesão). Assim, o PRP e seus fatores de crescimento (FCs) são considerados potentes estímulos no reparo de tecidos moles, uma vez que, estão envolvidos no processo angiogênico, reconstrução da matriz extracelular e tecido ósseo (Cole, Seroyer *et al.*, 2010).

A literatura está repleta de estudos sobre a ciência básica de FCs em relação à manutenção, proliferação e regeneração tecidual. A utilização do PRP na regeneração tecidual também tem sido tema de inúmeros trabalhos científicos e aplicações clínicas. Entretanto, apesar do intenso uso desta terapia na área médica e

de vários casos bem sucedidos, as causas de insucesso ainda não são bem entendidas. Um dos fatores críticos é a qualidade do PRP utilizado, que pode ser determinada por parâmetros como (i) centrifugação, que influencia diretamente a concentração e integridade das plaquetas e a presença de leucócitos e eritrócitos, (ii) tipo de agonistas utilizados na ativação do PRP, que influencia na velocidade de liberação dos FCs das plaquetas, bem como na formação da rede de fibrina (iii) rápida manipulação e utilização do PRP após a ativação, uma vez que os fatores de crescimento são lábeis e perdem rapidamente a sua atividade após serem liberados das plaquetas.

Devido à natureza autóloga do PRP, seu uso se popularizou muito rapidamente entre médicos e pacientes. Entretanto essa rápida popularização deve ser vista com cuidado uma vez que torna ainda mais difícil o controle adequado dos resultados. Além disso, algumas questões importantes a respeito do PRP ainda estão sem resposta, como a variação nas técnicas de preparação e na recuperação de plaquetas, a presença ou ausência de leucócitos e eritrócitos, a utilização de trombina para ativação das plaquetas e a variabilidade entre os doadores.

Uma busca no portal da *Web of Science*, com a palavra chave Plasma Rico em Plaquetas presente nos títulos das publicações científicas, mostra o salto no número de publicações sobre esse assunto na última década, como é mostrado na Figura 1.1(a). Vale ressaltar que concentrados de plaquetas são há muito tempo usado em transfusão sanguínea, em hematologia, e somente mais recentemente o Plasma Rico em Plaquetas passou a ser utilizado também para o produto autóloga rico em plaquetas utilizado para regeneração tecidual.

Dentre os estudos mais recentes envolvendo o PRP, a maioria trata das aplicações clínicas dos produtos em diversos tipos de tecidos como osso, músculos, tendões, ligamentos, menisco, além de aplicações em feridas e odontologia. Através de uma busca também no portal da *Web of Science* no mesmo período, observa-se que o número de estudos relacionados com a preparação do PRP é bem inferior aos estudos referentes às suas aplicações clínicas (Figura 1.1(b)).

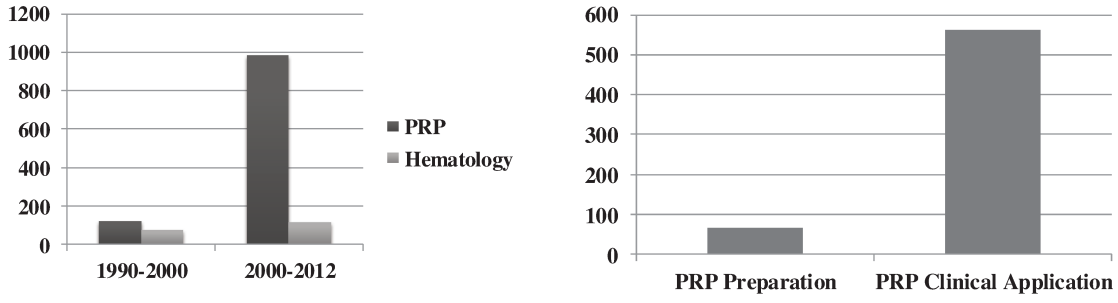

(a) (b)

Figure 1.1 Crescimento do número de estudos relacionados com Plasma Rico em Plaqueta aplicado à regeneração tecidual na última década em relação à década anterior (a) e número de publicações que estudam a preparação do PRP comparado ao número de publicações que se atém às aplicações clínicas do produto (b).

Busca feita no Web of Science em Novembro/2012

Os dados científicos relacionados com análise e/ou padronização das condições operacionais de cada etapa envolvida no preparo do PRP ainda são muito dispersos. Os estudos reportam várias preparações, que geram diferentes concentrações de plaquetas e FCs, e a falta de controle e padronização do PRP pode conduzir ao sucesso ou insucesso da terapia. Inúmeros protocolos de preparação, dispositivos (kits), centrífugas e métodos para a ativação plaquetária são propostos e usados no preparo de PRPs. Em geral, os principais fabricantes de produtos para ortopedia e medicina esportiva comercializam *kits* diferentes, com o apelo de produzir uma melhor qualidade e quantidade de PRP em relação aos seus concorrentes, para uma mesma quantidade de sangue do mesmo paciente. A variabilidade de custos é enorme: enquanto um kit comercial produz um PRP a um custo de várias centenas de dólares, um PRP preparado por técnica não automatizada (*in house*) na clínica pode custar muito menos. As metodologias usadas conduzem a diferentes produtos, com diferentes atividades biológicas,

havendo variações de cerca de 3 a 27 vezes na concentração de fatores de crescimento e na cinética de liberação.

Os trabalhos na literatura que estudam os aspectos envolvidos na preparação do PRP geralmente usam a estratégia causa-efeito. Avaliam a composição do PRP preparado em condições específicas, a partir da variação de alguma dessas condições. Como são muitas as variáveis envolvidas nesse processo, cada publicação obtém um PRP com uma composição diferente.

Nesse ponto, este estudo se diferencia dos demais da literatura, pois baseia-se na análise fenomenológica e estatística da preparação do PRP integrando as etapas de separação das células vermelhas do sangue e obtenção do primeiro concentrado de plaquetas, adicional concentração mantendo a sua integridade, ativação das plaquetas com seleção de redes de fibrina características, liberação dos fatores de crescimento e proliferação de células mesenquimais.

Além disso, como os fatores de crescimento são lábeis e a sua liberação prolongada beneficia a proliferação celular (Joshi, Mastrangelo *et al.*, 2009; Harrison, Vavken *et al.*, 2011), foi estudada a incorporação do PRP em hidrogéis de ácido hialurônico (AH) reticulados quimicamente com divinilsulfona (DVS) onde avaliou-se além da liberação dos FCs, a reologia dos géis formados e a sua capacidade de suportar o crescimento de celular.

1.3 Objetivo

O objetivo deste trabalho é estudar e caracterizar a preparação do Plasma Rico em Plaquetas como um processo integrado em todas as etapas, visando a sua padronização para aplicação em terapia regenerativa. Adicionalmente, este estudo contempla a incorporação de hidrogéis de ácido hialurônico ao PRP para a liberação controlada dos FCs e crescimento celular.

Este objetivo foi atingido através das seguintes metas:

- Implementação de metodologias para caracterização do PRP.
- Estudo da etapa de centrifugação através da construção de um modelo matemático fenomenológico.
- Estudo da influência dos agonistas soro autólogo e cálcio na formação da arquitetura da rede de fibrina através da construção de um modelo estatístico e estudo da influência dessas arquiteturas na liberação dos fatores de crescimento, na reologia e no crescimento celular.
- Estudo da encapsulação/incorporação do PRP em hidrogéis de AH quimicamente reticulados com divinilsulfona e sua capacidade de promover liberação controlada de seus FCs e o crescimento celular.

1.4 Principais contribuições deste trabalho

A padronização da preparação do PRP é um dos grandes desafios apresentados na literatura. Os inúmeros estudos referentes à aplicação clínica do PRP apontam para a necessidade da padronização do seu preparo, para que se possa assim comparar os resultados clínicos.

Entretanto, devido à própria natureza autóloga do produto, à necessidade de muitos dados experimentais e à interação entre às variáveis, os estudos de preparação do PRP geralmente utilizam métodos convencionais de análise, avaliando a composição do PRP preparado em faixas restritas, sem apontar tendências, tornando difíceis as predições quantitativas.

Um dos principais resultados alcançados com este trabalho foi o estabelecimento de uma estratégia de estudo que proporcionou a análise integrada dos dados através de metodologias que permitiram delinear o comportamento do sistema com um menor número de experimentos.

Essas metodologias basearam-se na construção de um modelo matemático do comportamento fenomenológico do sistema para o estudo da etapa de centrifugação e um modelo estatístico para etapa de ativação plaquetária e formação da rede de fibrina. As validações desses modelos mostraram a viabilidade desta estratégia que, integrada com a análise quantitativa da proliferação e diferenciação celular, permite que se chegue a PRPs preparados dentro de condições otimizadas e com controle de qualidade durante a sua preparação.

A Figura 1.2 apresenta de maneira esquemática a estratégia de análise integrada e padronização do PRP.

O desenvolvimento e consolidação desta estratégia resultaram na escrita de cinco artigos científicos submetidos à periódicos internacionais.

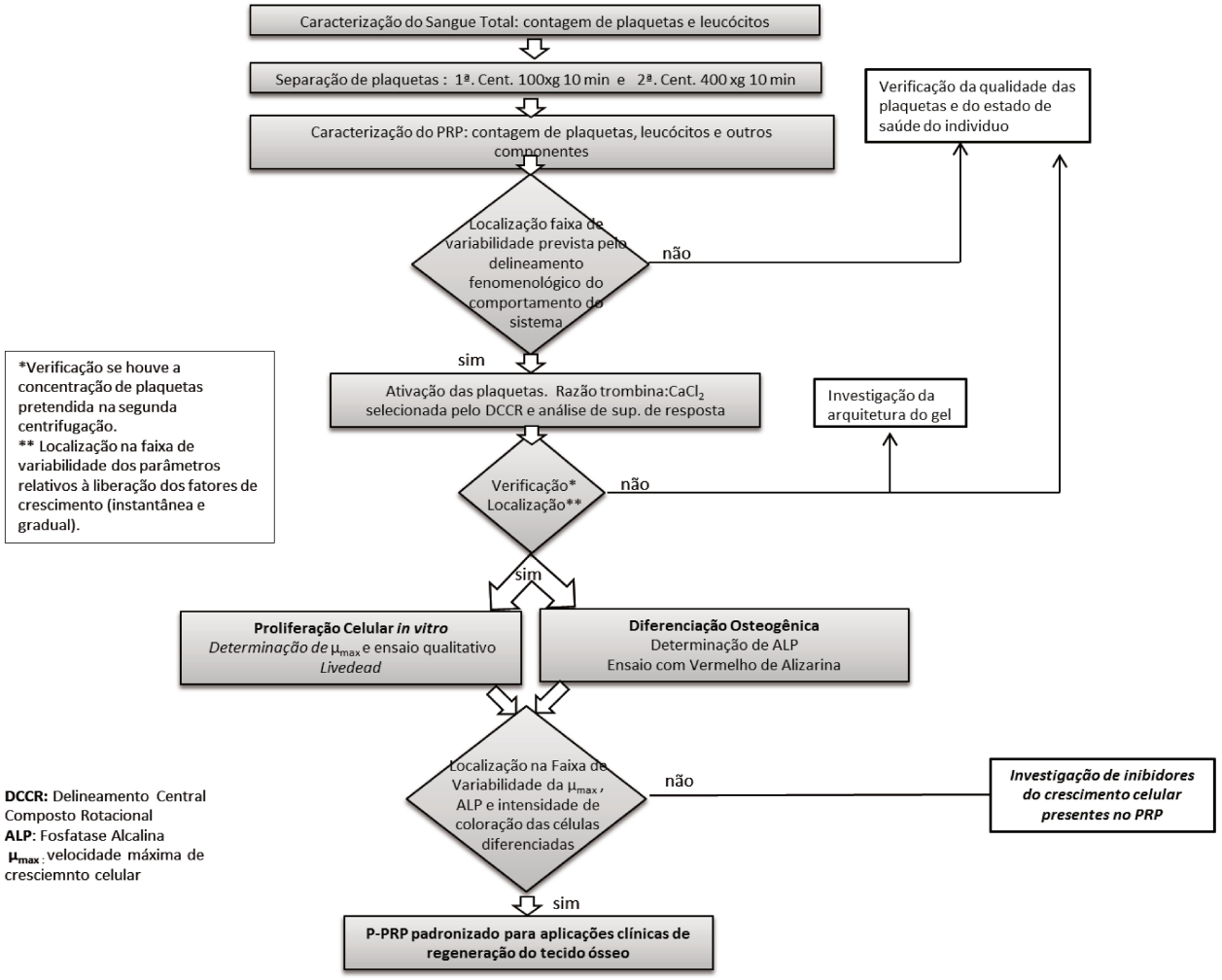

Figure 1.2 Estratégia de Análise Integrada e Padronização da Preparação do P-PRP para Aplicações Clínicas

Capítulo 2. Revisão Bibliográfica

2.1 Ciência Básica do Plasma Rico em Plaquetas

2.1.1 Introdução ao PRP

O Plasma rico em plaquetas (PRP) pode ser definido como uma fração do sangue autólogo com concentrações de plaquetas acima dos valores basais. As plaquetas por sua vez são ricas em fatores de crescimento que exercem um importante papel na cicatrização dos tecidos lesionados (Engebretsen, Steffen et al., 2010).

Os estudos do Plasma Rico em Plaquetas aplicado à cicatrização tecidual e regeneração óssea tiveram seu início na década de 90 (Everts, Devilee et al., 2006). Desde então inúmeras publicações tratam da aplicação clínica do PRP, com resultados notáveis nas mais diferentes áreas como odontologia (Anitua, 1999) cirurgia bucomaxilo facial, (Gentile, Bottini et al., 2010), cirurgia plástica, (Cervelli, Gentile et al., 2009), ortopedia (Dallari, Savarino et al., 2007) reumatologia (Filardo, Kon et al., 2012) e no tratamento de diferentes tipos de injúrias como feridas crônicas (Rozman e Bolta, 2007; Cieslik-Bielecka, Bielecki et al., 2009) e injúrias musculares. (Hammond, Hinton et al., 2009).

O PRP pode ser preparado por uma grande variedade de métodos, o que pode levar à preparações com diferentes composições, que podem impactar na sua composição e na eficácia do tratamento (Engebretsen, Steffen et al., 2010).

Apesar dessas variações na sua preparação, a maioria dos protocolos segue uma sequencia genérica (Figura 2.1) que contempla a coleta do sangue com anticoagulante, seguida de um primeiro processo de centrifugação para a separação do sangue em três camadas, o plasma sobrenadante; a camada de leucócitos intermediária e células vermelhas ao fundo (Dohan Ehrenfest, Rasmusson *et al.*, 2009). Alguns protocolos submetem o plasma a uma segunda centrifugação, obtendo-se uma concentração ainda maior de plaquetas (Landesberg, Roy *et al.*,

2000). Finalmente o PRP é aplicado no local da lesão, na presença de um ativador plaquetário, trombina e/ou cloreto de cálcio, que permite a ativação das plaquetas e a polimerização da fibrina (Dohan Ehrenfest, Rasmusson *et al.*, 2009).

Apesar dos estudos com PRP aplicado à regeneração tecidual serem relativamente recentes (cerca de 20 anos), estudos relacionados à formação da rede de fibrina e aplicação clínica da cola de fibrina como um adesivo cirúrgico natural é um assunto há muito investigado pelos pesquisadores.

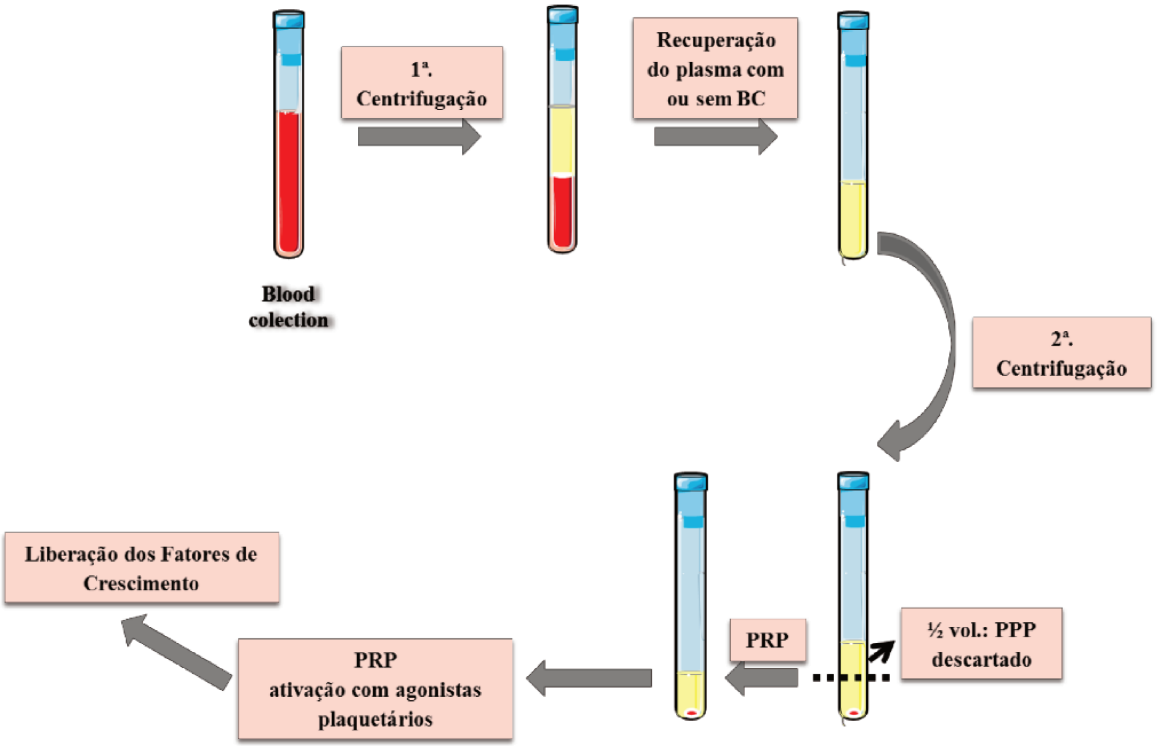

Figure 2.1 Sequencia genérica de preparação do Plasma Rico em Plaquetas

BC= Buffy coat

2.1.2 Da cola de fibrina ao PRP

A cola de fibrina (ou gel de fibrina) é um biomaterial que atua principalmente como agente hemostático e adesivo cirúrgico, no qual o fibrinogênio concentrado, o fator XIII (fator de *crosslinking* de fibrina) e a fibronectina são adicionados à trombina, ao cloreto de cálcio e a um inibidor de fibrinólise para a formação do coágulo de fibrina (Whitman, Berry *et al.*, 1997).

O interesse pelo uso de fibrinogênio como um adesivo cirúrgico natural surgiu nos primeiros anos de 1900. Mais tarde, tentativas mais sofisticadas usaram um sistema de coagulação constituído por fibrinogênio e trombina para ancorar enxertos de pele. Em geral, a qualidade adesiva dessas preparações era baixa, atribuída principalmente à falta de uma fonte concentrada de fibrinogênio (Gibble e Ness, 1990).

Em 1970 Matras descreveu pela primeira vez o uso da cola de fibrina, constituída de fibrinogênio concentrado (polimerização induzida por trombina e cálcio), para o fechamento de feridas e estímulo da cicatrização. Em 1978, o FDA (Food and Drud Administraion) órgão regulatório norte-americano revogou a licença para a comercialização dos concentrados de fibrina devido ao risco de transmissão de hepatite pelo fibrinogênio (Gibble e Ness, 1990).

Atualmente, colas de fibrina preparadas a partir de plasma humano, estão disponíveis comercialmente, a exemplo do Tisseel, da Baxter®, cuja aprovação para comercialização nos Estados Unidos ocorreu em 1998 (http://www.baxter.com). Porém, as colas de fibrina autóloga ainda possuem o inconveniente de ter seu uso limitado devido principalmente à complexidade e ao custo do processo de produção (Gibble e Ness, 1990), pois, é difícil a obtenção de altas concentrações de fibrinogênio para sua preparação (Dohan Ehrenfest, Choukroun *et al.*, 2006).

Assim, o uso de concentrado de plaquetas para melhorar a cicatrização e para a substituição das colas de fibrinas vem sendo muito explorado desde a década de

1990. O gel de plaquetas autólogo é uma modificação da cola de fibrina e que vem usado com sucesso em várias aplicações clínicas (Whitman, Berry *et al.*, 1997).

A principal diferença entre o gel de plaquetas e a cola de fibrina é a presença de altas concentrações de plaquetas e uma concentração nativa de fibrinogênio no gel de plaquetas (Whitman, Berry *et al.*, 1997).

Os géis ou *scaffolds* de fibrina podem ser obtidos a partir da reação do fibrinogênio e trombina isolados do plasma rico em plaquetas (PRP). Nas lesões teciduais *in vivo* o fibrinogênio é clivado pela trombina e é responsável pelos processos de hemostasia, adesão e agregação plaquetária (Zhao, Ma *et al.*, 2008).

Um dos parâmetros usados para a classificação do PRP é a formação da rede de fibrina (Dohan Ehrenfest, Rasmusson *et al.*, 2009), que é governada, principalmente, pelas razões entre as concentrações de fibrinogênio e trombina que determinam as propriedades biquímicas finais da rede. De acordo ainda com esses autores, altas concentrações de fibrinogênio e trombina promovem uma drástica ativação e polimerização que leva à formação de uma rede densa, que não é favorável à ligação dos fatores de crescimento e à migração celular. Entretanto, uma polimerização mais lenta e mais fisiológica, ou seja, onde as concentrações de fibrinogênio e trombina estão mais próximas das concentrações basais, permite à formação de uma rede flexível que é capaz de sustentar a migração celular e à ligação dos fatores de crescimento.

As propriedades físicas dos géis de fibrina têm sido bastante estudadas. Os estudos mostram que variações nas concentrações de fibrinogênio e trombina, assim como a força iônica levam à modificações na rede, principalmente na porosidade, diâmetro das fibras, permeabilidade do gel e adesão e migração celular (Carr, Gabriel *et al.*, 1986; Blomback, Carlsson *et al.*, 1989). Entretanto, a maioria dos estudos usa frequentemente fibrinogênio e trombina purificados, sem a presença de plaquetas.

Os principais estudos sobre a formação e caracterização da rede de fibrina são apresentados no item 2.1.3. deste capítulo.

2.1.3 Formação da Rede de Fibrina

A formação da rede de fibrina é um assunto bastante estudado na literatura (Carr e Hermans, 1978; Carr e Gabriel, 1980; Carr, Gabriel et al., 1986; Shah, Nair et al., 1987; Weisel e Nagaswami, 1993; Shah, Hospital et al., 1997; Weisel, 2007; Yeromonahos, Polack et al., 2007). Em geral, esses estudos utilizam fibrinogênio humano purificado e trombina bovina para avaliar a extensão da reação de hidrólise do fibrinogênio, a formação da rede de fibrina e a estabilidade dos *clots*.

O fibrinogênio é uma proteína trinodular com massa molar 340 KDa, presente em altas concentrações no plasma (2-4 mg/mL). É composto por até 3 pares de cadeias polipeptídicas $(A\alpha B\beta\gamma)_2$, incluindo os fibrnopeptídeos A e B, unidos por 29 ligações disulfeto .

Durante o processo de formação da rede de fibrina, inicialmente o fibrinogênio é hidrolisado pela ação da trombina e convertido à monômeros de fibrina. A trombina cliva primeiro as cadeias Aα, removendo o fibrinopeptídeo A, permitindo a formação das protofibrilas que crescem em comprimento. A remoção do fibrinopeptídeo B, na sequencia, parece estar associada ao crescimento lateral da cadeia, formando uma rede tridimensional. A rede de fibrina formada tem a consistência de um gel que, sob condições fisiológicas, é estabilizado através de ligações covalentes e não covalentes por cofatores que agem na cascata de coagulação. Portanto, a rede de fibrina é controlada principalmente por reações de polimerização da fibrina e decomposição do fibrinogênio. (Ferry e Morrison, 1947; Wolberg, 2007; Janmey, Winer *et al.*, 2009). O cálcio age como um cofator na hidrólise do fibrinogênio pela trombina, inibe o crescimento das protofibrilas por ação eletrostática e promove as ramificações laterais das protofibrilas (Falvo, Gorkun et al., 2010; Ryan, 2010).

As técnicas para monitoramento da formação e arquitetura da rede de fibrina têm envolvido, ao longo do tempo, desde monitoramento de medidas de densidade ótica em um só comprimento de onda (Ferry e Morrison, 1947), até o monitoramento da turbidez (derivada da densidade ótica - DO), em vários comprimentos de ondas (Carr e Hermans, 1978; Carr e Gabriel, 1980; Carr, Gabriel et al., 1986; Carr, 1990), análise dos espectros de espalhamento de luz (Ferri, Greco et al., 2001; Ferri, Greco et al., 2002) até técnicas mais sofisticadas como raios-X de baixo ângulo (Yeromonahos, Polack et al., 2007).

Um dos estudos mais antigos e mais citados sobre a formação da rede de fibrina relaciona turbidez dos géis de fibrina com o inverso do comprimento de onda elevado à terceira potência. Através dessa correlação é possível calcular a relação massa/comprimento e o raio das fibras (Carr e Hermans, 1978).

Os efeitos de diferentes componentes na formação da rede de fibrina são bastante investigados na literatura por diversas técnicas que vão desde o monitoramento de modificações na densidade ótica em um único comprimento de onda até análises de raio-x de baixo ângulo, como citado acima. A seguir serão apresentados estudos da influência de variações nas concentrações de trombina e cálcio, na formação da rede e consequentemente, nas suas propriedades físicas (Davis, Miller et al., 2011).

Elevadas concentrações de trombina não promovem quaisquer efeitos na rede quando da alteração da sua concentração. Porém, quando a trombina é utilizada em pequena quantidade, a variação na sua concentração promove alterações significativas na rede de fibrina. Em mais altas concentrações, a máxima turbidez gerada pelo gel é menor. Nessa condição, a clivagem do fibrinopeptídeo e a geração da protofibrila são mais rápidas comparadas à agregação lateral. Assim, o tempo de formação dos géis é menor, com a formação de fibras mais longas, antes que elas possam se agregar lateralmente (Weisel e Nagaswami, 1993).

Já o cálcio, em altas concentrações, promove o aumento da força eletrostática fraca das ligações laterais e, consequentemente, o crescimento lateral da fibra é

aumentado (Carr, Gabriel *et al.*, 1986). O aumento do tamanho da fibra, que ocorre mais por associação lateral do que por ligações terminais, reflete o aumento da turbidez do gel no ponto final (Carr e Gabriel, 1980). O cálcio está presente em todo o processo de associação do monômero e está intimamente envolvido com a força do gel, melhorando o módulo elástico (Carr, Gabriel *et al.*, 1986).

Com a utilização do PRP, outras variáveis podem influenciar a formação da rede de fibrina. As redes de fibrinas formadas por plasma, livre ou não de plaquetas, são diferentes daquelas produzidas com fibrinogênio purificado, mas exatamente quais componentes do plasma são responsáveis por essas diferenças não é totalmente conhecido (Shah, Nair *et al.*, 1987; Weisel e Nagaswami, 1992).

Os trabalhos que estudam a formação da rede de fibrina a partir do PRP ainda são poucos (Lucarelli, Beretta *et al.*, 2010; Dohan Ehrenfest, Bielecki *et al.*, 2012) .

Lucarelli (2010) estudou a formação do Plasma Rico em Matriz de Fibrina (PRMF- Fibrinet®), suas características morfológicas e a liberação de fatores de crescimento liberados das plaquetas A preparação do PRMF consiste na centrifugação do sangue (1100 xg por 6 min.) para separação do PRP. Em seguida o PRP é transferido para um tubo contendo 0,25 mL cloreto de cálcio 1M e submetido à centrifugação à 4500 xg por 25 minutos. O gel de fibrina formado apresentou fibras com diâmetro médio de 63,6 nm, caracterizado por Microscopia Eletrônica de Varredura (MEV). Segundo os autores, as propriedades mecânicas do gel foram superiores aos outros géis descritos na literatura. A liberação dos FC estudados (PDGF-AB, TGF-β1, VEGF, EGF e bFGF) mostrou-se muito mais pronunciada no primeiro dia (Lucarelli, Beretta *et al.*, 2010).

Donhan (2012) preparou dois tipos de PRPs, que resultaram em géis de fibrina com diferentes propriedades. O primeiro, o plasma rico em fator de crescimento (PRGF) foi preparado a partir de uma única etapa do sangue total, seguido pela ativação com $CaCl_2$ somente; o segundo, o plasma rico em fibrina e em leucócitos (L-PRF) foi preparado a partir da coleta do sangue total sem anticoagulante, seguido de uma etapa de centrifugação onde é formado o gel. Foi

observado que o gel de PRF apresentou-se muito mais resistente do que o gel de PRGF, uma vez que o primeiro já havia se dissolvido completamente em meio de cultura após o 5º. dia de cultura, enquanto o gel de PRGF permaneceu intacto o até o 7º. dia, último dia do estudo. A liberação de fatores de crescimento foi muito mais intensa no L-PRF comparado ao PRGF (Dohan Ehrenfest, Bielecki *et al.*, 2012). Entretanto os autores não mostram a quantificação de plaquetas em cada um dos géis preparados, o que pode levantar uma dúvida: a maior quantidade de FC liberado do L-PRF é devido à rede de fibrina formada ou à maior concentração de plaquetas que pode estar presente nesta preparação.

2.1.4 Plaquetas

As plaquetas possuem forma oval ou redonda e, com diâmetro entre 1-3 µm, são as menores células sanguíneas. A contagem média de plaquetas no sangue circulante está entre 150 a 400 x 10^3 plaquetas/mm^3 e sua meia-vida, *in vivo*, é de aproximadamente sete dias. As plaquetas são fragmentos citoplasmáticos de megacariócitos, um tipo de célula branca do sangue que é formada na medula óssea, anucleadas e com inúmeras estruturas citoplasmáticas como mitocôndrias, microtúbulos contráteis, contendo actina e miosina; grânulos densos, contendo ADP, ATP, serotonina e cálcio e os α grânulos, contendo os fatores de crescimento e outras proteínas (Everts, Devilee *et al.*, 2006).

Os α-grânulos por sua vez, possuem uma ampla variedade de proteínas adesivas de coagulação, fatores de crescimento e inibidores de proteases que estão envolvidos nos mecanismos de coagulação (Harrison e Cramer, 1993) e são capazes de promover a regeneração tecidual (Engebretsen, Steffen *et al.*, 2010).

As plaquetas são o primeiro tipo celular recrutado para o local da injuria tecidual e, particularmente, ativam uma resposta inflamatória precoce desencadeando, dessa forma, a liberação de fatores de crescimento após o processo de degranulação plaquetária. Os principais fatores de crescimento liberados consistem em fator de crescimento derivado de plaquetas (PDGF), fator de crescimento transformador (TGF-β), fator de crescimento vascular endotelial

(VEGF), fator de crescimento de fibroblastos (FGF), fator de crescimento semelhante à insulina (IGF) e fator de crescimento epidérmico (EGF) (Cole, Seroyer *et al.*, 2010).

A Figura 2.2 apresenta um desenho esquemático das plaquetas.

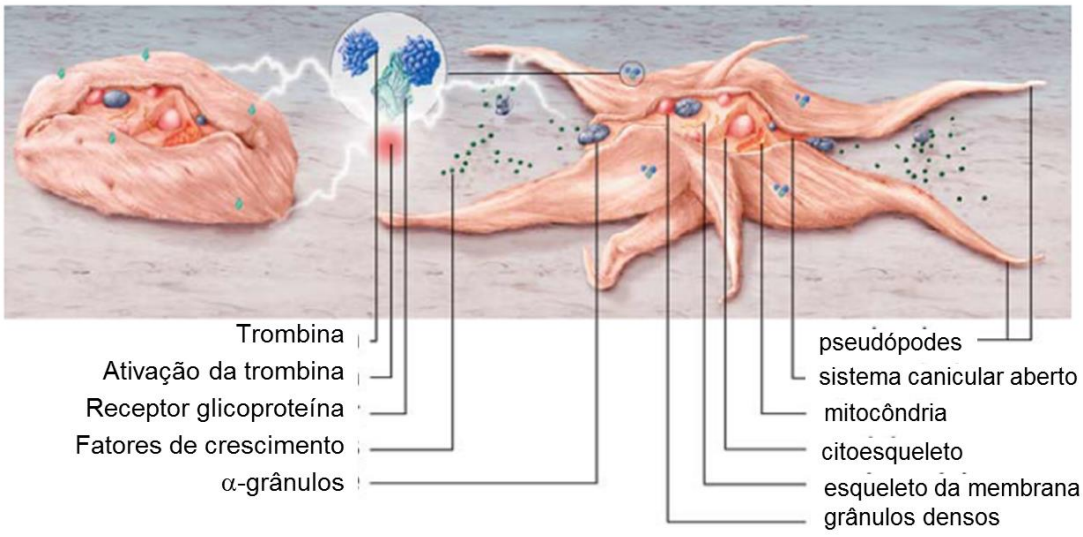

Figure 2.2 Desenho esquemático da morfologia das plaquetas antes e após a sua ativação. Adaptado de (Everts, Knape *et al.*, 2006)

2.1.4.1 Morfologia das Plaquetas

Com o objetivo de simplificar a estrutura das plaquetas e relacioná-la com suas atividades bioquímicas, pode-se dividi-la em três regiões maiores: periférica, sol-gel e de organelas.

A região periférica é composta por um sistema de membranas externas e internas que formam a superfície exposta das plaquetas e as paredes dos canais tortuosos que compõem a conexão da superfície com o sistema canicular aberto (OCS). A camada externa apresenta receptores que desencadeiam a ativação plaquetária e substratos para as reações de adesão-ativação plaquetária, como inúmeras glicoproteínas. O OCS desemboca na membrana plaquetária desempenhando um papel importante na liberação do conteúdo dos grânulos.

Imediatamente abaixo da membrana se encontra os canais do sistema tubular denso (DTS) onde se armazena o cálcio (Gresele, 2002).

A região sol-gel é a matriz do citoplasma plaquetário, composta principalmente por elementos do sistema contrátil, responsáveis pela mudança de forma, formação de pseudópodes, contração interna, e secreção (Hartwig, Barkalow *et al.*, 1999).

A região das organelas é composta por grânulos, corpos elétron-densos, peroxissomos, lisossomos, glicossomos e mitocôndrias, que estão dispersos no citoplasma de fome aleatória. Essas organelas são importantes para processo metabólico e o armazenamento de enzimas, serotonina, uma variedade de proteínas e cálcio destinado à secreção (Gresele, 2002).

Os α-grânulos concentram proteínas plasmáticas, como proteínas adesivas, fatores de coagulação e fatores mitogênicos, que exercem um papel crítico na hemostasia, cicatrização e na interação célula-matriz, estocando-as até que sejam necessárias no local da injúria. A transformação na morfologia das plaquetas associada à mudança de forma representam um forte indício da agregação plaquetária, sendo consideradas as primeiras repostas fisiológicas mensuráveis após a ativação por uma agonista plaquetário específico como o ADP ou trombina, e se inicia antes que ocorra uma agregação propriamente dita. A mudança de forma das plaquetas é caracterizada pela esferização e contração celular, rearranjos do citoesqueleto, dobra da superfície da membrana e formação de pseudópodes. Mudanças na sua morfologia também podem ocorrer após as plaquetas entrarem em contato com partículas ou superfícies estranhas, ao serem expostas à altas acelerações empregadas nos processos de centrifugação, ao calor, ao frio, ou devido à quelação com cálcio (como com EDTA) e pelo metabolismo energético deprimido (Weiss, 1995).

A ligação inicial das plaquetas à superfície e a subsequente coesão plaqueta-plaqueta são identificados como 2 estágios separados de formação do trombo, definidos como adesão e agregação, respectivamente; sendo que a adesão requer

um repertório maior de substratos e receptores plaquetários do que a agregação (Savage, Almus-Jacobs *et al.*, 1998; Ruggeri, Dent *et al.*, 1999).

A Figura 2.3 (a) e (b) apresentam um desenho esquemático da ultraestrutura das plaquetas e uma microscopia eletrônica de varredura

(a)

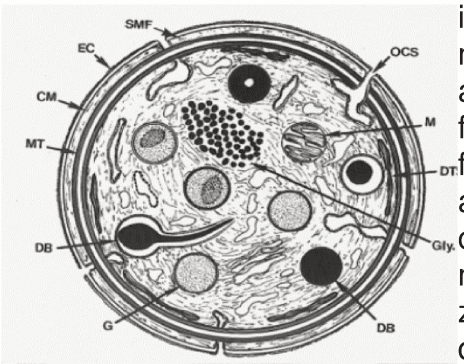

(b)

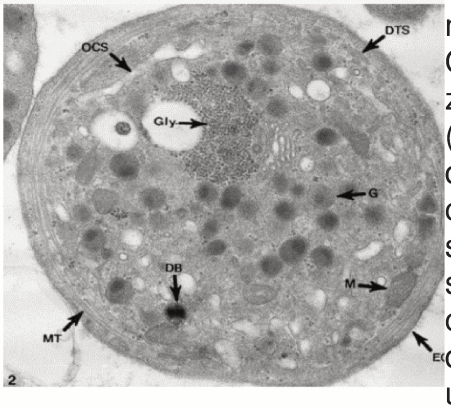

Figure 2.3 (a) e (b) Ultraestrutura das plaquetas discoides. Em (a) observa-se a ultraestrutura das plaquetas. Os componentes da zona periférica incluem o revestimento exterior (CE), membrana trilaminar (CM), e uma área da sub-membrana contendo filamentos especializados (SMF), que formam a parede das plaquetas e alinham os canais do sistema canalicular ligado à superfície (CS). A matriz do interior das plaquetas é a zona de sol-gel contendo filamentos de actina, a banda circunferencial dos microtúbulos (MT), e glicogênio (Gly). Os elementos celulares embutidos na zona de sol-gel incluem mitocôndrias (M), em grânulos, (G), e corpos densos (DB). Coletivamente eles constituem a zona organela. Os sistemas de membrana incluem a superfície de contato do sistema canalicular (CS) e o sistema tubular denso (DTS). Em 3(b) é apesentado um corte de plaquetas no plano equatorial, que revela a maior parte das estruturas indicadas em (a) (aumento 28 000 x). Imagens de (Gresele, 2002).

2.1.4.2 Adesão Plaquetária

As plaquetas discóides presentes no sangue circulante ou no PRP não são adesivas. O contato com o subendotélio ou outra superfície externa resulta na adesão e no início dos eventos da mudança de forma. Os receptores que cobrem a membrana plaquetária, facilitam a conversão da célula para sua forma adesiva. A ligação à proteínas da matriz extracelular é mediada primeiramente por uma família de proteínas hetero-diméricas da superfície celular, cada uma composta por subunidades α e β. α5β1 é um receptor para fibronectina, α6β1 é um receptor para laminina. Outras receptores plaquetários integrinas parecem ser menos específicos como o αvβ3, que é um receptor para vitronectina, trombospondina e fator de von willebrand (fvW). Além disso, as plaquetas possuem outros receptores não-integrinas em sua superfície como GP Ib–IX, receptor para o fvW e a GP IV que se liga à trombospondina e ao colágeno. A GP Ia– IIa (α2β1) também é um receptor para o colágeno como a GPVI. A mais importante integrina plaquetária é a αIIBβ3, cujo principal substrato é o fibrinogênio, mas também pode se ligar à vitronectina e ao fvW (Clemetson, 1995; Gresele, 2002).

Após a injúria tecidual, o fvW presente no plasma é o primeiro a se ligar ao colágeno exposto presente na parede do vaso. Em seguida ocorre a ligação das plaquetas através da interação do complexo receptor GPIb/V/IX com o fvW imobilizado. Além do complexo GPIb/V/IX, outros receptores estão envolvidos na adesão das plaquetas ao subendotélio, como os receptores de colágeno α2β1 e GPVI, receptor de fibronectina α5β1 e receptor de fibrinogênio αIIbβ3 (GPIIbIIIa). O aumento da extensão da superfície de contato das plaquetas, mediado pela glicoproteína GP IIbIIIa, sucede a adesão e é essencial para suportar as forças de cisalhamento exercidas pelo fluxo sanguíneo (Weiss, Turitto *et al.*, 1991; Gresele, 2002).

2.1.4.3 Agregação Plaquetária

Após a adesão plaquetária ao subendotélio, outras plaquetas migram da circulação para fixarem-se às plaquetas já aderidas, formando o agregado. Os agonistas, como trombina, colágeno e ADP, promovem a contração plaquetária, estreitando o anel microtubular que sustenta a membrana e empurrando os grânulos até o centro da célula. Essa contração promove a mudança na forma das plaquetas, que passam de discóides para esféricas, cobertas por pseudópodes.

Os diversos agonistas mobilizam o cálcio armazenado DTS e, com a concentração aumentada de íons cálcio no citoplasma, vem onda contrátil. Quando duas plaquetas em contração entram em contato, a superfície de contato de ambas se estende ao máximo. Este contato celular íntimo é necessário para a formação do agregado plaquetário. Além disso, a membrana das plaquetas adquire novas propriedades físico-químicas, com a formação de fosfolipídios específicos, aos quais os fatores de coagulação podem se fixar. O aumento da concentração citoplasmática de íons cálcio além de estimular a contração das plaquetas, estimula também a atividade da enzima plaquetaria fosfolipase A2. Essa enzima fragmenta fosfolipídios da membrana, liberando ácidos graxos, principalmente o ácido araquidônico. Esse serve como substrato para uma série de enzimas, como a cxiclooxigenase (COX), que está presente na parede vascular e no seio das plaquetas, e é responsável pela conversão do ácido araquidônico em endoperóxido. Esse endoperóxido por sua vez, é transformado em tromboxano A2 pela ação da enzima tromboxano-sintetase. O tromboxano A2 além de ser um poderoso vasoconstritor, promove a liberação do conteúdo dos grânulos (Gresele, 2002).

Por mais de três décadas a agregação plaquetária foi vista como um processo relativamente simples, requerendo apenas um estímulo plaquetário (agonista), uma proteína adesiva solúvel (fibrinogênio) e um receptor plaquetário ligado à membrana (Integrina αIIb β3 ou GPIIb-IIIa), levando a um modelo unificado simples de agregação plaquetária. Apesar desses elementos ainda serem fundamentais,

avanços técnicos, que estão permitindo a análise em tempo real da agregação plaquetária in vivo, mostram um processo muito mais complexo e dinâmico do que se acreditava anteriormente. Agora é amplamente aceito que um dos elementos chave que influenciam a agregação plaquetária é o fluxo sanguíneo, com evidências de que diferentes mecanismos de agregação operam em diferentes condições de cisalhamento (Jackson, 2007) .

Como mencionado, os agonistas plaquetários solúveis estimulam uma série de respostas bioquímicas e funcionais, incluindo o fluxo de cálcio citosólico, a mudança de forma das plaquetas e liberação dos seus grânulos, que coincidem com o rápido desenvolvimento dos agregados plaquetários (Nesbitt et AL, 2009).

Entretanto, com as recentes demonstrações de que as plaquetas podem formar agregados in vivo sem apresentar essas respostas biquímicas, ou seja, sem um aumento detectável de cálcio citosólico, sem sofrer mudança de forma sem secreção substancial de citocinas pelos α-grânulos nas fases iniciais do desenvolvimento do trombo e sem a expressão imediata da p-selectina na superfície das palquetas, tem se levantado a possibilidade de que mecanismos adicionais estejam envolvidos no fenômeno de agregação plaquetária. Um desses mecanismos pode estar envolvido com mudanças localizadas no fluxo sanguíneo (Nesbitt, Westein *et al.*, 2009).

Estudos recentes identificaram que, na faixa de taxa de cisalhamento fisiológica (1000 a 10000 s^{-1}), agregados discóides pequenos e transientes podem ser formados através de *tethers* nas membranas, enquanto que em taxas de cisalhamento patológicas (> 10000 s^{-1}) grandes agregados podem ser formados independente da ativação das plaquetas e integrina αIIb-β3 (Nesbitt, Westein *et al.*, 2009).

Embora se saiba há muito tempo que a agregação das plaquetas ocorre geralmente em locais onde o fluxo sanguíneo é perturbado, após uma injúria vascular; assumia-se que esse processo estava diretamente ligado com o acúmulo de agonistas plaquetários solúveis nesses locais. Essa hipótese foi modificada,

sugerindo-se que as plaquetas utilizam um mecanismo biomecânico de agregação. Eles demonstraram que micro gradientes de cisalhamento locais, que ocorre com a mudança da geometria dos vasos, expõe as plaquetas discóides há uma rápida mudança nas condições hemodinâmicas (especificamente aceleração no cisalhamento acompanhada de desaceleração), promovendo o desenvolvimento de agregados de plaquetas discóides estabilizados (Nesbitt, Westein *et al.*, 2009).

Mecanicamente, as plaquetas expostas à acelerações bruscas de cisalhamento desenvolvem *tethers* nas membranas (prolongamentos da bicamada lipídica) permitindo a formação de agregados de plaquetas discoides transientes (Nesbitt, Westein *et al.*, 2009).

(Nesbitt, Westein *et al.*, 2009) mostraram que após a subsequente desaceleração no cisalhamento, essas *tethers* se reestruturam, aumentando a força e a estabilidade dos agregados de plaquetas discoides, promovendo assim o crescimento do trombo. Esse mecanismo ocorre independentemente dos agonistas solúveis. No geral, suas descobertas mostraram que a formação do trombo envolve os dois mecanismos complementares; com a estabilização dos agregados de plaquetas discóides sendo o principal mecanismo que dirige a formação inicial do trombo e os agonistas solúveis estabilizando os agregados formados.

2.1.4.4 Agonistas Plaquetários

Os mais importantes agentes agonistas *in vivo* são o colágeno presente na parede dos vasos, o ADP dos glóbulos vermelhos ou liberados das próprias plaquetas, tromboxano A2 e trombina (Gresele, 2002).

O ADP pode participar da agregação espontânea que ocorre sob altas forças de cisalhamento ou em condições que ocorra hemólise. Essa agregação é muito maior no sangue total do que no PRP, uma vez que o ADP presente nos glóbulos vermelhos são, em parte, responsáveis por esse fenômeno. O ADP também pode ser liberado das plaquetas ativadas e atuam de maneira sinérgica com os outros agonistas que induzem a degranulação plaquetária. In vitro, em um meio contendo

concentrações fisiológica de íons cálcio, o ADP causa apenas uma agregação plaquetária primária, reversível, uma vez que não ocorra a formação de tromboxano A2 ou liberação significativa do conteúdo dos grânulos. Já em um meio com baixas concentrações de cálcio, como o PRP contendo citrato, a agregação plaquetária induzida pelo ADP em concentrações acima de 1-2 µM torna-se irreversível (Dong, Li *et al.*, 1994; Gresele, 2002).

O colágeno tipos I e III são efetivos agonistas. Uma vez aderidas ao colágeno, as plaquetas são induzidas a formarem o tromboxano A2 e a liberarem o ADP. O tromboxano A2 causa agregação e liberação do conteúdo dos grânulos plaquetários (Brass e Bensusan, 1974).

A trombina é o mais forte agregante plaquetário in vivo. A trombina causa a formação do tromboxano A2 e a liberação do ADP das plaquetas, porém, ela é capaz de promover a agregação sem a intervenção do tromboxano A2 ou ADP. A agregação plaquetária induzida por trombina não pode ser bem estudada no PRP devido à formação da fibrina; assim, os efeitos da trombina são estudados em suspensões de plaquetas lavadas em meio artificial (Gresele, 2002).

As plaquetas podem agregar na ausência de agonistas, quando são submetidas à altas tensões de cisalhamento do fluido in vitro, com por exemplo em dispositivos como um viscosímetro cone e placa (Hardwick, Hellums *et al.*, 1981; Chow, Hellums *et al.*, 1992).

A agregação espontânea pode ser induzida após a agitação do sangue com anticoagulante ou do PRP ou após reaquecimento e agitação de plaquetas refrigeradas na presença de fibrinogênio.

2.1.4.5 Marcadores da ativação plaquetária

P-selectina

As selectinas são uma classe de moléculas especializadas na adesão celular. As selectinas são designadas por prefixos, de acordo com o tipo de células em que

essas moléculas foram identificadas pela primeira vez: L-selectina é expressa na maioria dos tipos de leucócitos; E-selectina é expressa no endotélio ativado e P-selectina, primeiro encontrada armazenada nos alfa-grânulos das plaquetas, mas também é expressa pelas células endoteliais (Vestweber e Blanks, 1999).

P-selectina (CD62P; anteriormente chamada GMP-140 ou PADGEM) possui massa molar de aproximadamente 140 KDa e é uma proteína rica em cisteína, contendo várias cadeias oligossacarídicas unidas por ligação-N. O domínio extracelular é organizado da seguinte maneira: um domínio lecitina (o grupo amino-terminal contendo 120 resíduos de aminoácido), um domínio do fator de crescimento epidérmico e nove regiões regulatórias do complemento (cada uma com aproximadamente 60 resíduos de aminoácido em comprimento). Além disso, a p-selectina apresenta um domínio transmembrana e uma cauda citoplasmática (Bevilacqua, 1993; Blann e Lip, 1997), conforme representado esquematicamente na Figura 2.4.

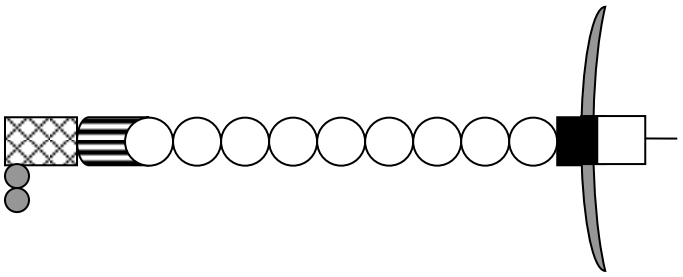

Figure 2.4 Representação esquemática da molécula de P-selectina

● Resíduos de Carboidrato

⊠ Lecitina

Região do EGF

○ Proteínas regulatórias do complemento

■ Domínio trasnmembrana

▭ Cauda citoplasmática

A P-selectina está presente nas células endoteliais vasculares, assim como nas plaquetas e em suas células precursoras, os megacariócitos. São armazenadas na membrana de grânulos secretores de armazenamento, os alfa-grânulos (no caso das plaquetas) e os corpos de Weibel-Palade, no caso das células endoteliais (Bonfanti, Furie *et al.*, 1989; Mcever, Beckstead *et al.*, 1989).

Após a ativação por trombina e fusão da membrana, a P-selectina presente nos α-grânulos das plaquetas são expostos na superfície da membrana plasmática (Stenberg, Mcever *et al.*, 1985).

A P-selectina solúvel, presente no plasma, possui massa molar aproximadamente 3 KDa menor (Chong, Murray *et al.*, 1994). Após a ativação plaquetária, essa P-selectina também é secretada no plasma e portanto, pode também funcionar como um marcador da ativação plaquetária (Blann e Lip, 1997; Ferroni, Martini *et al.*, 2009). Daí vem a importância da sua quantificação após a etapa de centrifugação no preparo do PRP, com o objetivo de indicar a ativação precoce das plaquetas devido às altas forças empregadas nas etapas de centrifugação.

2.1.5 Fatores de crescimento

Os fatores de crescimento (FC) são proteínas que atuam como agentes sinalizadores para as células. Suas funções fazem parte de uma vasta rede de comunicação celular que influenciam funções críticas como a divisão celular, a síntese da matriz e a diferenciação tecidual. Os resultados de estudos experimentais estabeleceram que os FCs exercem um importante papel na formação da cartilagem e do osso, na consolidação da fratura e no reparo de outros tecidos musculo-esqueléticos (Lieberman, Daluiski *et al.*, 2002). A seguir será apresentado, esquematicamente, o mecanismo pelo qual os fatores de crescimento regulam o comportamento celular (Figura 2.5). Uma molécula sinalizadora celular (ligante), presente no meio extracelular se liga ao domínio extracelular do seu receptor. Essa ligação ligante-receptor ativa o domínio intracelular do receptor. Para muitos receptores de fatores de crescimento, esse domínio quinase possui a habilidade

enzimática de transferir grupos fosfato para proteínas (atividade quinase), um importante passo de sinalização na comunicação celular. O receptor ativado por sua vez ativa uma série de etapas adicionais de fosforilação (cascata quinase) em associação com outros fatores regulatórios no citoplasma. Essa castata culmina no núcleo com a ligação de fatores de transcrição (proteínas que se ligam a sequências regulatórias específicas do DNA) para ativar a transcrição de um gene no interior do RNA mensageiro (mRNA). O mRNA é então transcrito em proteína para ser utilizado no interior da célula ou ser exportado para a produção da matriz ou outras funções teciduais (Trippel, 1997).

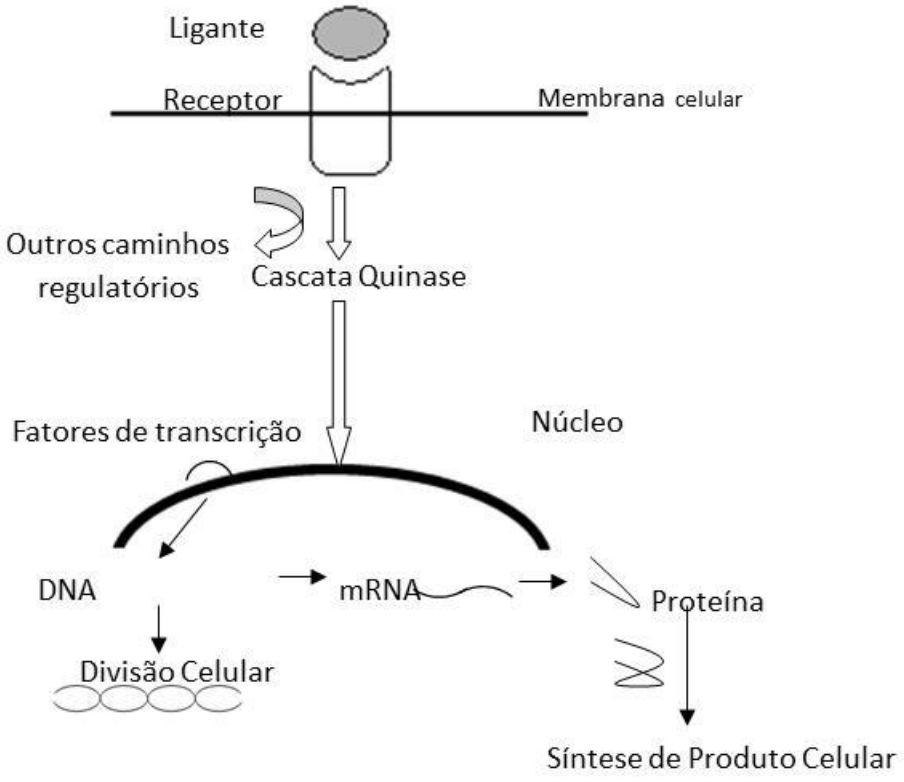

Figure 2.5 Ação dos Fatores de Crescimento nas células

Os FCs podem agir no organismo, basicamente, por três vias distintas: (i) autócrina, a qual é caracterizada pela auto-ativação celular, ou seja, por essa via os

fatores de crescimento agem sobre as células que os originaram ou sobre células fenotipicamente idênticas a essas; (ii) parácrina, via pela qual os FCs secretados localmente agem sobre as células vizinhas e (iii) endócrina, onde os FC secretados por uma determinada célula são liberados na corrente sanguínea e agem em células-alvo em um local distante de onde foram originalmente secretados (Trippel, 1997; Lieberman, Daluiski *et al.*, 2002).

Os fatores de crescimento, em geral, não atuam de maneira endócrina. Eles se difundem pouco através da matriz extracelular e atuam localmente devido à sua curta meia-vida e à lenta difusão. Os fatores de crescimento possuem a capacidade de levar uma mensagem específica à sub-populações de células distintas. Isso se deve não somente ao tipo de fator de crescimento ou à sua capacidade de se difundir através da matriz extracelular, mas se deve também ao tipo de receptor, ao número de células alvo e à transdução do sinal no interior da célula, subseqüente à ligação do FC. Assim, a mensagem transmitida por um determinado FC pode variar de acordo com o tipo de célula ou o tipo de receptor à que ele se liga. Ainda que se tenha um mesmo receptor, ele poderá transmitir mensagens diferentes, de acordo com os atalhos de transdução do sinal no interior da célula, o que pode diferir de um tipo de célula para o outro (Trippel, 1997; Lieberman, Daluiski *et al.*, 2002).

Outros fatores que podem influenciar a resposta das células-alvo à um determinado FC são: localização das células alvo, concentração dos FC, a capacidade desses fatores se ligarem à matriz extracelular e a degradação dessa matriz (Lamalice, Le Boeuf *et al.*, 2007; Lee, Silva *et al.*, 2011).

Os nomes específicos como, por exemplo, fator de crescimento semelhante à insulina (IGF), fator de crescimento de fibroblasto (FGF) e fator de crescimento derivado de plaquetas (PDGF), são advindos das descrições iniciais da ação ou da fonte desses FCs. Esses nomes são tradicionalmente aceitos até hoje, porém, não fornecem uma descrição significante da função desses fatores de crescimento (Trippel, 1997).

A cicatrização dos tecidos moles envolve a reepitelização, angiogenese, e deposição de matriz extracelular. Diferentes tipos de fatores de crescimento regulam as diferentes fases do processo de cicatrização.

A seguir serão apresentados os dois fatores de crescimento mais bem descritos presentes nas plaquetas, o PDGF e o TGF-β.

2.1.5.1 Fator de crescimento derivado de plaquetas (PDGF)

Os α-grânulos das plaquetas são a principal fonte se PDGF, embora esse fator de crescimento também seja produzido por vários outros tipos celulares como fibroblastos, macrófagos, dentre outros (Heldin e Westermark, 1999).

O PDGF existe como três isômeros distintos (AA, AB e BB), que diferem na constituição da cadeia polipeptídica (Angel, Sgaglione *et al.*, 2006).

A cicatrização de tecidos moles envolve a reepitelização, angiogênese e deposição da matriz extracelular. Diferentes tipos de fatores de crescimento regulam os diferentes tipos de processos de cicatrização. O PDGF atua sobre diferentes tipos celulares envolvidos na cicatrização. Ele estimula a mitose e a quimiotaxia de fibroblastos e células musculares lisas e a quimiotaxia de neutrófilos e macrófagos. Ele também estimula os macrófagos a produzirem outros fatores de crescimento, importantes para várias fases do processo de cicatrização. Além disso, o PDGF estimula a produção de várias matrizes, como fibronectina, colágeno, proteoglicanos e ácido hialurônico. O PDGF também é importante na cicatrização tardia de feridas, uma vez que estimula a contração da matrizes de colágeno in vitro. Na fase de remodelamento da cicatrização, o PDGF estimula a produção e secreção de colagenase pelos fibroblastos (Heldin e Westermark, 1999).

Para que o PDGF atue sobre a cicatrização in vivo, ele deve estar presentes no local da lesão. As primeiras observações revelaram que PDGF é liberado pelas plaquetas e secretado por macrófagos ativados, por células endoteliais estimuladas por trombina, por células musculares lisas de artérias

danificadas, por fibroblastos ativados, bem como por queratinócitos epidérmicos, sugerindo que a PDGF está presente no local da lesão (Heldin e Westermark, 1999).

Lesões tratadas com PDGF mostraram um aumento no tecido de granulação rico em fibroblastos e glicosaminoglicanos e um aumento na taxa de reepitelização e neovascularização. Assim PDGF não altera a seqüência normal de cicatrização, mas aumenta a sua taxa. Ensaios clínicos mostraram que o PDGF-BB aumenta a cicatrização e úlceras de decúbito. Análise de seções de feridas humanas mostraram que o PDGF-BB induz a proliferação e diferenciação de fibroblastos. O PDGF-BB também é capaz de aumentar a capacidade de cicatrização em pacientes com capacidade de cicatrização diminuída, como os diabéticos (Heldin e Westermark, 1999).

Em fraturas ósseas, durante a resposta imediata à lesão, o PDGF e TGF-beta são os primeiros fatores de crescimento liberados pela degranulação plaquetária, seguida pela infiltração de macrófagos e outras células inflamatórias que secretam FGF e PDGF e TGF-beta adicionais (Barnes, Kostenuik *et al.*, 1999).

2.1.5.2 Fator de crescimento transformador (TGF)

A família TGF contém três isoformas que estão presentes nos seres humanos, o TGF-β1, TGF- β 2 e TGF- β 3 que, apesar das similaridades no domínio C terminal (64-82%), possuem atividade biológica bastante diferentes. O TGF-β 1 e o TGF-β 2 parecem ser os mais importantes no que se refere ao reparo do tecido conectivo e à regeneração óssea. O TGF-β é encontrado predominantemente nas plaquetas, que corresponde à 95% do total, e pode ser encontrado também, em sua forma latente, nos macrófagos (Everts, Knape *et al.*, 2006).

Os fatores de crescimento TGF- β's possuem efeitos autócrinos e parácrinos, o que dão à esses FC o poder de cicatrização a longo prazo e capacidade de regeneração óssea (Everts, Knape *et al.*, 2006). Essa citocina é de grande importância durante a embriogênese e na manutenção da hemostasia tecidual durante a vida.

O TGF- β 1 regula uma ampla gama de processos biológicos, como proliferação, diferenciação e migração celular, além da produção da matriz extracelular. A ação combinada dessas respostas celulares media os efeitos globais do TGF- β1 nas respostas imunes, anfigênese, cicatrização, desenvolvimento e formação óssea (Janssens, Ten Dijke *et al.*, 2005).

Inúmeros estudos in vitro demonstram o papel do TGF- β1 em cada estágio da formação do osso, mostrando que o TGF- β1 aumenta a formação do osso in vitro principalmente por recrutar células progenitoras de osteoblastos e estimular sua proliferação, ampliando assim o número de osteoblastos, bem como a promoção de estágios iniciais de diferenciação (produção de matriz óssea). Por outro lado, ele bloqueia as fases finais de diferenciação e mineralização. Esses últimos estágios são regulados por outros fatores de crescimento como as Proteínas Morfogenéticas do Osso (BMP). A apoptose dos osteoblastos é bloqueada pelo TGF- β1 através da sua manutenção durante a transdiferenciação em osteócitos (Janssens, Ten Dijke *et al.*, 2005).

O TGF- β1 é responsável ainda, no processo de reabsorção óssea, pelos os eventos ligados ao recrutamento dos precursores dos osteoclastos para o tecido ósseo, pela diferenciação em osteoclastos maduros, pela reabsorção óssea e pela apoptose dos osteoclastos (Janssens, Ten Dijke *et al.*, 2005).

No Plasma Rico em Plaquetas, ambos o PDGF e o TGF-β estão presentes, o que implica em que uma mistura combinada desses fatores de crescimento sempre estarão presentes nos tecidos. Esse efeito parece ser benéfico para os tecidos desde que vários resultados são relatados na literatura, reportando o efeito sinérgico de diferentes fatores de crescimento (Everts, Knape *et al.*, 2006).

Contudo, outros fatores de crescimento participam durante os eventos de reparo tecidual. O fator de crescimento vascular endotelial (VEGF) é considerado um dos principais fatores de crescimento envolvidos na regulação da angiogênese, criando o suprimento sanguíneo requerido para formação tecidual. O fator de crescimento epidérmico (EGF) estimula a diferenciação celular, angiogênese e

proliferação de células mesenquimais e epiteliais (Everts, Knape *et al.*, 2006). O fator de crescimento fibroblástico (FGF), produzido principalmente por fibroblastos e células endoteliais, apresenta ação mitogênica para células envolvidas na cicatrização, tais como: células endoteliais, fibroblastos, osteoblastos, condrócitos, células musculares lisas e esqueléticas. O fator de crescimento semelhante à insulina (IGF), por sua vez, aumenta a formação óssea por induzir a proliferação dos osteoblastos e células precursoras (Cole, Seroyer *et al.*, 2010).

2.2 Preparação do Plasma Rico em Plaquetas

2.2.1 Sequencia básica de preparação do PRP

A literatura está repleta de protocolos diferentes para a preparação do plasma rico e plaquetas. Apesar disso, a preparação do PRP segue uma sequencia básica que contempla três etapas principais, ilustradas na Figura 2.1: a coleta do sangue, as etapas de centrifugação para separação e concentração das plaquetas e a ativação plaquetária para liberação dos fatores de crescimento, conforme brevemente descritas a seguir.

2.2.1.1 Coleta do sangue

A punção venosa segue os mesmos princípios de um acesso venoso tradicional, optando preferencialmente pelas veias dos membros superiores (veia mediana, basílica e/ou cefálica) (Everts, Knape *et al.*, 2006). O sangue é coletado com anticoagulante para evitar a ativação e degranulação plaquetária (Dohan Ehrenfest, Choukroun *et al.*, 2006). Os anticoagulantes mais comumente usados são o citrato de sódio a 10% e o ácido citrato dextrose (ACD), que impedem a formação do coágulo captando e neutralizando os íons cálcio do sangue. Além disso, não alteram os receptores de membrana das plaquetas e, consequentemente, o processo pode ser revertido através da adição de cloreto de cálcio e posterior formação do gel de plaquetas (Macedo, 2004).

2.2.1.2 Centrifugação

Após a coleta do sangue total, a separação do plasma e fração leucocitária é feita por centrifugação do sangue autólogo, permitindo assim, a concentração de um grande número de plaquetas em pequenos volumes de plasma. A centrifugação ocorre por gradiente de densidade, e o plasma assim obtido contém maior concentração de plaquetas quando comparada com a contagem basal do sangue periférico. A concentração plaquetária e os fatores de crescimento são os responsáveis imediatos pelo processo cicatricial (Cole, Seroyer *et al.*, 2010).

Os vários protocolos descritos na literatura diferem no número de centrifugações e tempo de processamento. Alguns autores, dentre eles, (Anitua, 1999) sugerem protocolo com apenas uma centrifugação, enquanto outras referências utilizam dupla centrifugação (Sonnleitner, Huemer *et al.*, 2000). Alguns trabalhos têm demonstrado que com duas centrifugações obtém-se uma maior concentração de plaquetas, entretanto, com menor viabilidade e função plaquetária (Macedo, 2004).

A primeira centrifugação geralmente é mais branda e permite a separação do sangue em três camadas distintas (Figura 2.1), as células vermelhas no fundo do tubo; no topo do tubo está presente a camada de plasma, que é constituída principalmente de moléculas plasmáticas circulantes (principalmente o fibrinogênio), plaquetas e alguns leucócitos; entre essas duas camadas há uma camada intermediaria chamada *buffy coat* (BC) ou camada leucocitária, onde estão presente a maioria dos leucócitos. As plaquetas podem estar em maior ou menor concentração no BC, de acordo com a força e o tempo aplicados nesta etapa de centrifugação. Com o auxílio de uma pipeta o plasma, com ou sem a camada leucocitária são transferidas para um tubo seco sem anticoagulante (Dohan Ehrenfest, Choukroun *et al.*, 2006).

Na sequencia, é realizada uma segunda etapa de centrifugação, que geralmente usa velocidades e intervalos de tempo maiores. Assim são obtidas duas camadas distintas: o plasma pobre em plaquetas (PPP), que corresponde a cerca de 80% (em volume) do plasma um *pellet* no fundo do tubo onde estão presentes as

plaquetas, o BC e eventualmente, algumas hemácias que vieram da separação do plasma após a primeira etapa de centrifugação (Dohan Ehrenfest, Choukroun *et al.*, 2006).

2.2.1.3 Ativação plaquetária

A ativação e degranulação plaquetária é necessária para desencadear a liberação dos fatores de crescimento (Everts, Knape *et al.*, 2006). Geralmente, o processo de degranulação inicia-se 10 minutos após a exposição aos fatores da cascata de coagulação, tais como trombina, considerada como um potente ativador plaquetário capaz de induzir a liberação dos fatores de crescimento. A maioria destes fatores é liberada na primeira hora, contudo, uma liberação contínua persiste durante o período de viabilidade plaquetária (7dias) (Cole, Seroyer *et al.*, 2010).

2.2.2 Principais métodos de Preparação do PRP descritos na literatura

Os trabalhos na literatura que estudam os aspectos envolvidos na preparação do PRP geralmente usam a estratégia causa-efeito. Avaliam a composição do PRP preparado em condições específicas, a partir da variação de algumas condições. Além disso, muitos trabalhos não deixam claro como e quais condições foram utilizadas na preparação do PRP. Como são muitas as variáveis envolvidas nesse processo, cada publicação obtém um PRP com uma composição diferente.

A seguir são apresentados alguns trabalhos que focam no estudo da preparação do PRP.

Um dos estudos mais antigos da literatura que trata da preparação de concentrado de plaquetas para outras aplicações que não a regeneração tecidual, foi realizado por Kahn e colaboradores (Kahn, Cossette *et al.*, 1976). Eles estudaram experimentalmente a centrifugação de 478 mL de sangue total utilizando acelerações centrífugas no intervalo de 1600 a 4000 g, por tempos que variaram de 0,5 a 5 minutos. Os autores concluíram que quanto maior a velocidade de centrifugação e o tempo, maior é a separação, ou recuperação do plasma, atingindo um máximo de 80%. A recuperação de plaquetas aumentou com a aceleração centrífuga para

tempos até 1 minuto, atingindo o máximo de 100% à acelerações de 2300 e 3000 g, decaindo para tempos maiores em todas as acelerações. Para a segunda etapa de centrifugação, foram utilizadas acelerações centrífugas entre 2300 e 3731 g, por 4 a 12 minutos. A melhor condição encontrada foi 3731 xg por 4 minutos, onde houve recuperação de 94% das plaquetas advindas da primeira centrifugação.

Slichter e colaboradores (Slichter e Harker, 1976) estudaram a recuperação das plaquetas a partir da centrifugação de amostras contendo 250 a 450 mL de sangue total. Na primeira centrifugação, estudando seis acelerações centrífugas entre 175 e 1600 xg, por períodos entre 3 a 14 minutos, foi observado que a melhor recuperação de plaquetas, 89%, foi obtida a 1000 xg por 9 minutos. Na segunda etapa de centrifugação, foram estudadas acelerações entre 1500 e 4000 xg por 10 a 30 minutos. Os autores observaram que a integridade plaquetária começa a cair com a aplicação de acelerações centrífugas a partir de 3000 g por 20 minutos.

Landesberg et al. (2000) prepararam PRP processando 5 mL de sangue total, anticoagulado com citrato de sódio, a 100 e 200 xg por tempos entre 2 e 20 minutos na primeira etapa de centrifugação, Para a segunda centrifugação eles processaram o plasma a 100, 200, 250 e 400xg por tempos entre 2 a 10 minutos. Ao final, foram obtidos PRPs com concentrações plaquetária cerca de 3,2 vezes superior à concentração no sangue total, com um processo de 2 centrifugações à 200 xg por 10 minutos cada uma (Landesberg, Roy *et al.*, 2000).

Jo e colaboradores (2011) estudaram a preparação do PRP a partir de 9 mL de ST, utilizando acelerações centrífugas entre 500 xg e 1900 xg com incremento de 200 xg por 5 minutos, e de 100 xg a 1300 xg com incrementos de 200 xg por 10 minutos. Para a segunda etapa de centrifugação, o plasma foi submetido à acelerações e tempo de 1000 xg-15min, 1500 xg-15min, 2000 xg-5min e 3000 xg-5min, e ainda 1000 xg-10min e 1500 xg-10min. Eles observaram melhores eficiências (92%) aplicando acelerações de 900 xg por 5 minutos na primeira etapa de centrifugação. Já na segunda centrifugação, as melhores eficiências (84%) foram

conseguidas quando aplicada aceleração de 1500 xg por 15 minutos (Jo, Roh *et al*., 2011).

Bausset et al. obtiveram melhores resultados na recuperação de plaquetas (concentração plaquetária 3,47 vezes superior à concentração basal) processando 8,5 mL de ST, aplicando acelerações centrífugas de 130 xg e 250 xg por 15 minutos no processo de preparação do PRP, para a primeira e segunda centrifugações, respectivamente. No estudo da segunda etapa de centrifugação foram avaliadas diversas acelerações (130,250, 400 e 1000 xg) por 15 minutos. A integridade das plaquetas, avaliada por citometria de fluxo, através da determinação da p-selectina e por alterações morfológicas observadas por microscopia eletrônica de transmissão, começou a ser afetada após a 2ª. centrifugação a 400xg (Bausset, Giraudo *et al*., 2012).

Estudando a primeira etapa de centrifugação do ST, Araki et al. (2012) obtiveram recuperação de 70-80% das plaquetas e 10-35% de leucócitos quando aplicadas acelerações de 70 xg por 10 minutos. Ao aplicar acelerações entre 230-270 xg por 10 minutos, a recuperação de plaquetas foi semelhante, entretanto, a recuperação dos leucócitos permaneceu entre 4-6%. Na segunda etapa de centrifugação à 2300 xg por 10 minutos a recuperação das plaquetas foi cerca de 70% e s concentração plaquetária em relação à concentração basal foi cerca de 7,4 vezes após a remoção de cerca de 90% do volume de sobrenadante (plasma pobre em plaquetas), quando o EDTA foi aplicado como anticoagulante. Para o ST anticoagulado com ACD-A a eficiência de recuperação das plaquetas foi de apenas 35%. Os autores atribuem essa diferença à alterações na integridade das plaquetas promovida pelos anticoagulantes (Araki, Jona *et al*., 2012).

Franco et al obtiveram PRPs com concentração média de plaquetas cerca de 3,8 vezes superior à concentração basal, utilizando aceleração de 400 xg por 10 minutos na primeira etapa de centrifugação e 800 xg por 10 minutos na segunda etapa de centrifugação.

Muitos outros estudos (Fernandez-Barbero, Galindo-Moreno *et al.*, 2006; Su, Kuo *et al.*, 2008; Mazzocca, Mccarthy *et al.*, 2012) especificam as etapas de centrifugações em rotação por minuto (RPM) ao invés de força centrífuga relativa, sem especificar o raio da centrífuga, dificultando a comparação com outros resultados e a reprodução.

Além dos trabalhos descritos na literatura, atualmente há diversos tipos de kits para o preparo do PRP disponíveis no mercado, contendo basicamente tubos com anticoagulantes e centrífugas. Os protocolos utilizados para gerar esses concentrados de plaquetas diferem quanto à quantidade de sangue total, ao uso de anticoagulante, ao tempo e velocidade de centrifugação, ao volume final e ao número de plaquetas (Cole, Seroyer *et al.*, 2010), como mostrado na Tabela 2.1.

Table 2.1 Principais dispositivos (*kits*) disponíveis comercialmente para o preparo de PRP.

Dispositivo	Anti coagulante	No. de Centrifugações/ velocidade/tempo	Buffy coat	Ativador Plaquetário	Sangue requerido (mL)	PRP obtido (mL)	Concentração de plaquetas
GPS III (Biomet Co.)	ACD-A	1/ 1100g /15 min	Sim	Tb autóloga e $CaCl_2$ 10%	27-110	3-12	x2-x3
Cascade (MTF Musculoskeletal Tissue Foundation)	Citrato de sódio	1/ 1100g / 6 min.	Não	$CaCl_2$ 10%	9-18	4-9	x3-x8
Magellan, (Medtronic, Minneapolis)	ACD-A	1/ 1200g / 17 min.	Sim	CaCl2 10%	26	6	x3-x7
ACP-DS (Arthrex)	ACD-A	1/ 5 min / não encontrada a velocidade	Não	Não usa	9	3	x2-x3
PRGF kit (BTI Biotechnology Institute)	Citrato de sódio	1/ 460g/ 8 min	Não	$CaCl_2$ 10%	9-72	4-32	x2-x3
SmartPrep®2 (Harvest Technologies)	ACD-A	2 máximo 1000g	Sim	Tb bovina e $CaCl_2$ 10%	20-120	3-20	x4-x5

2.3 Classificação do PRP

Os principais autores da área vêm discutindo nos últimos anos a nomenclatura mais adequada para o concentrado de plaquetas, em uma tentativa de uniformização dos nomes, sem sucesso até o momento.

Dohan Ehrenfest e colaboradores (Dohan Ehrenfest, Rasmusson *et al.*, 2009) propuseram uma classificação para o Plasma Rico em Plaquetas baseada na presença ou ausência de leucócitos e na densidade da rede de fibrina, visando enquadrar os diferentes tipos de PRPs em uma de quatro categorias a seguir, o P-PRP - Plasma Rico em Plaquetas Puro, que corresponde ao PRP com baixa concentração de leucócitos como o PRGF (Plasma Rico em Fator de Crescimento) do Anitua (1999) e o Vivostat PRP (kit comercial para o preparo de PRP); o L-PRP - Plasma Rico em Plaquetas e leucócitos, um PRP com alta concentração de leucócitos, nessa classificação se enquadrariam produtos como o Curasan, Regen, Plateltex, SmartPReP, PCCS, Magellan ou GPS- PRP (todos kits comerciais disponíveis no mercado); o P-PRF- Plasma Rico em Fibrina Puro, sem leucócitos, como o Fibrinet e finalmente o L-PRF- Plasma Rico em Fibrina com leucócitos, como o PRF de Choukroun. Essa foi a tentativa mais completa, presente na literatura até o momento, de classificação dos concentrados de plaquetas.

Já, segundo Everts e colaboradores, os concentrados de plaquetas devem receber nomes distintos antes e após a ativação plaquetária. Eles defendem que o PRP, por si só, é uma substância não ativa com altas concentrações de plaquetas, plasma e leucócitos; sendo que após a sua ativação com um agonista, e subseqüente degranulação plaquetária, liberação de FC e formação da rede de fibrina, o que se tem é uma massa de gel, ou gel de plaquetas (PG-*Platelet Gel*). Assim eles denominam Plasma Rico em Plaquetas e Leucócitos (platelet-leukocyte-rich plasma P-LRP), os concentrados plaquetários não ativados, ricos em leucócitos, que após a ativação plaquetária, serão denominados Gel de plaquetas e leucócitos (platelet-leukocyte gel - PLG) (Everts, Knape *et al.*, 2006; Everts, Overdevest *et al.*, 2007).

Anitua et al. (2009) propõem o conceito do Plasma Rico em Fatores de Crescimento (PRGF – Platelet-Rich Growth Factor) para identificar um produto 100% autólogo e biocompatível, preparado utilizando uma única etapa de centrifugação, utilizando citrato de sódio e cloreto de cálcio como anticoagulante e ativador, respectivamente. A ausência de leucócitos nesse produto é justificada pelos efeitos pró-inflamatórios das proteases e hidrolases ácidas presentes nos leucócitos .

A nomenclatura defendida por Anitua (Anitua, Sanchez *et al.*, 2009) é criticada por Dohan (Dohan Ehrenfest, Rasmusson *et al.*, 2009), que menciona conflito de interesse na classificação proposta por Anitua, uma vez que a marca PRGF (Platelet Rich in Growth Factor) e suas patentes associadas são de propriedade do Dr. Anitua e do Instituto de Biotecnologia (BTI, uma companhia de implante dentário, também de propriedade do Dr. Anitua), conforme publicado no banco de dados de marcas e patentes internacionais da Organização Mundial de Propriedade Intelectual; Dohan enfatiza ainda que só poderia ser dado um nome específico ao produto de Dr. Anitua caso haja alguma evidência científica que esse produto seja diferente dos outros PRPs.

Contudo, Plasma Rico em Plaquetas ainda é um conceito excessivamente vago e controverso, que requer um termo mais preciso (Anitua, Sanchez *et al.*, 2009), sendo muito importante se chegar a um consenso para evitar confusões nesse amplo e complexo campo de pesquisa, principalmente quanto aos papéis dos leucócitos e da arquitetura da rede de fibrina (Dohan Ehrenfest, Rasmusson *et al.*, 2009).

2.4 Principais Aplicações do PRP

A seguir serão apresentadas algumas importantes aplicações do PRP, com a descrição de alguns estudos apresentados na literatura. Entretanto, aqui são apresentados apenas alguns poucos estudos uma vez que, como mencionado na Introdução deste trabalho, a quantidade de estudos clínicos com PRP é imensa, muito maior que os estudos envolvendo a sua preparação, que é o nosso campo de

interesse. Portanto, atermo-nos muito às aplicações clínicas do PRP sairia um pouco do foco deste trabalho.

2.4.1 Odontologia

O PRP vem sendo aplicado às mais diversas áreas da odontologia desde o seu surgimento na década de 1990. O primeiro resultado clínico com PRP foi reportado em 1998 por Marx et al. Eles utilizaram o PRP para melhorar a incorporação de enxertos na reconstrução mandibular após remoção do tumor, em pacientes que receberam enxertos de medula óssea trabecular. Os resultados mostraram que a adição de PRP aos enxertos aumentaram a taxa e o grau de formação óssea (Marx, Carlson *et al.*, 1998).

Anitua estudou a aplicação de PRP em pacientes nos quais a extração dentária era indicada, por doença periodontal severa ou fratura vertical. Após a extração, 10 pacientes receberam uma mistura de enxerto ósseo autólogo e PRP, enquanto o grupo controle recebeu apenas enxerto ósseo autólogo. Os resultados mostraram que aqueles que receberam PRP tiveram melhor epitelização e ossos maduros compactos (Anitua, 1999).

Vários estudos também tem demostrado o sucesso da aplicação do PRP em casos de cobertura recessão gengival (Tozum, 2003; Naik, Ramesh *et al.*, 2013).

2.4.2 Ortopedia e Traumatologia

A utilização do PRP em cirurgia ortopédica com o objetivo de acelerar a reconstrução e reparar os tecidos musculoesqueléticos vem sendo bastante estudada na literatura, com resultados bastante promissores.

2.4.2.1 Tendão

Aplicando PRP em 15 pacientes com tendinose crônica do cotovelo Mishra e Pavelko (Mishra e Pavelko, 2006) demonstraram uma melhora na dor sentida por após aplicação única. Comparando ao grupo controle, tratado com bupivacaína, foi observada a redução da dor no grupo tratado com PRP em 93% dos casos.

Em um estudo de controle de caso, Sanchez et al investigaram o efeito do PRP na ruptura do tendão de Aquiles atletas submetidos ao reparo aberto. O efeito da aplicação do PRP junto com o procedimento de reparo mostrou-se superior ao procedimento de reparo sem a aplicação do PRP. Os atletas que receberam PRP recuperaram todos os movimentos e levaram menos tempo para voltarem aos treinos (Sánchez, Anitua *et al.*, 2007).

Um estudo piloto feito por Randelli et al mostrou que o PRP foi eficaz no tratamento de reparação do manguito rotador. Os 14 pacientes que receberam PRP após o reparo da ruptura mostraram, após 24 meses mostraram redução significativa da dor e melhora dos movimentos (Randelli, Arrigoni *et al.*, 2008).

2.4.2.2 Osso

Atualmente, existem poucos estudos que investigam o papel do PRP na cicatrização óssea após o trauma ortopédico. A maioria está relacionado à cirurgia oral ou craniana.

Lowery et al (Lowery, Kulkarni *et al.*, 1999) utilizaram PRP combinado com enxerto ósseo autólogo durante a fusão espinhal com a obtenção de união em todos os seus pacientes.

Bielecki et al (Bielecki, Gazdzik *et al.*, 2008) estudaram a injeção percutânea de PRP rico em leucócitos em 32 pacientes com união tardia e não união óssea. No grupo com união tardia, o tempo médio em que ocorreu a união foi de 9,3 semanas após a injeção do PRP e a união foi alcançada em todos os casos. No grupo de não união, a união foi alcançada em 13 dos 20 pacientes, e o tempo médio foi de 10,3 semanas. Um fator essencial ressaltado pelos autores é que a união óssea não foi alcançada nos pacientes cuja fratura ou a a última cirurgia havia ocorrido há mais de 11 meses.

2.4.2.3 Cartilagem

O uso de fatores de crescimento para o crescimento e regeneração tecidual é proposto como uma poderosa ferramenta no tratamento de lesões de cartilagem (Blunk, Sieminski *et al.*, 2002).

Kon et al (Kon, Buda *et al.*, 2010) estudando o tratamento da doença articular degenerativa do joelho com injeção de PRP autólogo observaram que o tratamento foi capaz de reduzir a dor, melhorar as funções do joelho e a qualidade de vida.

Em um estudo de caso reportado por Sanchez (Sanchez, Azofra *et al.*, 2003) , um atleta com lesão na cartilagem articular do joelho foi submetido a uma artroscopia associada à injeção de PRP, resultando em aceleração da cicatrização e completa recuperação funcional.

2.4.2.4 Feridas

A cicatrização normal de feridas requer boa circulação, nutrição, estado imunológico e ausência de forças mecânicas negativas. O processo geralmente leva de 3 a 14 dias e compreende três fases: inflamação, proliferação e remodelamento com contração da ferida. Uma ferida crônica é definida como uma abertura na pele de longa duração (mais do que semanas) ou frequentemente recorrente (Fonder, Lazarus *et al.*, 2008).

No inicio da década de 90, fatores de crescimento derivados de plaquetas foram utilizados para cicatrização de ulcerações neuropáticas em pés diabéticos, mostrando-se mais eficiente quando comparado às terapias tradicionais, sendo capaz de promover a regulação da cicatrização através da formação de tecido de granulação na fase inicial da cicatrização (Margolis, Kantor *et al.*, 2001).

Driver et al (Driver, Hanft et al., 2006) em estudo clínico, duplo cego, randomizado, controlado conduzido sob a supervisão da FDA (*Food and Drugs Administration*) avaliaram o efeito do gel de PRP no tratamento de úlceras em pés diabéticos. A aplicação do PRP foi comparada ao controle, tratado com salina. Cerca

de 81,3% das feridas tratadas com PRP foram completamente curadas, contra 42,1% das tratadas com salina. A diferença no tempo de cicatrização entre os dois grupos também foi altamente significativa, cerca de 28 dias.

2.5 Incorporação do PRP em matrizes

O crescimento de novos tecidos, tanto *in vivo* durante o desenvolvimento ou *in vitro* para aplicações em engenharia tecidual é um processo complexo que requer a interação entre células, matriz extracelular tridimensional, forças mecânicas e inúmeras proteínas sinalizadoras, como os fatores de crescimento (Kobsa e Saltzman, 2008).

Como visto na seção 2.1.5, os FCs exercem um papel crucial, acelerando a proliferação e a diferenciação celular de células recrutadas ou implantadas e promove a regeneração de tecidos e órgãos que não cicatrizariam sem essas substâncias.

Os fatores de crescimento exógenos, naturais ou recombinantes, aceleram a cicatrização normal. Entretanto, eles ainda não são muito utilizados devido ao alto custo, a potencial resposta imunogênica, e também por que muitos poucos estão disponíveis para uso clínico (Sawamura, Ikeda et al., 2009; Ito, Morimoto et al., 2013; Shuko Suzuki, 2013). Além disso, a injeção de FCs exógenos, na sua forma solúvel, não é efetiva pelo seu baixo tempo de meia-vida, devido à proteólise e devido à sua rápida dispersão no local de injeção (Tabata, 2003; Ito, Morimoto et al., 2013).

O PRP surge como uma alternativa como fonte de FCs, com as vantagens de ser natural, autólogo e apresentar uma mistura de FCs e outras substâncias bioativas em proporções fisiológicas.

Entretanto, os FCs derivados do PRP são liberados praticamente na primeira hora após a ativação plaquetária, nos processos convencionais de preparo do PRP (Cole, Seroyer *et al.*, 2010). Por outro lado, o processo de regeneração tecidual, requer que a liberação dos FCs ocorra como em uma cascata fisiológica, de acordo

com as exigências do tecido a ser reparado (Hokugo, Sawada *et al.*, 2007; Rossi, Faccendini *et al.*, 2013).

Para contornar as dificuldades de espalhamento, instabilidade e liberação rápida dos FCs, aumentando a sua biodisponibilidade e aumentando seu potencial de cicatrização e regeneração tecidual muitos estudos na literatura tem investigado a incorporação do PRP em matrizes poliméricas.

Tabata, 2003, no seu trabalho de revisão sobre regeneração tecidual baseado na liberação de fatores de crescimento, recomenda a utilização de sistemas carreadores para a proteção dos FCs contra proteólise e prolongamento da sua atividade in vivo. O carreador deve ser biodegradável, e capaz de proporcionar um ambiente adequado para a indução da regeneração de tecidos, combinando assim as funções de *scaffold* e tecnologia de liberação controlada (Tabata, 2003).

A seguir serão descritos alguns estudos na literatura que visam à incorporação do PRP em diferentes tipos de matrizes como gelatina, colágeno, alginato, dentre outas.

Hokugo e colaboradores (2007) prepararam um hidrogel de gelatina reticulado com glutaraldeído, incorporando PRP. Quando em contato com a gelatina, os fatores de crescimento são liberados do PRP e imobilizados no hidrogel através de interações físico-químicas com as moléculas de gelatina, e posteriormente liberados para o meio externo com a degradação do hidrogel. Nesse trabalho promoveu-se um defeito ósseo em coelhos, que em seguida foram tratados com (i) hidrogel de gelatina incorporando PRP, (ii) PRP livre e (iii) hidrogel de gelatina vazio. Através de exames radiográficos, feitos quatro semanas após a aplicação desses materiais, atribuindo-se a maior velocidade de regeneração ao hidrogel de gelatina incorporando PRP, devido à liberação controlada dos FCs derivados do PRP (Hokugo, Sawada *et al.*, 2007).

Investigando se a adição de diferentes concentrações de trombina a um gel de colágeno-PRP alteraria as propriedades mecânicas deste gel ou a migração e

proliferação celular ou a produção de colágeno por células de fibroblastos humanos, Murray (2006) concluiu que maiores concentrações de trombina (42 U/mL) promoveram a diminuição significativa da força do gel e a menor taxa de migração das células, enquanto nos géis controle (sem trombina) e com baixa concentração de trombina (10,5 U/mL), observou-se a máxima distância de migração das células com o tempo (Murray, Forsythe *et al.*, 2006).

Lu e colaboradores (2008) estudaram a liberação controlada de FCs derivados do PRP, utilizando cápsulas e partículas de alginato de sódio reticuladas com cálcio como carreadores. Os resultados mostraram que a liberação dos FCs para o meio externo depende do tipo de carreador e das interações entre os FCs e a matriz de alginato. As repostas celulares também variaram de acordo com o tipo de carreador utilizado. Maior proliferação celular foi quantificada no terceiro dia em cultura de osteoblastos contendo as partículas de alginato + PRP, enquanto uma resposta similar foi encontrada para as cápsulas de alginato + PRP, somente no décimo quarto dia (Lu, Vo *et al.*, 2008).

Considerando o papel das plaquetas na liberação dos FCs, e a importância do arcabouço tridimensional dos *scaffolds* na diferenciação e proliferação celular, Moroz et al., 2009, estudaram a possibilidade de uso de PRP como um arcabouço 3D em forma de gel, como sistema de cultura de células. Os géis foram preparados na geometria esférica e plana utilizando PRP, gluconato de cálcio e concentrações variadas de trombina. O estudo ainda preliminar, apresentou resultados promissores e representou uma inovação na tecnologia de produção de *scaffolds* 3D para cultura celular, por usar as próprias plaquetas diretamente no suporte mecânico às células (Moroz, Bittencourt *et al.*, 2009).

Abreu e colaboradores avaliaram a influência da densidade de colágeno na formação de um hidrogel de colágeno + PRP. Para isso eles estudaram géis formados com diferentes concentrações de colágeno: 2, 3 e 4 mg/mL. Eles notaram que os parâmetros G' e G'' dos géis foram diretamente proporcionais à concentração de colágeno enquanto o tempo de formação do gel foi inversamente proporcional.

Porém, o perfil de liberação para o fator de crescimento PDGF-AB não foi afetado pela concentração de colágeno, sendo que a maior parte dos FCs foi liberada nas primeiras 12 horas. Além disso, eles estudaram a proliferação de fibroblastos e a retração dos géis. Notou-se que, apesar de os géis formados com maiores concentrações de colágeno serem mais rígidos, a proliferação de fibroblastos foi maior no hiddrogel formado com a menor concentração de colágeno (Abreu, Palmer *et al.*, 2010).

Em um estudo recente, um extrato rico em fator de crescimento, proveniente de uma preparação de PRF (Plasma Rico em Fibrina) foi incorporado em uma solução de gelatina, que em seguida foi reticulada com glutaraldeído. Os hidrogéis de gelatina formados foram capazes de reter os fatores de crescimento, liberando-os ao longo de um longo período de tempo. Além disso, este gel foi responsável por promover angiogênese, formação de tecido de granulação e reparação total de defeito na pele (Shuko Suzuki, 2013).

Scaffolds de gelatina/colágeno reticulados com glutaraldeído foram incorporados à lisados de plaquetas (PL) com o objetivo de promover o crescimento de tecido epidérmico. As plaquetas foram lisadas por processo de congelamento e descongelamento. Os PLs foram liofilizados e em seguida reconstituídos com ¼ de solução salina correspondente ao seu volume original, para produzir PLs concentrado 4 x, que na sequencia foram diluídos para formarem lisados concentrados 3x, 2x e 1x . A concentração de fatores de crescimento foi diretamente proporcional à concentração dos PLs. Os resultados mostraram que os *scaffolds* de colágeno/gelatina podm liberar os fatores de crescimento de uma maneira sustentada e, além disso, mostraram que a formação do tecido epidérmico foi mais acelerada com a aplicação dos *scaffolds* nos quais foram incorporados os PLs concentrados 2x (Ito, Morimoto *et al.*, 2013). Esse resultado indica que altas concentrações de fatores de crescimento nem sempre é sinônimo de melhor cicatrização.

A quitosana (CS) e o ácido hialurônico (AH) também tem sido estudados como matrizes para a incorporação de fatores de crescimento derivados do PRP. Três tipos de *scaffolds* em forma de esponjas foram preparados utilizando a Glicina (Gly) como crioprotetor: CS-GLY; HA-GLY e CS-GLY-Glicerofosfato (GP), através da mistura desses componentes com lisado de plaquetas e posterior congelamento e liofilização. O crescimento de fibroblastos foi avaliado em cada gel e foi comparável àqueles que continham o lisado de plaquetas fresco. (Rossi, Faccendini *et al.*, 2013)

2.5.1 Ácido Hialurônico (AH)

O ácido hialurônico (HA) é um glicosaminoglicano de alta massa molar, não ramificado, composto por repetidas unidades dissacarídicas (β1-3D-N-acetilglicosamina, β1-4 D-ácido glucurônico) (Hardingham, 2004).

O AH é o principal glicosaminoglicano encontrado na matriz extracelular dos mamíferos (West e Kumar, 1989) e possui propriedades físico-químicas como: viscosidade, elasticidade, lubrificação e alta capacidade de se ligar água. Exerce também importante papel no metabolismo celular, através de seus receptores CD44 and RHAMM, influenciam na mobilidade, proliferação e diferenciação celular e na produção de substâncias celulares fisiológicas. Portanto, as aplicações médicas do AH podem se dar pelas suas propriedades físico-químicas, pelas suas funções biológicas ou ambas (Asari, 2004).

Até aonde nós sabemos, não encontramos estudos na literatura que analisem o perfil de liberação de fatores de crescimento derivados do PRP a partir de matrizes de AH. A maioria dos estudos com AH e PRP são estudos clínicos que comparam a ação do PRP com a do AH, mostrando a superioridade do tratamento com PRP (Kon, Mandelbaum *et al.*, 2011; Cerza, Carnì *et al.*, 2012; Spaková, Rosocha *et al.*, 2012), mas alguns deles como o trabalho reportado por Filardo (Filardo, Kon et al., 2012), mostram que o PRP não oferece melhores resultados em comparação com AH para pacientes de meia-idade com sinais moderados de osteoartrite.

Devido à sua biocompatibilidade, propriedades físicas atrativas e possibilidade de modificações químicas na sua molécula, AH é um polissacarídeo bastante estudado para o desenvolvimento de sistemas de liberação para aplicação em engenharia tecidual. Entretanto, o AH não modificado em solução aquosa apresenta propriedades mecânicas pobres. Portanto, o AH requer estabilização física e/ou química para se tornar adequado para o carreamento de proteínas. Os grupos carboxílico e hidroxílico são os principais grupos funcionais que podem ser modificados quimicamente na molécula de AH.

No presente trabalho o ácido hialurônico, através de seu grupo hidroxílico foi reticulado quimicamente com divinilsulfona (DVS) para a preparação dos géis. A preparação desses géis foi desenvolvida e implementada em nosso grupo de pesquisa por Shimojo (Shimojo, Pires *et al.*, 2012).

2.5.1.1 Principais Aplicações do Ácido Hialurônico

2.5.1.1.1 Cirurgia de catarata

O AH é um dos principais componentes do corpo vítreo dos olhos, sendo portanto bastante utilizados em cirurgias oftálmicas como as de catarata. AH de alta MM (1900 a 3900 KDa) são utilizados principalmente para manter espaço operativo enquanto os de baixa MM (600 a 1200 KDa) possuem maior dispersividade e são usados principalmente para proteger a camada endotelial (Liesegang, 1990).

2.5.1.1.2 Osteoartrite

A osteoartrite (OA) é uma doença degenerativa da cartilagem hialina articular que acomete principalmente indivíduos acima dos 55 anos de idade (Silva, Montandon *et al.*, 2008).

O AH é amplamente utilizado no tratamento da OA. Vários estudos demostram que o AH suprime a degeneração da cartilagem, protege a superfície da cartilagem articular, normaliza as propriedades do fluído sinovial e reduz a dor. O AH influencia as propriedades físicas como a viscoelasticidade e a lubrificação do

estroma, sendo que seu efeito é dependente da MM. AH de maior MM é recomendado para o tratamento da OA por ser mais eficaz na absorção de impactos (Asari, 2004).

2.5.1.1.3 Drug Delivery

O ácido hialurônico em gel para o carreamento de ativos foi usado pela primeira vez no início dos anos 80 após o desenvolvimento do Hyaln B . O Hylan B é um derivado de AH reticulado com divinilsulfona, que produz um gel viscoelástico, insolúvel em água, altamente hidratado (> 99,5% de água), mas que pode sofrer digestão enzimática com hyaluronidase. Esse gel vem sendo bastante estudado como sistema carreadores para diversos agentes farmacêuticos (Balazs, 2004).

Hylan Gel foi estudado e se mostrou eficaz como sistema carreador de fármacos antibacterianos como a gentamicina ou outros como a pilocarpina, betaxolol ou serotonina. Os ativos, incorporados à fase aquosa do gel, estendem drasticamente a taxa de liberação. (Larsen e Balazs, 1991; Meyer, Whitcomb *et al*., 1995).

A liberação controlada de FCs humanos com AH foi reportada por Meyer et al (Meyer, Whitcomb *et al*., 1995), que estudaram AHs de várias massas molares como carreadores para a liberação *in vivo* do fator estimulador de granulócitos humanos (rHG-CSF). Eles concluíram que a mistura com AH de várias viscosidades promoveu a ação sustentada desse FC, sendo que a liberação mais prolongada foi obtida com a maior concentração e com o AH de maior MM.

Prisell et al estudaram a liberação in vitro de hIGF-I a partir de AH de alta MM em diferentes concentrações. Eles também concluíram que o controle da liberação desse FC é mais efetivo quanto maior a concentração de AH (Prisell, Camber *et al*., 1992).

2.5.1.1.4 Engenharia Tecidual

O ácido hialurônico vem sendo bastante utilizando na engenharia tecidual. Durante o desenvolvimento embrionário, regeneração tecidual e a cicatrização, a matriz extracelular ao redor das células que estão migrando e proliferando é rica em AH. O AH está envolvido com a morfogênese e a organização do tecido (Asari, 2004).

Scaffolds de AH quimicamente modificados permitem a proliferação de condrócitos humanos, com a produção de colágeno tipo II e portanto vem sendo utilizados para a reparação de defeitos da cartilagem articular (Yoon, Chung *et al.*, 2011).

Queratinócitos e fibroblastos quando cultivados em *scaffolds* de AH são capazes de formar tecidos que mimetizam a derme e a epiderme, respectivamente, podendo juntos formarem uma nova pele (Hollander, Stein *et al.*, 1999; Galassi, Brun *et al.*, 2000).

AH quimicamente modificados podem ser utilizados na forma de gel, filme, esponja, que podem ser aplicados para crescimento e diferenciação de vários tipos de células e tecidos de acordo com a sua forma. Além das propriedades físico-químicas, as interações do AH com as células podem influenciar o comportamento das últimas (Hall, Wang *et al.*, 1994). Portanto, a aplicação do AH para engenharia de tecidos ou cicatrização é baseada tanto nas suas propriedades físico-químicas quanto nas suas funções biológicas celulares (Asari, 2004).

2.6 Referências Bibliográficas

ABREU, E. L.; PALMER, M. P.; MURRAY, M. M. Collagen density significantly affects the functional properties of an engineered provisional scaffold. **Journal of Biomedical Materials Research Part A,** v. 93A, n. 1, p. 150-157, 2010. ISSN 1552-4965. Disponível em: < http://dx.doi.org/10.1002/jbm.a.32508 >.

ANGEL, M. J.; SGAGLIONE, N. A.; GRANDE, D. A. Clinical applications of bioactive factors in sports medicine - Current concepts and future trends. **Sports Medicine and Arthroscopy Review,** v. 14, n. 3, p. 138-145, 2006. ISSN 1062-8592. Disponível em: < <Go to ISI>://000247022000005 >.

ANITUA, E. Plasma rich in growth factors: preliminary results of use in the preparation of future sites for implants. **Int J Oral Maxillofac Implants,** v. 14, n. 4, p. 529-35, Jul-Aug 1999. ISSN 0882-2786 (Print)0882-2786 (Linking). Disponível em: < http://dx.doi.org/ >.

ANITUA, E. et al. Platelet-released growth factors enhance the secretion of hyaluronic acid and induce hepatocyte growth factor production by synovial fibroblasts from arthritic patients. **Rheumatology (Oxford),** v. 46, n. 12, p. 1769-72, 2007. ISSN 1462-0332 (Electronic)1462-0324 (Linking). Disponível em: < http://dx.doi.org/10.1093/rheumatology/kem234 >.

ANITUA, E. et al. Shedding light in the controversial terminology for platelet rich products. **Journal of Biomedical Materials Research Part A,** v. 90, n. 4, p. 1262, 2009. ISSN 1549-3296.

ARAKI, J. et al. Optimized preparation method of platelet-concentrated plasma and noncoagulating platelet-derived factor concentrates: maximization of platelet concentration and removal of fibrinogen. **Tissue Eng Part C Methods,** v. 18, n. 3, p. 176-85, Mar 2012. ISSN 1937-3392 (Electronic)1937-3384 (Linking). Disponível em: < http://dx.doi.org/10.1089/ten.TEC.2011.0308 >.

ASARI, A. Chapter 21 - Medical Application of Hyaluronan. In: HARI, G. G.;PH.D*, et al* (Ed.). **Chemistry and Biology of Hyaluronan**. Oxford: Elsevier Science Ltd, 2004. p.457-473. ISBN 978-0-08-044382-9.

BALAZS, E. A. Chapter 20 - Viscoelastic Properties of Hyaluronan and Its Therapeutic Use. In: HARI, G. G.;PH.D*, et al* (Ed.). **Chemistry and Biology of Hyaluronan**. Oxford: Elsevier Science Ltd, 2004. p.415-455. ISBN 978-0-08-044382-9.

BARNES, G. L. et al. Growth factor regulation of fracture repair. **Journal of Bone and Mineral Research,** v. 14, n. 11, p. 1805-1815, 1999. ISSN 1523-4681.

BAUSSET, O. et al. Formulation and Storage of Platelet-Rich Plasma Homemade Product. 2012-07-18 2012. Disponível em: < http://online.liebertpub.com/doi/abs/10.1089/biores.2012.0225 >.

BEVILACQUA, M. P. Endothelial-leukocyte adhesion molecules. **Annu Rev Immunol,** v. 11, p. 767-804, 1993. ISSN 0732-0582 (Print) 0732-0582 (Linking).

BIELECKI, T.; GAZDZIK, T.; SZCZEPANSKI, T. Benefit of percutaneous injection of autologous platelet-leukocyte-rich gel in patients with delayed union and nonunion. **European Surgical Research,** v. 40, n. 3, p. 289-296, 2008. ISSN 1421-9921.

BLANN, A. D.; LIP, G. Y. Hypothesis: is soluble P-selectin a new marker of platelet activation? **Atherosclerosis,** v. 128, n. 2, p. 135-8, Feb 10 1997. ISSN 0021-9150 (Print) 0021-9150 (Linking).

BLOMBACK, B. et al. Native fibrin gel networks observed by 3D microscopy, permeation and turbidity. **Biochim Biophys Acta,** v. 997, n. 1-2, p. 96-110, 1989. ISSN 0006-3002 (Print)0006-3002 (Linking). Disponível em: < http://dx.doi.org/ >.

BLUNK, T. et al. Differential effects of growth factors on tissue-engineered cartilage. **Tissue engineering,** v. 8, n. 1, p. 73-84, 2002. ISSN 1076-3279.

BONFANTI, R. et al. PADGEM (GMP140) is a component of Weibel-Palade bodies of human endothelial cells. **Blood,** v. 73, n. 5, p. 1109-12, Apr 1989. ISSN 0006-4971 (Print) 0006-4971 (Linking).

BRASS, L. F.; BENSUSAN, H. B. The role of collagen quaternary structure in the platelet: collagen interaction. **Journal of clinical investigation,** v. 54, n. 6, p. 1480, 1974.

CARR, M. E. Patent US5118182 - Method for determining fibrin fiber size from a single gel optical density measurement 1990.

CARR, M. E.; GABRIEL, D. A. Dextran-Induced Changes in Fibrin Fiber Size and Density Based on Wavelength Dependence of Gel Turbidity. May 1, 2002 1980. Disponível em: < http://pubs.acs.org/doi/abs/10.1021/ma60078a022 >.

CARR, M. E.; HERMANS, J. Size and Density of Fibrin Fibers from Turbidity. May 1, 2002 1978. Disponível em: < http://pubs.acs.org/doi/abs/10.1021/ma60061a009 >.

CARR, M. E., JR.; GABRIEL, D. A.; MCDONAGH, J. Influence of Ca2+ on the structure of reptilase-derived and thrombin-derived fibrin gels. **Biochem J,** v. 239, n. 3, p. 513-6, Nov 1 1986. ISSN 0264-6021 (Print)0264-6021 (Linking). Disponível em: < http://dx.doi.org/ >.

CERVELLI, V. et al. Application of platelet-rich plasma in plastic surgery: clinical and in vitro evaluation. **Tissue Eng Part C Methods,** v. 15, n. 4, p. 625-34, Dec 2009. ISSN 1937-3392 (Electronic)1937-3384 (Linking). Disponível em: < http://dx.doi.org/10.1089/ten.TEC.2008.0518 >.

CERZA, F. et al. Comparison between hyaluronic acid and platelet-rich plasma, intra-articular infiltration in the treatment of gonarthrosis. **The American journal of sports medicine,** v. 40, n. 12, p. 2822-2827, 2012. ISSN 0363-5465.

CHONG, B. et al. Plasma P-selectin is increased in thrombotic consumptive platelet disorders. **Blood,** v. 83, n. 6, p. 1535-1541, March 15, 1994 1994. Disponível em: < http://bloodjournal.hematologylibrary.org/content/83/6/1535.abstract >.

CHOW, T. W. et al. Shear stress-induced von Willebrand factor binding to platelet glycoprotein Ib initiates calcium influx associated with aggregation. **Blood,** v. 80, n. 1, p. 113-120, 1992. ISSN 0006-4971.

CIESLIK-BIELECKA, A. et al. Autologous platelets and leukocytes can improve healing of infected high-energy soft tissue injury. In: (Ed.). **Transfus Apher Sci**. England, v.41, 2009. p.9-12. ISBN 1473-0502 (Print)1473-0502 (Linking).

CLEMETSON, K. Platelet activation: signal transduction via membrane receptors. **Thrombosis and haemostasis,** v. 74, n. 1, p. 111, 1995. ISSN 0340-6245.

COLE, B. J. et al. Platelet-Rich Plasma: Where Are We Now and Where Are We Going? **Sports Health: A Multidisciplinary Approach,** v. 2, n. 3, p. 203-210, May/June 2010 2010. Disponível em: < http://sph.sagepub.com/content/2/3/203.abstract >.

DALLARI, D. et al. Enhanced tibial osteotomy healing with use of bone grafts supplemented with platelet gel or platelet gel and bone marrow stromal cells. In: (Ed.). **J Bone Joint Surg Am**. United States, v.89, 2007. p.2413-20. ISBN 1535-1386 (Electronic).

DAVIS, H. E. et al. Supplementation of fibrin gels with sodium chloride enhances physical properties and ensuing osteogenic response. **Acta Biomater,** v. 7, n. 2, p. 691-9, 2011. ISSN 1878-7568 (Electronic)1742-7061 (Linking). Disponível em: < http://dx.doi.org/10.1016/j.actbio.2010.09.007 >.

DOHAN EHRENFEST, D. M. et al. Do the fibrin architecture and leukocyte content influence the growth factor release of platelet concentrates? An evidence-based answer comparing a pure platelet-rich plasma (P-PRP) gel and a leukocyte-

and platelet-rich fibrin (L-PRF). **Curr Pharm Biotechnol,** v. 13, n. 7, p. 1145-52, Jun 2012. ISSN 1873-4316 (Electronic) 1389-2010 (Linking).

DOHAN EHRENFEST, D. M. et al. Platelet-rich fibrin (PRF): A second-generation platelet concentrate. Part I: Technological concepts and evolution. **Oral surgery, oral medicine, oral pathology, oral radiology, and endodontics,** v. 101, n. 3, p. e37-e44, 2006. ISSN 1079-2104. Disponível em: < http://linkinghub.elsevier.com/retrieve/pii/S107921040500586X?showall=true >.

DOHAN EHRENFEST, D. M.; RASMUSSON, L.; ALBREKTSSON, T. Classification of platelet concentrates: from pure platelet-rich plasma (P-PRP) to leucocyte- and platelet-rich fibrin (L-PRF). **Trends Biotechnol,** v. 27, n. 3, p. 158-67, 2009. ISSN 0167-7799 (Print)0167-7799 (Linking). Disponível em: < http://dx.doi.org/10.1016/j.tibtech.2008.11.009 >.

DONG, J.-F.; LI, C. Q.; LOPEZ, J. A. Tyrosine sulfation of the glycoprotein Ib-IX complex: identification of sulfated residues and effect on ligand binding. **Biochemistry,** v. 33, n. 46, p. 13946-13953, 1994. ISSN 0006-2960.

DRIVER, V. R. et al. A prospective, randomized, controlled trial of autologous platelet-rich plasma gel for the treatment of diabetic foot ulcers. **Ostomy wound management,** v. 52, n. 6, p. 68, 2006. ISSN 0889-5899.

ENGEBRETSEN, L. et al. IOC consensus paper on the use of platelet-rich plasma in sports medicine. **Br J Sports Med,** v. 44, n. 15, p. 1072-81, 2010. ISSN 1473-0480 (Electronic)0306-3674 (Linking). Disponível em: < http://dx.doi.org/10.1136/bjsm.2010.079822 >.

EVERTS, P. A. et al. Platelet gel and fibrin sealant reduce allogeneic blood transfusions in total knee arthroplasty. **Acta Anaesthesiol Scand,** v. 50, n. 5, p. 593-9, 2006. ISSN 0001-5172 (Print)0001-5172 (Linking). Disponível em: < http://dx.doi.org/10.1111/j.1399-6576.2006.001005.x >.

EVERTS, P. A. et al. Platelet-rich plasma and platelet gel: a review. **J Extra Corpor Technol,** v. 38, n. 2, p. 174-87, Jun 2006. ISSN 0022-1058 (Print)0022-1058 (Linking). Disponível em: < http://dx.doi.org/ >.

EVERTS, P. A. et al. The use of autologous platelet-leukocyte gels to enhance the healing process in surgery, a review. **Surg Endosc,** v. 21, n. 11, p. 2063-8, Nov 2007. ISSN 1432-2218 (Electronic)0930-2794 (Linking). Disponível em: < http://dx.doi.org/10.1007/s00464-007-9293-x >.

FALVO, M. R.; GORKUN, O. V.; LORD, S. T. The molecular origins of the mechanical properties of fibrin. **Biophys Chem,** v. 152, n. 1-3, p. 15-20, 2010. ISSN 1873-4200 (Electronic)0301-4622 (Linking). Disponível em: < http://dx.doi.org/10.1016/j.bpc.2010.08.009 >.

FERNANDEZ-BARBERO, J. E. et al. Flow cytometric and morphological characterization of platelet-rich plasma gel. In: (Ed.). **Clin Oral Implants Res**. Denmark, v.17, 2006. p.687-93. ISBN 0905-7161 (Print)0905-7161 (Linking).

FERRI, F. et al. Growth kinetics and structure of fibrin gels. **Physical Review E,** v. 63, n. 3, p. 031401, 2001. Disponível em: < http://link.aps.org/doi/10.1103/PhysRevE.63.031401 >.

FERRI, F. et al. Structure of fibrin gels studied by elastic light scattering techniques: Dependence of fractal dimension, gel crossover length, fiber diameter, and fiber density on monomer concentration. **Physical Review E,** v. 66, n. 1, p. 011913, 2002. Disponível em: < http://link.aps.org/doi/10.1103/PhysRevE.66.011913 >.

FERRONI, P. et al. Soluble P-selectin as a marker of in vivo platelet activation. **Clinica Chimica Acta,** v. 399, n. 1–2, p. 88-91, 2009. ISSN 0009-8981. Disponível em: < http://www.sciencedirect.com/science/article/pii/S0009898108004713 >.

FERRY, J. D.; MORRISON, P. R. Preparation and Properties of Serum and Plasma Proteins. VIII. The Conversion of Human Fibrinogen to Fibrin under Various Conditions1,2. **Journal of the American Chemical Society,** v. 69, n. 2, p. 388-400, 1947/02/01 1947. ISSN 0002-7863. Disponível em: < http://dx.doi.org/10.1021/ja01194a066 >. Acesso em: 2012/11/14.

FILARDO, G. et al. Platelet-rich plasma intra-articular injections for cartilage degeneration and osteoarthritis: single- versus double-spinning approach. **Knee Surg Sports Traumatol Arthrosc,** v. 20, n. 10, p. 2078-87, Oct 2012. ISSN 1433-7347 (Electronic)0942-2056 (Linking). Disponível em: < http://dx.doi.org/10.1007/s00167-011-1837-x >.

FONDER, M. A. et al. Treating the chronic wound: a practical approach to the care of nonhealing wounds and wound care dressings. **Journal of the American Academy of Dermatology,** v. 58, n. 2, p. 185-206, 2008. ISSN 0190-9622.

GALASSI, G. et al. In vitro reconstructed dermis implanted in human wounds: degradation studies of the HA-based supporting scaffold. **Biomaterials,** v. 21, n. 21, p. 2183-2191, 2000. ISSN 0142-9612.

GENTILE, P. et al. Application of platelet-rich plasma in maxillofacial surgery: clinical evaluation. In: (Ed.). **J Craniofac Surg**. United States, v.21, 2010. p.900-4. ISBN 1536-3732 (Electronic)1049-2275 (Linking).

GIBBLE, J. W.; NESS, P. M. Fibrin glue: the perfect operative sealant? **Transfusion,** v. 30, n. 8, p. 741-747, 1990. ISSN 1537-2995. Disponível em: < http://dx.doi.org/10.1046/j.1537-2995.1990.30891020337.x >.

GRESELE, P. **Platelets in Thrombotic and Non-thrombotic Disorders : Pathophysiology, Pharmacology and Therapeutics**. Port Chester, NY, USA: Cambridge University Press; 1 edition (July 8, 2002), 2002. 1124.

HALL, C. L. et al. Hyaluronan and the hyaluronan receptor RHAMM promote focal adhesion turnover and transient tyrosine kinase activity. **The Journal of cell biology,** v. 126, n. 2, p. 575-588, 1994. ISSN 0021-9525.

HAMMOND, J. W. et al. Use of autologous platelet-rich plasma to treat muscle strain injuries. In: (Ed.). **Am J Sports Med**. United States, v.37, 2009. p.1135-42. ISBN 1552-3365 (Electronic)0363-5465 (Linking).

HARDINGHAM, T. Chapter 1 - Solution Properties of Hyaluronan. In: HARI, G. G.;PH.D*, et al* (Ed.). **Chemistry and Biology of Hyaluronan**. Oxford: Elsevier Science Ltd, 2004. p.1-19. ISBN 978-0-08-044382-9.

HARDWICK, R. et al. The effect of PGI2 and theophylline on the response of platelets subjected to shear stress. **Blood,** v. 58, n. 4, p. 678-681, 1981. ISSN 0006-4971.

HARRISON, P.; CRAMER, E. M. Platelet alpha-granules. **Blood Rev,** v. 7, n. 1, p. 52-62, Mar 1993. ISSN 0268-960X (Print)0268-960X (Linking). Disponível em: < http://dx.doi.org/ >.

HARRISON, S. et al. Platelet Activation by Collagen Provides Sustained Release of Anabolic Cytokines. 2011-04-01 2011. Disponível em: < http://ajs.sagepub.com/content/39/4/729.short >.

HARTWIG, J. H. et al. The elegant platelet: signals controlling actin assembly. **Thromb Haemost,** v. 82, n. 2, p. 392-8, Aug 1999. ISSN 0340-6245 (Print) 0340-6245 (Linking).

HELDIN, C.-H.; WESTERMARK, B. Mechanism of action and in vivo role of platelet-derived growth factor. **Physiological reviews,** v. 79, n. 4, p. 1283-1316, 1999. ISSN 0031-9333.

HOKUGO, A. et al. Controlled release of platelet growth factors enhances bone regeneration at rabbit calvaria. **Oral Surgery, Oral Medicine, Oral Pathology, Oral Radiology, and Endodontology,** v. 104, n. 1, p. 44-48, 2007. ISSN 1079-

2104. Disponível em: < http://www.sciencedirect.com/science/article/pii/S107921040600936X >.

HOLLANDER, D. et al. Autologous keratinocytes cultured on benzylester hyaluronic acid membranes in the treatment of chronic full-thickness ulcers. **Journal of wound care,** v. 8, n. 7, p. 351-355, 1999. ISSN 0969-0700.

ITO, R. et al. Efficacy of the Controlled Release of Concentrated Platelet Lysate from a Collagen/Gelatin Scaffold for Dermis-Like Tissue Regeneration. **Tissue Engineering**, n. ja, 2013. ISSN 1937-3341.

JACKSON, S. P. The growing complexity of platelet aggregation. **Blood,** v. 109, n. 12, p. 5087-5095, 2007. Disponível em: < http://europepmc.org/abstract/MED/17311994 >.

JANMEY, P. A.; WINER, J. P.; WEISEL, J. W. Fibrin gels and their clinical and bioengineering applications. **Journal of the Royal Society, Interface / the Royal Society,** v. 6, n. 30, p. 1-10, 2009. Disponível em: < http://europepmc.org/abstract/MED/18801715 >.

JANSSENS, K. et al. Transforming growth factor-β1 to the bone. **Endocrine reviews,** v. 26, n. 6, p. 743-774, 2005. ISSN 0163-769X.

JO, C. H. et al. Optimizing Platelet-Rich Plasma Gel Formation by Varying Time and Gravitational Forces During Centrifugation. **http://dx.doi.org/10.1563/AAID-JOI-D-10-00155**, 2011-04-11 2011. Disponível em: < http://www.joionline.org/doi/abs/10.1563/AAID-JOI-D-10-00155?journalCode=orim >.

JOSHI, S. M. et al. Collagen-platelet composite enhances biomechanical and histologic healing of the porcine anterior cruciate ligament. **The American journal of sports medicine,** v. 37, n. 12, p. 2401-2410, 2009. ISSN 0363-5465.

KAHN, R. A.; COSSETTE, I.; FRIEDMAN, L. I. Optimum centrifugation conditions for the preparation of platelet and plasma products. **Transfusion,** v. 16, n.

2, p. 162-5, Mar-Apr 1976. ISSN 0041-1132 (Print)0041-1132 (Linking). Disponível em: < http://dx.doi.org/ >.

KOBSA, S.; SALTZMAN, W. M. Bioengineering approaches to controlled protein delivery. **Pediatric research,** v. 63, n. 5, p. 513-519, 2008. ISSN 0031-3998.

KON, E. et al. Platelet-rich plasma: intra-articular knee injections produced favorable results on degenerative cartilage lesions. **Knee Surgery, Sports Traumatology, Arthroscopy,** v. 18, n. 4, p. 472-479, 2010. ISSN 0942-2056.

KON, E. et al. Platelet-rich plasma intra-articular injection versus hyaluronic acid viscosupplementation as treatments for cartilage pathology: from early degeneration to osteoarthritis. **Arthroscopy: The Journal of Arthroscopic & Related Surgery,** v. 27, n. 11, p. 1490-1501, 2011. ISSN 0749-8063.

LAMALICE, L.; LE BOEUF, F.; HUOT, J. Endothelial cell migration during angiogenesis. **Circulation research,** v. 100, n. 6, p. 782-794, 2007. ISSN 0009-7330.

LANDESBERG, R.; ROY, M.; GLICKMAN, R. S. Quantification of growth factor levels using a simplified method of platelet-rich plasma gel preparation. **Journal of Oral and Maxillofacial Surgery,** v. 58, n. 3, p. 297-300, 2000. ISSN 0278-2391. Disponível em: < http://www.sciencedirect.com/science/article/pii/S0278239100900582 >.

LARSEN, N. E.; BALAZS, E. A. Drug delivery systems using hyaluronan and its derivatives. **Advanced drug delivery reviews,** v. 7, n. 2, p. 279-293, 1991. ISSN 0169-409X.

LEE, K.; SILVA, E. A.; MOONEY, D. J. Growth factor delivery-based tissue engineering: general approaches and a review of recent developments. **Journal of The Royal Society Interface,** v. 8, n. 55, p. 153-170, 2011. ISSN 1742-5689.

LIEBERMAN, J. R.; DALUISKI, A.; EINHORN, T. A. The role of growth factors in the repair of bone biology and clinical applications. **The Journal of Bone & Joint Surgery,** v. 84, n. 6, p. 1032-1044, 2002. ISSN 0021-9355.

LIESEGANG, T. J. Viscoelastic substances in ophthalmology. **Survey of ophthalmology,** v. 34, n. 4, p. 268-293, 1990. ISSN 0039-6257.

LOWERY, G.; KULKARNI, S.; PENNISI, A. Use of autologous growth factors in lumbar spinal fusion. **Bone,** v. 25, n. 2, p. 47S-50S, 1999. ISSN 8756-3282.

LU, H. H. et al. Controlled delivery of platelet-rich plasma-derived growth factors for bone formation. **Journal of Biomedical Materials Research Part A,** v. 86A, n. 4, p. 1128-1136, 2008. ISSN 1552-4965. Disponível em: < http://dx.doi.org/10.1002/jbm.a.31740 >.

LUCARELLI, E. et al. A recently developed bifacial platelet-rich fibrin matrix. **European cells & materials,** v. 20, p. 13-23, 2010. Disponível em: < http://europepmc.org/abstract/MED/20597062 >.

MACEDO, A. P. **Plasma Rico Em Plaquetas: Uma Análise Quantitativa E Qualitativa De Dois Protocolos De Obtenção**. 2004. Dissertação De Mestrado Em Odontologia, Universidade Federal De Santa Catarina, Brazil.

MARGOLIS, D. J. et al. Effectiveness of platelet releasate for the treatment of diabetic neuropathic foot ulcers. **Diabetes care,** v. 24, n. 3, p. 483-488, 2001. ISSN 0149-5992.

MARX, R. E. et al. Platelet-rich plasma: growth factor enhancement for bone grafts. **Oral Surgery, Oral Medicine, Oral Pathology, Oral Radiology, and Endodontology,** v. 85, n. 6, p. 638-646, 1998. ISSN 1079-2104.

MAZZOCCA, A. D. et al. Platelet-Rich Plasma Differs According to Preparation Method and Human Variability. **The Journal of Bone & Joint Surgery,** v. 94, n. 4, p. 308-316, 2012/02/15 2012. ISSN 0021-9355. Disponível em: < http://jbjs.org/data/Journals/JBJS/12134/308.pdf >.

MCEVER, R. P. et al. GMP-140, a platelet alpha-granule membrane protein, is also synthesized by vascular endothelial cells and is localized in Weibel-Palade bodies. **J Clin Invest,** v. 84, n. 1, p. 92-9, Jul 1989. ISSN 0021-9738 (Print) 0021-9738 (Linking).

MEYER, J. et al. Sustained in vivo activity of recombinant human granulocyte colony stimulating factor (rHG-CSF) incorporated into hyaluronan. **Journal of Controlled Release,** v. 35, n. 1, p. 67-72, 1995. ISSN 0168-3659. Disponível em: < http://www.sciencedirect.com/science/article/pii/0168365995000209 >.

MISHRA, A.; PAVELKO, T. Treatment of chronic elbow tendinosis with buffered platelet-rich plasma. **Am J Sports Med,** v. 34, n. 11, p. 1774-8, 2006. ISSN 0363-5465 (Print)0363-5465 (Linking). Disponível em: < http://dx.doi.org/10.1177/0363546506288850 >.

MOROZ, A. et al. Gel de plaquetas: arcabouço 3D para cultura celular. **Acta Ortopédica Brasileira,** v. 17, p. 43-45, 2009. ISSN 1413-7852. Disponível em: < http://www.scielo.br/scielo.php?script=sci_arttext&pid=S1413-78522009000200008&nrm=iso >.

MURRAY, M. M. et al. The effect of thrombin on ACL fibroblast interactions with collagen hydrogels. **Journal of Orthopaedic Research,** v. 24, n. 3, p. 508-515, 2006. ISSN 1554-527X. Disponível em: < http://dx.doi.org/10.1002/jor.20054 >.

NAIK, A. et al. Use of autologous platelet rich plasma to treat gingival recession in esthetic periodontal surgery. **Journal of Indian Society of Periodontology,** v. 17, n. 3, p. 345, 2013. ISSN 0972-124X.

NESBITT, W. S. et al. A shear gradient-dependent platelet aggregation mechanism drives thrombus formation. **Nat Med,** v. 15, n. 6, p. 665-673, 2009. ISSN 1078-8956. Disponível em: < http://dx.doi.org/10.1038/nm.1955 >.

PRISELL, P. T. et al. Evaluation of hyaluronan as a vehicle for peptide growth factors. **International Journal of Pharmaceutics,** v. 85, n. 1–3, p. 51-56, 1992.

ISSN 0378-5173. Disponível em: < http://www.sciencedirect.com/science/article/pii/037851739290133M >.

RANDELLI, P. S. et al. Autologous platelet rich plasma for arthroscopic rotator cuff repair. A pilot study. **Disability & Rehabilitation,** v. 30, n. 20-22, p. 1584-1589, 2008. ISSN 0963-8288.

ROSSI, S. et al. “Sponge-like” dressings based on biopolymers for the delivery of platelet lysate to skin chronic wounds. **International Journal of Pharmaceutics,** v. 440, n. 2, p. 207-215, 2013. ISSN 0378-5173. Disponível em: < http://www.sciencedirect.com/science/article/pii/S0378517312007776 >.

ROZMAN, P.; BOLTA, Z. Use of platelet growth factors in treating wounds and soft-tissue injuries. In: (Ed.). **Acta Dermatovenerol Alp Panonica Adriat**. Slovenia, v.16, 2007. p.156-65. ISBN 1318-4458 (Print)1318-4458 (Linking).

RUGGERI, Z. M.; DENT, J. A.; SALDÍVAR, E. Contribution of distinct adhesive interactions to platelet aggregation in flowing blood. **Blood,** v. 94, n. 1, p. 172-178, 1999. Disponível em: < http://europepmc.org/abstract/MED/10381510 >.

RYAN, E., MOCKROS, LF, WEISEL, JW, LORAND, L. Scientific Commons: Structural origins of fibrin clot rheology. 2010-08-11T16:09:11Z 2010. Disponível em: < http://en.scientificcommons.org/12076477 >.

SÁNCHEZ, M. et al. Comparison of surgically repaired Achilles tendon tears using platelet-rich fibrin matrices. **The American journal of sports medicine,** v. 35, n. 2, p. 245-251, 2007. ISSN 0363-5465.

SANCHEZ, M. et al. Plasma rich in growth factors to treat an articular cartilage avulsion: A case report. **Medicine and science in sports and exercise,** v. 35, n. 10, p. 1648-1652, 2003. ISSN 0195-9131.

SAVAGE, B.; ALMUS-JACOBS, F.; RUGGERI, Z. M. Specific Synergy of Multiple Substrate Receptor Interactions in Platelet Thrombus Formation under Flow.

Cell, v. 94, n. 5, p. 657-666, 1998. ISSN 0092-8674. Disponível em: < http://linkinghub.elsevier.com/retrieve/pii/S0092867400816074 >.

SAWAMURA, K. et al. Characterization of in vivo effects of platelet-rich plasma and biodegradable gelatin hydrogel microspheres on degenerated intervertebral discs. **Tissue Engineering Part A,** v. 15, n. 12, p. 3719-3727, 2009. ISSN 1937-3341.

SHAH, G. A.; NAIR, C. H.; DHALL, D. P. Comparison of fibrin networks in plasma and fibrinogen solution. **Thromb Res,** v. 45, n. 3, p. 257-64, Feb 1 1987. ISSN 0049-3848 (Print)0049-3848 (Linking). Disponível em: < http://dx.doi.org/ >.

SHAH, J. V. et al. Strain hardening of fibrin gels and plasma clots. **Rheologica Acta,** v. 36, n. 3, p. 262-268, 1997. ISSN 1435-1528. Disponível em: < http://link.springer.com/article/10.1007/BF00366667http://link.springer.com/content/pdf/10.1007/BF00366667 >.

SHIMOJO, A. A. M. et al. Influence of particle size and fluid fraction on rheological and extrusion properties of crosslinked hyaluronic acid hydrogel dispersions. **Journal of Applied Polymer Science**, 2012. ISSN 1097-4628.

SHUKO SUZUKI, N. M., YOSHITO IKADA. Gelatin gel as a carrier of platelet-derived growth factors **Journal of Biomaterials Applications,** v. 27, n. 6, 2013.

SILVA, N. A. D.; MONTANDON, A. C. D. O.; CABRAL, M. V. D. S. P. Doenças osteoarticulares degenerativas periféricas; Peripheral degenerative joint diseases. **Einstein (São Paulo),** v. 6, n. supl. 1, p. S21-S28, 2008. ISSN 1679-4508.

SLICHTER, S. J.; HARKER, L. A. Preparation and Storage of Platelet Concentrates: I. FACTORS INFLUENCING THE HARVEST OF VIABLE PLATELETS FROM WHOLE BLOOD. **British Journal of Haematology,** v. 34, n. 3, p. 395-402, 1976. ISSN 1365-2141. Disponível em: < http://dx.doi.org/10.1111/j.1365-2141.1976.tb03586.x >.

SONNLEITNER, D.; HUEMER, P.; SULLIVAN, D. Y. A simplified technique for producing platelet-rich plasma and platelet concentrate for intraoral bone grafting techniques: a technical note. **Int J Oral Maxillofac Implants,** v. 15, n. 6, p. 879-82, Nov-Dec 2000. ISSN 0882-2786 (Print) 0882-2786 (Linking).

SPAKOVÁ, T. et al. Treatment of Knee Joint Osteoarthritis with Autologous Platelet-Rich Plasma in Comparison with Hyaluronic Acid. **American Journal of Physical Medicine & Rehabilitation,** v. 91, n. 5, p. 411-417 10.1097/PHM.0b013e3182aab72, 2012. ISSN 0894-9115. Disponível em: < http://journals.lww.com/ajpmr/Fulltext/2012/05000/Treatment_of_Knee_Joint_Osteoarthritis_with.5.aspx >.

STENBERG, P. E. et al. A platelet alpha-granule membrane protein (GMP-140) is expressed on the plasma membrane after activation. **The Journal of cell biology,** v. 101, n. 3, p. 880-886, 1985. Disponível em: < http://europepmc.org/abstract/MED/2411738 >.

SU, C. Y. et al. Quantitative assessment of the kinetics of growth factors release from platelet gel. In: (Ed.). **Transfusion**. United States, v.48, 2008. p.2414-20. ISBN 1537-2995 (Electronic)0041-1132 (Linking).

TABATA, Y. Tissue regeneration based on growth factor release. **Tissue engineering,** v. 9 Suppl 1, p. S5-15, 2003. Disponível em: < http://europepmc.org/abstract/MED/14511467 >.

TOZUM, T. F. A promising periodontal procedure for the treatment of adjacent gingival recession defects. **Journal-Canadian Dental Association,** v. 69, n. 3, p. 155-159, 2003. ISSN 0709-8936.

TRIPPEL, S. B. Growth factors as therapeutic agents. **INSTRUCTIONAL COURSE LECTURES-AMERICAN ACADEMY OF ORTHOPAEDIC SURGEONS,** v. 46, p. 473-476, 1997. ISSN 0065-6895.

VESTWEBER, D.; BLANKS, J. E. Mechanisms that regulate the function of the selectins and their ligands. **Physiological reviews,** v. 79, n. 1, p. 181-213, 1999. Disponível em: < http://europepmc.org/abstract/MED/9922371 >.

WEISEL, J.; NAGASWAMI, C. Computer modeling of fibrin polymerization kinetics correlated with electron microscope and turbidity observations: clot structure and assembly are kinetically controlled. **Biophysical Journal,** v. 63, n. 1, p. 111, 1992. ISSN 0006-3495.

WEISEL, J. W. Structure of fibrin: impact on clot stability. **Journal of Thrombosis and Haemostasis,** v. 5, n. s1, p. 116-124, 2007. ISSN 1538-7836. Disponível em: < http://onlinelibrary.wiley.com/doi/10.1111/j.1538-7836.2007.02504.x/abstracthttp://onlinelibrary.wiley.com/doi/10.1111/j.1538-7836.2007.02504.x/full http://onlinelibrary.wiley.com/doi/10.1111/j.1538-7836.2007.02504.x/pdf >.

WEISEL, J. W.; NAGASWAMI, C. Computer modeling of fibrin polymerization kinetics correlated with electron microscope and turbidity observations: clot structure and assembly are kinetically controlled. 1993. Disponível em: < http://dx.doi.org/10.1016/S0006-3495(92)81594-1 >.

WEISS, H. Flow-related platelet deposition on subendothelium. **Thrombosis and haemostasis,** v. 74, n. 1, p. 117-122, 1995. ISSN 0340-6245.

WEISS, H.; TURITTO, V.; BAUMGARTNER, H. Further evidence that glycoprotein IIb-IIIa mediates platelet spreading on subendothelium. **Thrombosis and haemostasis,** v. 65, n. 2, p. 202, 1991. ISSN 0340-6245.

WEST, D. C.; KUMAR, S. The effect of hyaluronate and its oligosaccharides on endothelial cell proliferation and monolayer integrity. **Experimental Cell Research,** v. 183, n. 1, p. 179-196, 1989. ISSN 0014-4827. Disponível em: < http://www.sciencedirect.com/science/article/pii/001448278990428X >.

WHITMAN, D. H.; BERRY, R. L.; GREEN, D. M. Platelet gel: An autologous alternative to fibrin glue with applications in oral and maxillofacial surgery. **Journal of oral and maxillofacial surgery : official journal of the American Association of Oral and Maxillofacial Surgeons,** v. 55, n. 11, p. 1294-1299, 1997. ISSN 0278-2391. Disponível em: < http://linkinghub.elsevier.com/retrieve/pii/S0278239197901877?showall=true >.

WOLBERG, A. S. Thrombin generation and fibrin clot structure. **Blood Reviews,** v. 21, n. 3, p. 131-142, 2007. ISSN 0268-960X. Disponível em: < http://www.sciencedirect.com/science/article/pii/S0268960X0600066X >.

YEROMONAHOS, C.; POLACK, B.; CATON, F. Nanostructure of the FibrinClot. **Biophysical Journal** v. 99, n. 7, p. 2018-2027, 2007. Disponível em: < http://dx.doi.org/10.1016/j.bpj.2010.04.059 >.

YOON, I.-S. et al. Proliferation and chondrogenic differentiation of human adipose-derived mesenchymal stem cells in porous hyaluronic acid scaffold. **Journal of Bioscience and Bioengineering,** v. 112, n. 4, p. 402-408, 2011. ISSN 1389-1723. Disponível em: < http://www.sciencedirect.com/science/article/pii/S1389172311002593 >.

ZHAO, H. et al. Fabrication and physical and biological properties of fibrin gel derived from human plasma. **Biomed Mater**, England**,** v. 3, n. 1, p. 015001, 2008. ISSN 1748-605X (Electronic)1748-6041 (Linking). Disponível em: < http://dx.doi.org/10.1088/1748-6041/3/1/015001 >.

Capítulo 3. Relevant Aspects of Centrifugation Step in the Preparation of Platelet-Rich Plasma

Amanda G. M. Perez,[1] José Fábio. S.D. Lana,[2] Ana Amélia Rodrigues,[3] Angela Cristina M. Luzo,[4] William D. Belangero[3] and Maria Helena A. Santana[1]*.

[1]Department of Engineering of Materials and Bioprocesses - School of Chemical Engineering, University of Campinas, Campinas-SP, Brazil, Phone: 55-19-35213921, FAX: 55-19-35213890, E-mail: mariahelena.santana@gmail.com

[2]Research Institute of Sports Medicine, Orthopedics and Regeneration - iMOR, Uberaba- MG, Brazil, Phone: 55-34-33317777, Fax: 55-34-33317777, E-mail: josefabiolana@gmail.com

[3]Department of Orthopedics and Traumatology - Faculty of Medical Sciences, University of Campinas, Campinas-SP, Brazil, Phone: 55-19-35217498. E-mail: belangerowd@gmail.com

[4]Haematology and Hemotherapy Center, Umbilical Cord Blood Bank, University of Campinas, Campinas-SP, Brazil. E-mail: angela.luzo@gmail.com

*Corresponding author

Abstract: This work highlights relevant aspects of the centrifugation step of the Platelet-Rich Plasma (PRP) preparation and discusses its implications for the overall quality of the PRP. Moreover, understanding these aspects helps researchers to analyze results and select reproducible protocols. Reliable sampling and maintenance of platelet integrity during the centrifugation step are key factors in ensuring reproducible and consistent data. The effects of the volume of whole blood processed, time, centrifugal acceleration and number of spins on the composition of

PRP are illustrated and discussed in relation to the physical basis of centrifugation. The recovery efficiency of platelets and white blood cells along with the concentration factor of platelets, are essential factors in the process' performance. Finally, the performance of a centrifugation consisting of two spins was measured by observing the highlighted aspects and characterizing the composition of Pure Platelet-Rich Plasma (P-PRP). In addition, optimal operating conditions and the robustness of protocols that have been reported in other studies on centrifugation are discussed. In conclusion, despite the PRP being an autologous product, the observance of the highlighted aspects of the PRP preparation can produce reliable and consistent data and reproducible PRP compositions. Although this study highlights certain aspects of the centrifugation step of the PRP preparation, a complete understanding of this step is still required to correctly predict optimal conditions and to validate results.

Keywords: Platelet-rich plasma, blood centrifugation, centrifugation, platelet separation.

3.1 Introduction

Platelet- Rich Plasma (PRP) is an autologous preparation that concentrates platelets in a small volume of plasma [1]. Platelets are rich in growth factors, which play an important role in tissue healing. Numerous studies have demonstrated the clinical application and notable results of PRP in dentistry [2]. oral maxilla facial surgery [3], plastic surgery [4], orthopedics [5], rheumatology [6], and the treatment of different types of injuries that include chronic wounds [7, 8] and muscle injuries [9].

The wide variation in the reported protocols for obtaining PRP may lead to samples with different compositions that may induce different biological responses.[1] Despite these variations, all protocols follow a generic sequence that consists of blood collection, an initial centrifugation to separate red blood cells (RBC), subsequent centrifugations to concentrate platelets and other components and an activation of the sample by adding a platelet agonist, as summarized in Figure 3.1. Prior to the platelet activation step, variables in the process that may influence the platelet integrity along with the composition and effectiveness of the PRP include the

initial volume of collected whole blood (WB), number of spins, centrifugal accelerations, time period of centrifugation and selection of anticoagulant and agonist [10]. In addition to the platelets, the white blood cells (WBC) composition may also be analyzed, as the concentration of these cells is also an important factor in tissue healing [11].

There is currently disagreement in the literature over whether the presence of WBC in PRP provides any benefit. Proponents of PRP containing high WBC concentrations (Leukocyte and Platelet-Rich Plasma (L-PRP) according to Ehrenfest[12]) believe that the presence of WBC provides natural protection against infections and allergic responses [13].

Other authors do not recommend the presence of high WBC concentration in PRP (Pure Platelet-Rich Plasma (P-PRP) according to Ehrenfest).[12] The presence of neutrophils, which are 65% of WBC and more than 95% of granulocytes, may be harmful because they destroy surrounding tissue, even if the tissue is not injured. These neutrophils release non-selective and toxic reactive oxygen species that include hypochlorite, superoxide and hydroxyl radicals at high levels.[14, 15] Some studies have also shown that WBC concentration is directly correlated to catabolic gene expression in the tendon and ligaments. High catabolic gene expression may impair tissue healing [11, 16].

There are numerous protocols in the current literature that describe the optimal conditions for centrifugation. However, these various protocols have been optimized with respect to different volumes of processed WB. Considering the complexity of an autologous product such as PRP and the need for quality control in clinical applications, it is crucial to demonstrate process´s ability to reproduce consistent results. There is currently no studies that measures the effects of the complete set of variables in the process, such as volume of processed WB, number of spins, time period of centrifugation and centrifugal accelerations, on the quality of obtained PRP. Without these studies on centrifugation, the optimization and standardization of the PRP preparation cannot be achieved. Clear protocols for centrifugation should be

selected and followed to achieve the desired result. Therefore, the purpose of this study is to highlight the relevant aspects involved in the centrifugation step of the PRP preparation and to discuss their implications for the final composition of the PRP product.

3.2 Materials and Methods

3.2.1 Blood Collection

This study was approved by the Ethics Committee of the Medical Sciences School of the University of Campinas (UNICAMP), CAAE: 0972.0.146.000-11.

In the preparation of P-PRP, approximately 3.15 mL of WB was collected in 3.5 mL tubes (Vacuette, Ref. 454327; Greiner Bio-One) that contained 0.35 mL of 3.2% sodium citrate, an anticoagulant.

3.2.2 P-PRP Preparation

3.2.2.1 First Spin

For the first spin, WB was centrifuged at different centrifugal forces ranging from 50 to 820 xg (50, 70, 100, 190, 280, 370, 460, 550 and 820 xg) for 10 min in a Routine 380R centrifuge model (Hettich, Zentrifugen). After the formation of three layers (a bottom layer composed of RBC; an upper layer composed of plasma, platelets and some WBCs; and an intermediate layer, or buffy coat, composed mostly of WBCs), the upper layer was collected with a pipette. This collection was performed carefully to avoid disturbing the bottom layer of RBC and the buffy coat layer. Depending on the centrifugal force of the spin, the collected volume ranged from 1 to 2 mL. The collected sample was then transferred to an empty siliconized glass tube to be homogenized. After the sample was homogenized, a blood cell count was performed with cell counting equipment (Micros ES 60 Horiba®).

The procedure at 100 xg for 10 min was repeated with approximately 20 donors to validate the recovery of platelets obtained for a single donor.

3.2.2.2 Second Spin

The WB was initially centrifuged at 100 xg for 10 min for the first spin step. Approximately 1.2 mL of the upper layer of the sample that underwent the first spin step was collected and transferred to 6 empty tubes. The tubes were centrifuged again for 10 min at various centrifugal forces: 200, 400, 800, 1200 and 1600 xg.

The upper half of the plasma volume, platelet poor plasma (PPP), was removed. The remaining volume of P-PRP was homogenized and analyzed for platelets and WBC. The P-PRP was characterized by (i) measuring the platelet concentration gradient prior to PPP removal; (ii) observing cell composition after the removal of PPP and subsequent sample homogenization, and (iii) examining the integrity of the platelets.

3.2.3 P-PRP Characterization

3.2.3.1 Composition after the first Spin

After the first spin step, the concentration of platelets and WBCs in the upper layer was measured to calculate the recovery efficiencies of plasma (E_{Pl}), platelets (E_{Pt}) and WBC (E_{WBC}) as well as the platelet concentration factor (Fc_{Pt}). These values were calculated using equations (1), (2), (3) and (4).

WBC composition was also analyzed by measuring the concentration of lymphocytes, monocytes and granulocytes.

$$E_{Pl=}\frac{Volume\ of\ upper\ layer}{Total\ volume\ of\ WB\ x\ (1-hematocrit)} \times 100 \qquad (1)$$

$$E_{Pt} = \frac{N_{Pt\ (upper\ layer)}}{N_{Pt\ (WB)}} \times 100 \qquad (2)$$

$$E_{WBC} = \frac{N_{WBC\ (upperlayer)}}{N_{WBC\ (WB)}} \times 100 \quad (3)$$

$$Fc_{Pt} = \frac{C_{Pt\ (upper\ layer)}}{C_{Pt\ (WB)}} \quad (4)$$

Where $N_{Pt\ (upper\ layer)}$ and $N_{Pt(WB)}$ refer to the number of platelets in the respective upper layer and in WB (counts /(mm^3) x 1000 x volumes in mL); $N_{WBC(WB)}$ and $N_{WBC\ (upper\ layer)}$ refer to the number of WBC in the respective upper layer and in WB; and $Ct_{Pt\ (upper\ layer)}$ and $Ct_{Pt\ (WB)}$ are the concentrations of platelets in the upper layer and in WB, respectively.

The effect of time of centrifugation on the first spin step was demonstrated by comparing the composition of platelets and WBC in the upper layer between 6 and 10 min periods of centrifugation at 100xg.

3.2.3.2 Composition after the second Spin

After the second spin step and the separation of PPP (2/3 or 1/2 of the upper volume) from the P-PRP sample, the recovery efficiencies of platelets and WBC, along with the platelet concentration factor, were calculated by equations (5), (6) and (7) for both PPP and P-PRP volumes.

$$E_{Pt\ (PPP\ or\ P-PRP)} = \frac{N_{Pt\ (PRP\ or\ P-PRP)}}{N_{Pt\ (upper\ layer)}} \times 100 \quad (5)$$

$$E_{WBC\ (PPP\ or\ P-PRP)} = \frac{N_{WBC\ (PPP\ or\ P-PRP)}}{N_{WBC\ (upper\ layer)}} \times 100 \quad (6)$$

$$Fc_{Pt} = \frac{C_{Pt\ (P-PRP)}}{C_{Pt\ (WB)}} \quad (7)$$

where $N_{Pt\ (P\text{-}PRP\ or\ PPP)}$is the platelet number in P-PRP or PPP; $N_{WBC\ (P\text{-}PRP\ or\ PPP)}$ is the WBC number in P-PRP or PPP; and $C_{Pt(P\text{-}PRP)}$ is the concentration of platelets in P-PRP.

The effect of the volume of plasma centrifuged in the second spin step was quantified in terms of the recovery efficiency of platelets that remained in the PPP volume.

3.2.3.3 Platelet concentration gradient

The platelet concentration gradient in the samples was analyzed immediately after the second spin step by positioning the needle of the hematological counter at various points along the tube.

3.2.3.4 The influence of homogenization

The effect of homogenizing the samples after the second spin step was evaluated**.** After the removal of the PPP (1/2 of the upper volume), the remaining P-PRP volume was homogenized and analyzed with respect to platelet recovery. The homogenization step was performed manually for 30 seconds and in a tube homogenizer for 30 and 60 min.

3.2.3.5 Platelet integrity

The influence of the centrifugal acceleration on the integrity of platelets in the P-PRP sample was evaluated by measuring the sP-selectin after the second spin step. This protein can be used to quantify the activation of platelets [17].

All assays were performed using enzyme-linked immunosorbent assay (ELISA) kits (R&D Systems) according to the manufacturer's instructions and specifications.

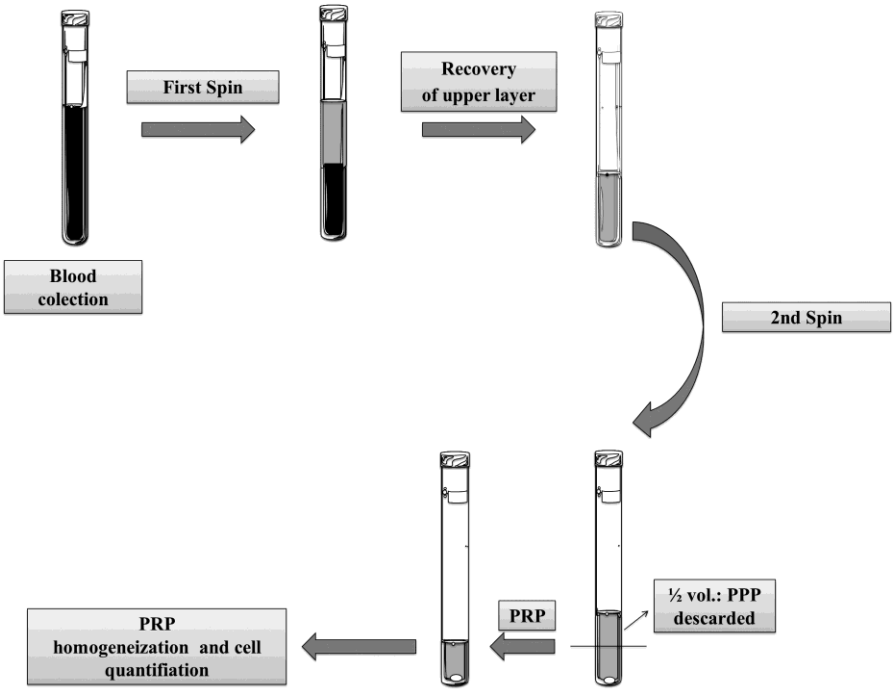

Figure 3.1 Flow chart describing the general preparation process of PRP. WB is initially collected in tubes that contain anticoagulants. The first spin step is performed at constant acceleration to separate RBCs from the remaining WB volume. After the first spin step, the WB separates into three layers: an upper layer that contains mostly platelets and WBC, an intermediate layer that is known as the buffy coat and that is rich in WBCs and a bottom layer that consists mostly of RBCs. Only the upper layer or the upper layer plus buffy coat are transferred to an empty tube. The second spin step is then performed. The upper portion of the volume that is composed mostly of PPP (platelet poor plasma) is removed to create the PRP (platelet rich plasma).The concentrations of platelets and WBC in each of the various layers are measured to characterize the quality of PRP.

3.3 Results

3.3.1 Experimental aspects

3.3.1.1 Effects of time and volume in centrifugation

Table 3.1 compares the recovery efficiencies of plasma, platelets and WBC in the upper layer after the first spin step. The first spin step was performed at 100 xg for

either 6 or 10 min. According to the physics of the centrifugation process, time and acceleration are the fundamental parameters that define the composition of the PRP sample after the first spin step**.** The effect of centrifugation time at a low spin setting was evaluated with respect to the concentration of WBC in the upper layer. Based on the data collected after the first spin step, it appears that longer time periods slightly increased platelet recovery and decreased the concentrations of WBC in the upper layer. Therefore, time could be a control parameter when low levels of WBC, such as granulocytes and lymphocytes, are required in the PRP sample.

Table 3.1 Comparison of the recovery efficiencies of plasma, platelets and WBC in the upper layer after the first spin step of 100 xg for 6 or 10 min. Volume of WB: 3.5 mL

	Recovery Efficiencies (%)(± SD)			**WBC Composition(± SD)**		
	Plasma	Platelets	WBC	Lymphocytes ($10^3/mm^3$)	Monocytes ($10^3/mm^3$)	Granulocytes ($10^3/mm^3$)
Blood	-	-	-	1.72±0.64	0.31±0.14	4.01±1.71
10 min	66.6± 4.5	79.0 ±7.8	8.7 ±3,7	0.71± 0.34	0.062± 0.05	0.32± 0.15
6 min	43.9± 6.2	72.3±2.9	26.6 ±11,4	3.18±0.77	0.47±0.34	1.20±0.43

Table 3.2 shows the effect of the volume of plasma transferred to the second spin step. It is evident that the percentage of remaining platelets in the PPP volume is higher when the volume of plasma is increased. Therefore, when a greater volume of P-PRP is desired, the centrifugal acceleration and time should be adjusted to maintain the same recovery efficiency.

Table 3.2 Effect of plasma volume on the percentage of platelets remaining in the PPP volume after the second spin step (400 xg for 10 min).

Volume of plasma after second spin step (mL)	Platelets remaining in PPP (%)
1.2	0.42
1.4	0.75
2.5	6.55
3.1	5.20

3.3.1.2 Platelet concentration gradient

Platelet concentration gradients form after both spin steps. However, this gradient is more critical after the second spin step because some RBC are inevitably present in the upper volume that was transferred from the first spin step. The presence of these remaining RBC can generate a pellet at the bottom of the tube. This pellet may adsorb platelets and WBCs on its surface. This possibility was evident in this study and is depicted in Figure 3.2.

From the measurements of platelet concentrations at various points along the tube (illustrated in Figure 3.2), it appears that at 200 xg, the concentration of platelets from points 1 to 4 were approximately 100,000 to 150,000 Pq/mm3. For spins centrifugal forces greater than 200 xg, the concentration values at these points were much lower, as expected. The platelet gradient data show the importance of homogenizing the P-PRP located in the bottom layer of volume sample prior to measuring the components of the sample.

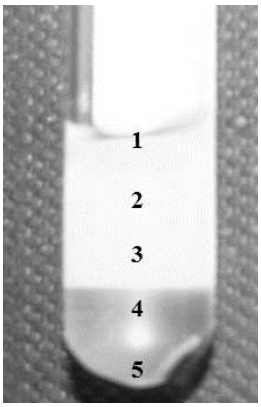

Figure 3.2: Illustration of the RBC pellet. After the second spin step, gradients of platelets and WBC were present. The points indicate where the concentrations of platelets and WBC were measured.

Figure 3.3 (a) illustrates the effects of homogenization after the second spin step on P-PRP samples spun at various centrifugal accelerations in terms of recovery efficiency of platelets in P-PRP. We can conclude that manually homogenizing the sample for a short period of time was insufficient to completely resuspend the platelets. In addition, the recovery efficiency of platelets in P-PRP was 50% or less, indicating poor homogenization. Samples spun for 30 or 60min had an improved recovery efficiency of platelets in P-PRP, regardless of the centrifugal acceleration that was applied, according to Tukey's test ($p>0.05$), The recovery efficiency was approximately 75-80%. Thus, approximately 20% of platelets remained adsorbed in the RBC pellet. Figure 3.3 (b) shows that the residual of platelets in PPP was minimal when centrifugal accelerations of 400 xg or higher were applied.

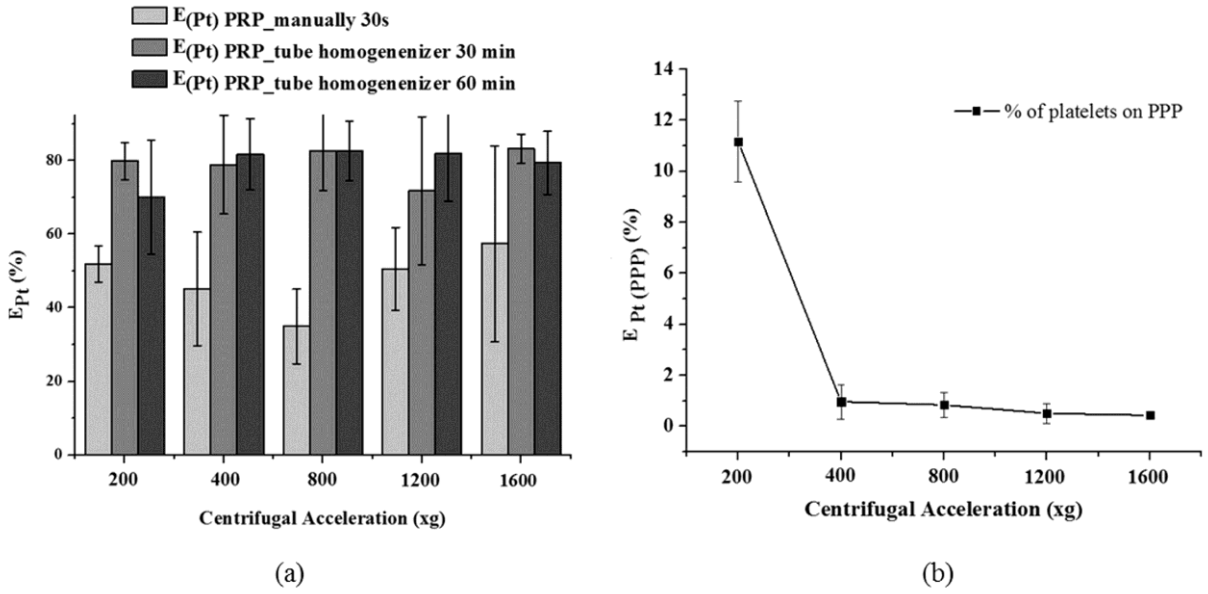

Figure 3.3: (a) Effect of homogenization after the second spin step (10 min) on the recovery efficiency of platelets in the PRP samples (n=3); (b) Percentage of platelets in the PPP layer. Total volumes of P-PRP and PPP ranged from 0.5 to 0.7 mL.

3.3.1.3 Platelet Integrity

The initial plasma concentrations of sP-selectin for two of the donors ranged from 18 to 40 ng/mL. These values are considered to be in the normal range of concentration values for human plasma[18]. Figure 3.4 shows that the concentration of sP-selectin from both donors increased when the centrifugal acceleration was 800 xg and 1200 xg.

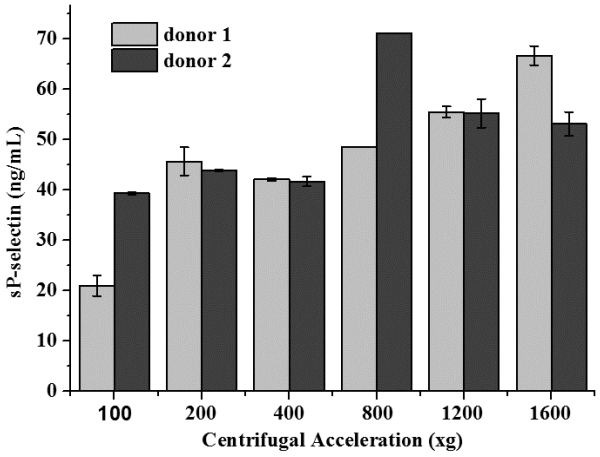

Figure 3.4: .Effects of centrifugal acceleration on concentration of sP-selectin the after second spin step.

3.3.1.4 Performance of centrifugation step and P-PRP composition in two spins

3.3.1.4.1 First spin

The composition of P-PRP samples spun at various centrifugal accelerations is shown in Figure 3.5(a). The mean platelet count in WB for all donors was 249.977 Pq/mm^3 (± 45.167).

As expected, the recovery efficiency of platelets increased as the centrifugal acceleration increased from 50 to 70 xg. The recovery efficiency peaked in the 70 to 100 xg range and began to decrease in the 190 to 820 xg range. The recovery efficiency of plasma increased with centrifugal force. The recovery of WBC remained between 5 and 10%, regardless of the applied centrifugal accelerations.

The setting of 100 xg for centrifugal acceleration and a centrifugation time of 10 min was determined to yield the maximum recovery of platelets; these settings were repeated with 20 donors for data validation. Figure 3.5(b) shows that the mean recovery of platelets, plasma and WBC was approximately 80%, 65% and8%, respectively.

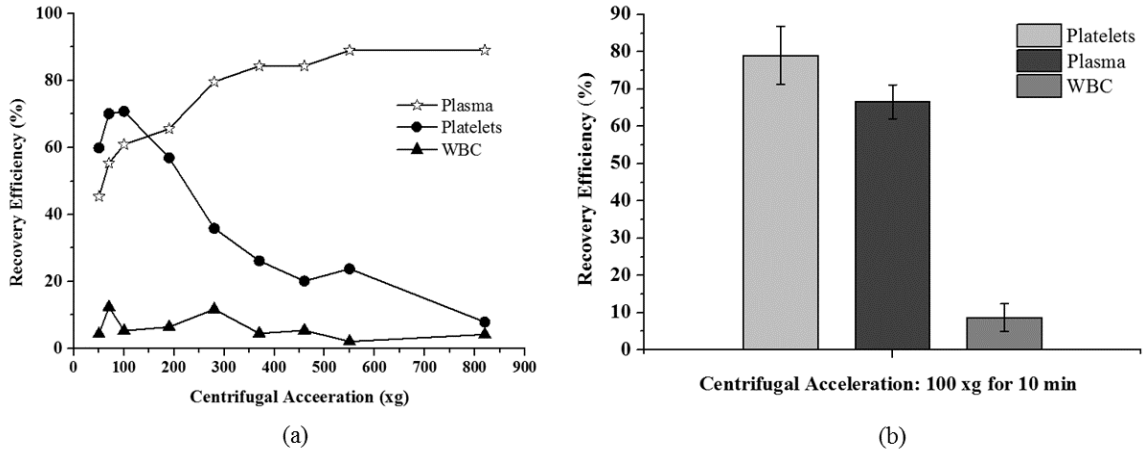

Figure 3.5: Recovery efficiency of platelets, plasma and WBC after the first spin step of WB: (a) Centrifugal acceleration from 50 to 820 xg for 10 min (n=1); (b) Centrifugal acceleration of 100 xg for 10 min (n=20).

3.3.1.4.2 Second spin

After removal of the upper 1/2 of the plasma volume (PPP layer), the platelet concentration in the remaining P-PRP sample was approximately 3 times greater than the baseline concentration. To achieve a platelet concentration that was 5 times greater than baseline, it was necessary to remove 2/3 of the plasma volume after the second spin step (Table 3.3).

For the second spin step, settings with the centrifugal acceleration ranging from 400 to 1600 xg yielded a WBC concentration of 0 x 10^3/mm^3 in the PPP layer. This value suggests that all the WBC had settled. Therefore, the final WBC concentration in the P-PRP samples (Table 3.3) only depends on the WBC recovered in the first spin step and the volume of PPP removed in the second spin step.

Table 3.3 Composition of platelets and WBCs in the P-PRP samples after the second spin step (400 xg and 10 min). According to the hematocrit of the donor, volumes of the upper phase after first spin ranged from 1.0 to1.4 mL.

		Fc_{Pt}	Platelet x $10^3/mm^3$ (± SD)	WBC x $10^3/mm^3$ (± SD)
P-PRP after second spin step	Blood	-	232 ±28	-
	1/2 of volume of PPP removed	3.1±0.3	668 ±34	2.2±0.4
	1/3 of volume of PPP removed	5.2±0.5	1.222 ±166	3.3±0.4

Despite the variable nature of PRP, it is possible to optimize the centrifugation process to produce PRP samples with consistent compositions.

3.4 Discussion

Centrifugation is one of the most widely used processes in liquid-liquid or solid-liquid separation. It is based on the application of a centrifugal force that exceeds the force of gravity. The difference in density between the various phases is the driving force responsible for the phase separation. Therefore, the centrifugation process is based on the difference in the physical properties of the components in the sample.

When a rigid particle moves through fluid, the particle is being acting upon by numerous forces: gravitational force in the downward direction, buoyant force in the upward direction, and drag force in the opposing direction of the particle. Figure 3.6(a) and (b) show the numerous forces acting upon a particle during centrifuging.

The frictional force is directly related to the particle velocity. During the process of centrifugation, the movement of the particle is driven by centrifugal force. This force is acted upon by a frictional force that is proportional to the particle's velocity. As a result, the forces are quickly balanced. Figure 3.6(c) shows the movement of a suspended particle traveling away from the axis of the centrifuged tube.[19, 20]

After centrifugation of WB, a concentration gradient is formed within the tube for various blood components. Thus, the concentration gradient of each component must be considered. To ensure reliable measurements of the sample, the sample should be homogenized. In the second spin step, concentration gradients are more intense. This effect on the concentration gradients occurs because the platelets are adsorbing to the surface of the remaining RBC. The presence of some RBC in the volume transferred from the first spin step is unavoidable.

Another important variable that affects recovery efficiency of platelets is the volume of WB processed. When the volume of WB increases, the recovery efficiency of platelets decreases. Therefore, the centrifugal force must be adjusted to maintain the desired recovery efficiency.

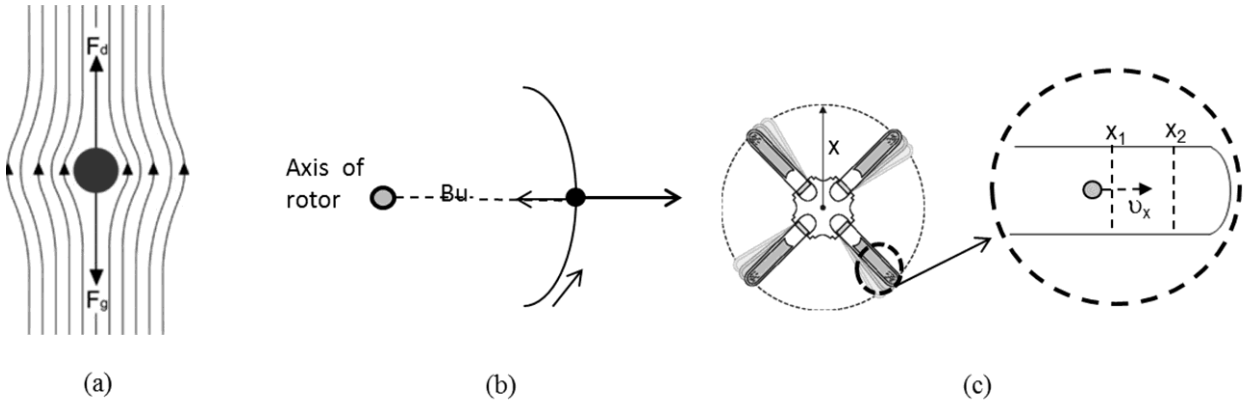

Figure 3.6: Illustration of forces acting upon the particle and particle displacement during the centrifugation process. (a) The forces acting upon a particle that is settling under gravity. F_g is the difference between the gravitational force and the force generated from the displacement of fluid. F_d is the frictional force. (b) The forces acting upon a particle under a centrifugal field. Bu is the friction coefficient that quantifies how strongly the surrounding fluid resists the motion of the particle. (c) The scheme of a discontinue centrifuge in which the tubes are positioned relative to the rotor. The rotor has a radius that is designated as x and rotates with an angular velocity ω (left). The displacement of a particle at velocity υ_x between points x_1 and x_2 (bottom of the tube) is because of the centrifugal acceleration.

To compare protocols that are described in the literature, it is important to use the same initial volume of WB. Even with the same centrifugal acceleration and time of centrifugation, different WB volumes may lead to PRP preparations with differing compositions. In addition to the volume of WB, the transferred volume of the upper layer from the first centrifugation has an impact on the composition of the PRP. Anitua et al.[21] used only one centrifugation spin step and collected the volume immediately above the RBC layer. This protocol obtained a platelet concentration factor of 2.67 above the baseline value. When all of the volume of the upper layer is collected, regardless of whether the buffy coat layer is included, additional spins can be performed to achieve higher platelet concentration factors (> 3x) [22, 23].

The homogenization of the samples is essential for reliable measurements of the components in the PRP samples. As shown, the integrity of platelets mainly depends on centrifugal acceleration. Therefore, these factors should be evaluated when optimizing the centrifugation procedure.

Numerous protocols have attempted to optimize the centrifugation procedure using various processed volumes and performance standards.

Kahn et al. (1976) determined that a centrifugal acceleration of 3730 xg for a period of 4 min was the optimal condition for obtaining the highest platelet concentration from 478 mL of WB[24]. The highest platelet recovery efficiency obtained by Slichter and Harker (1976) was 80%, using a sample of 250-450 mL of WB centrifuged at 1000 xg for a period of 9 min[25]. It was observed that a subsequent centrifugation step of 3000 xg for a period of 20 min decreased the platelet viability.

Landesberg et al. obtained PRP samples that had approximately 3.2 times the concentration of the WB baseline. The centrifugation procedure processed 5 mL of WB for two spins at 200 xg for 10 min per spin [23]. In most of these studies, the authors only refer to the final concentration factor instead of recovery efficiency. Thus, the performance of theses protocols cannot be precisely measured. In our study, a maximum recovery of platelets (70-80%) was obtained from the first spin step when an acceleration of 100 xg for 10 min was applied to 3.5 mL of WB (Figure 3.4). This processed sample had a concentration factor that was 2 times greater than the baseline concentration. After the second spin step, the platelet concentration factor of the PRP was 3 to 5 times greater than the baseline concentration by removing 1/2 or 1/3 of the upper volume.

In the same study, it was observed that centrifugal accelerations greater than 250 xg resulted in a pellet of platelets that could not be resuspended [23]. In our study, it was shown that resuspension of approximately 85% of pellet was possible by homogenizing the sample for 30 min. The resuspension of the pellet was successful even when high accelerations, such as 1600 xg for 10min, were applied.

Jo et al. achieved better efficiency (92%) by applying an acceleration of 900 xg for 5 min for the first spin step [22]. A total of 9 mL of WB was processed, and the platelet concentration was measured to be 310.7 ±78.5 x 103/mm3. The maximum efficiency for the second spin step (84%) was obtained by applying1500 xg for 15 min. The platelet concentration was 633.2 ±91.6 x 103/mm3, which was 4.2 times greater than the baseline concentration. However, the integrity of platelets was not evaluated. Our results show that it is possible to achieve a concentration factor that is 5 times greater than baseline by applying a lower centrifugal acceleration in the second spin step (400 xg) for less time (10 min). This setting ensures platelet integrity.

Bausset et al.[26] found that a centrifugation of 130 or 250 xg for a period of 15 min was optimal when performing a procedure that involved two spins. A platelet concentration factor of 3.47 was obtained from the 8.5 mL WB processed, and 2.0 mL of plasma was processed in the second spin step. Although different methods were used, the authors evaluated the platelet integrity, and the data are consistent with those of our study.

Studding the first spin step, Araki et al. obtained a PRP sample that had 70-80% recovery of platelets and 10-35% recover of WBC by applying low accelerations of 70 xg for 10 min.[27] At 230-270 xg, they achieved similar platelet recovery; however, the WBC recovery efficiency was only 4-6%. For the second spin step, an acceleration of 2300 xg for 10 min was applied. The platelet concentration factor was 7.4 times greater than the baseline after removing approximately 1/10 of the PPP and adding ethylenediaminetetraacetic acid (EDTA) as an anticoagulant. However, when ACD was used, the platelet recovery efficiency was only 35%. The authors attributed this difference to the anticoagulant diminishingthe platelet integrity in the sample. Therefore, the integrity of platelets is an important parameter that should be evaluated.

Mazzocca et al.[28] analyzed 3 protocols for preparing PRP samples with different compositions: a low platelet ($382x10^3/mm^3$) and low WBC ($0.6\ x10^3/mm^3$)

process with one spin step at 1500 rpm for 5 min (10 mL WB); a high platelet ($940x10^3/mm^3$) and high WBC ($17x10^3/mm^3$) process with one spin stepat 3200 rpm for 15 min (27 mL WB); and a double-spin process (1500 rpm for 5 min and 6300 rpm for 20 min) that produced a higher platelet concentration ($472\ x10^3/mm^3$) and lower white blood cell concentration ($1.5x10^3/mm^3$). Many other studies [29, 30] specify centrifugal accelerations in rotations per minute (RPM) instead of in xg, complicating the task of comparing and reproducing their results.

Therefore, it is important to observe the aspects highlighted in this study when choosing a protocol for centrifugation. By following the observations made in this study, it is possible to obtain the required composition of PRP, supported by reliable measurements along and selected variables in the process.

3.5 Conclusion

Although the PRP being an autologous product, its composition can be controlled by a set of variables in the preparation process. The measurements must be reliable and the integrity of platelets preserved. Clear and reproducible protocols ensure the quality of the prepared PRP.

Conflict of Interest

The authors declare that they have no conflict of interests.

Acknowledgments

The authors acknowledge the financial support of FAPESP (Fundação de Amparo à Pesquisa do Estado de São Paulo), project's number 2010/11758-3 and 2010/17434/5, and the University of Campinas.

References

[1] Engebretsen, L.; Steffen, K.; Alsousou, J.; Anitua, E.; Bachl, N.; Devilee, R.; Everts, P.; Hamilton, B.; Huard, J.; Jenoure, P.; Kelberine, F.; Kon, E.; Maffulli, N.; Matheson, G.; Mei-Dan, O.; Menetrey, J.; Philippon, M.; Randelli, P.; Schamasch, P.; Schwellnus, M.; Vernec, A.; Verrall, G., IOC consensus paper on the use of platelet-rich plasma in sports medicine. *Br J Sports Med* **2010,** *44* (15), 1072-81.

[2] Anitua, E., Plasma rich in growth factors: preliminary results of use in the preparation of future sites for implants. *Int J Oral Maxillofac Implants* **1999,** *14* (4), 529-35.

[3] Gentile, P.; Bottini, D. J.; Spallone, D.; Curcio, B. C.; Cervelli, V., Application of platelet-rich plasma in maxillofacial surgery: clinical evaluation. In *J Craniofac Surg*, United States, 2010; Vol. 21, pp 900-4.

[4] Cervelli, V.; Gentile, P.; Scioli, M. G.; Grimaldi, M.; Casciani, C. U.; Spagnoli, L. G.; Orlandi, A., Application of platelet-rich plasma in plastic surgery: clinical and in vitro evaluation. *Tissue Eng Part C Methods* **2009,** *15* (4), 625-34.

[5] Dallari, D.; Savarino, L.; Stagni, C.; Cenni, E.; Cenacchi, A.; Fornasari, P. M.; Albisinni, U.; Rimondi, E.; Baldini, N.; Giunti, A., Enhanced tibial osteotomy healing with use of bone grafts supplemented with platelet gel or platelet gel and bone marrow stromal cells. In *J Bone Joint Surg Am*, United States, 2007; Vol. 89, pp 2413-20.

[6] Filardo, G.; Kon, E.; Pereira Ruiz, M. T.; Vaccaro, F.; Guitaldi, R.; Di Martino, A.; Cenacchi, A.; Fornasari, P. M.; Marcacci, M., Platelet-rich plasma intra-articular injections for cartilage degeneration and osteoarthritis: single- versus double-spinning approach. *Knee Surg Sports Traumatol Arthrosc* **2012,** *20* (10), 2078-87.

[7] Cieslik-Bielecka, A.; Bielecki, T.; Gazdzik, T. S.; Arendt, J.; Krol, W.; Szczepanski, T., Autologous platelets and leukocytes can improve healing of infected high-energy soft tissue injury. In *Transfus Apher Sci*, England, 2009; Vol. 41, pp 9-12.

[8] Rozman, P.; Bolta, Z., Use of platelet growth factors in treating wounds and soft-tissue injuries. In *Acta Dermatovenerol Alp Panonica Adriat*, Slovenia, 2007; Vol. 16, pp 156-65.

[9] Hammond, J. W.; Hinton, R. Y.; Curl, L. A.; Muriel, J. M.; Lovering, R. M., Use of autologous platelet-rich plasma to treat muscle strain injuries. In *Am J Sports Med*, United States, 2009; Vol. 37, pp 1135-42.

[10] Harrison, S.; Vavken, P.; Kevy, S.; Jacobson, M.; Zurakowski, D.; Murray, M. M., Platelet activation by collagen provides sustained release of anabolic cytokines. *Am J Sports Med* **2011,** *39* (4), 729-34.

[11] Sundman, E. A.; Cole, B. J.; Fortier, L. A., Growth factor and catabolic cytokine concentrations are influenced by the cellular composition of platelet-rich plasma. In *Am J Sports Med*, United States, 2011; Vol. 39, pp 2135-40.

[12] Dohan Ehrenfest, D. M.; Rasmusson, L.; Albrektsson, T., Classification of platelet concentrates: from pure platelet-rich plasma (P-PRP) to leucocyte- and platelet-rich fibrin (L-PRF). *Trends Biotechnol* **2009,** *27* (3), 158-67.

[13] Everts, P. A.; Overdevest, E. P.; Jakimowicz, J. J.; Oosterbos, C. J.; Schonberger, J. P.; Knape, J. T.; van Zundert, A., The use of autologous platelet-leukocyte gels to enhance the healing process in surgery, a review. *Surg Endosc* **2007,** *21* (11), 2063-8.

[14] Scott, A.; Khan, K.; Roberts, C.; Cook, J.; Duronio, V., What do we mean by the term "inflammation"? A contemporary basic science update for sports medicine. *Br J Sports Med* **2004,** *38* (3), 372-80.

[15] Toumi, H.; Best, T., The inflammatory response: friend or enemy for muscle injury? *Br J Sports Med* **2003,** *37* (4), 284-6.

[16] McCarrel, T.; Fortier, L., Temporal growth factor release from platelet-rich plasma, trehalose lyophilized platelets, and bone marrow aspirate and their effect on tendon and ligament gene expression. *J Orthop Res* **2009,** *27* (8), 1033-42.

[17] Kostelijk EH, F. R., Nieuwenhuis HK, Gouwerok CW, de Korte D, Soluble P-selectin as parameter for platelet activation during storage. - Abstract - UK PubMed Central. *Thrombosis and Haemostasis* **1996,** *76* (6), 1086-1089.

[18] R&D Systems, I. Human soluble P-Selectin/CD62P Immunoassay. http://www.rndsystems.com/pdf/bbe6.pdf (accessed 05/10/2012).

[19] Bird , B., Steart, EW.,; Lightfoot, E., *Transport Phenomena*. 2nd ed.; USA, 2007; p 920.

[20] Hunter, R. J., *Foundations of Colloid Science*. Oxford University Press: USA, 2001; p 816

[21] Anitua, E.; Aguirre, J. J.; Algorta, J.; Ayerdi, E.; Cabezas, A. I.; Orive, G.; Andia, I., Effectiveness of autologous preparation rich in growth factors for the treatment of chronic cutaneous ulcers. *J Biomed Mater Res B Appl Biomater* **2008,** *84* (2), 415-21.

[22] Jo, C. H.; Roh, Y. H.; Kim, J. E.; Shin, S.; Yoon, K. S.; Noh, J. H., Optimizing Platelet-Rich Plasma Gel Formation by Varying Time and Gravitational Forces During Centrifugation. *J Oral Implantol* **2011**.

[23] Landesberg, R.; Roy, M.; Glickman, R. S., Quantification of growth factor levels using a simplified method of platelet-rich plasma gel preparation. *Journal of Oral and Maxillofacial Surgery* **2000,** *58* (3), 297-300.

[24] Kahn, R. A.; Cossette, I.; Friedman, L. I., Optimum centrifugation conditions for the preparation of platelet and plasma products. *Transfusion* **1976,** *16* (2), 162-5.

[25] Slichter, S. J.; Harker, L. A., Preparation and Storage of Platelet Concentrates: I. FACTORS INFLUENCING THE HARVEST OF VIABLE PLATELETS FROM WHOLE BLOOD. *British Journal of Haematology* **1976,** *34* (3), 395-402.

[26] Bausset, O.; Giraudo, L.; Veran, J.; Magalon, J.; Coudreuse, J.-M.; Magalon, G.; Dubois, C.; Serratrice, N.; Dignat-George, F.; Sabatier, F., Formulation and Storage of Platelet-Rich Plasma Homemade Product. **2012**.

[27] Araki, J.; Jona, M.; Eto, H.; Aoi, N.; Kato, H.; Suga, H.; Doi, K.; Yatomi, Y.; Yoshimura, K., Optimized preparation method of platelet-concentrated plasma and noncoagulating platelet-derived factor concentrates: maximization of platelet concentration and removal of fibrinogen. *Tissue Eng Part C Methods* **2012,** *18* (3), 176-85.

[28] Mazzocca, A. D.; McCarthy, M. B. R.; Chowaniec, D. M.; Cote, M. P.; Romeo, A. A.; Bradley, J. P.; Arciero, R. A.; Beitzel, K., Platelet-Rich Plasma Differs According to Preparation Method and Human Variability. *The Journal of Bone & Joint Surgery* **2012,** *94* (4), 308-316.

[29] Fernandez-Barbero, J. E.; Galindo-Moreno, P.; Avila-Ortiz, G.; Caba, O.; Sanchez-Fernandez, E.; Wang, H. L., Flow cytometric and morphological characterization of platelet-rich plasma gel. In *Clin Oral Implants Res*, Denmark, 2006; Vol. 17, pp 687-93.

[30] Su, C. Y.; Kuo, Y. P.; Nieh, H. L.; Tseng, Y. H.; Burnouf, T., Quantitative assessment of the kinetics of growth factors release from platelet gel. In *Transfusion*, United States, 2008; Vol. 48, pp 2414-20.

Capítulo 4. Prediction and Modulation of Platelet Recovery by Discontinuous Centrifugation of Whole Blood for the Preparation of Pure Platelet-Rich Plasma.

Amanda G. M. Perez, B.S., M.Sc.,[1]Rafael Lichy, B.E.,[1]José Fábio S.D. Lana, M.D.[1,2,3] Ana Amélia Rodrigues, B.S., D.Sc.,[3] Ângela Cristina M. Luzo, M.D., D.Sc.,[4] William D. Belangero, M.D., D.Sc.,[3] and Maria Helena A. Santana,B.E., D.Sc. [1*]

[1]Department of Materials and Bioprocesses Engineering - School of Chemical Engineering, University of Campinas, Albert Einstein Av., 500, Campinas-SP, Brazil, Phone: 55-19-35213921, FAX: 55-19-35213890, E-mails: mariahelena.santana@gmail.com, amandamarcelino@gmail.com

[2]Research Institute of Sports Medicine, Orthopedics and Regeneration - iMOR, Uberaba- MG, Brazil, E-mail: josefabiolana@gmail.com

[3]Department of Orthopaedic and Traumatology - Faculty of Medical Sciences, University of Campinas, Campinas-SP, Brazil, belangerow@gmail.com, anaarodrigues@gmail.com

[4]Haematology and Hemotherapy Center, Umbilical Cord Blood Bank, University of Campinas, Campinas-SP, Brazil, angela.luzo@gmail.com

*Corresponding author

Abstract The aim of this study was to describe the behavior of the separation of red blood cells (RBCs) by discontinuous centrifugation (DC) of whole blood to modulate and control the platelet recovery in the preparation of Pure Platelet-Rich Plasma (P-PRP). P-PRP is a platelet-rich plasma (PRP) in which the white blood cell layer is not included. To achieve this goal, an analytical model was derived that takes into

account the packing of RBCs and predicts the behavior of platelet and plasma recovery efficiencies (PtPlRE) based on the volume of whole blood, the hematocrit and the volume of supernatant, as a function of the operating variables, centrifugal acceleration and time. The model was derived from the basic equation of DC, which originates from the equilibrium balance of forces on a particle, and included the addition of one factor that corrected the terminal velocity of RBCs and was also correlated to the PtPlRE in the supernatant. This factor was the ratio between the fractional volume concentrations of plasma and RBCs in the centrifugation pellet after centrifugation. The model was validated and the variability of the data was determined using experimental data from 10 healthy donors in the age range of 25-35 years. The predicted behavior for the packing of RBCs and the PtPlRE was consistent with the behavior seen in the experimental data. Thus, the PtPlRE could be modulated and controlled through centrifugal acceleration, time and hematocrit. Use of this model based on a physical description of events is the first step of a reliable standardization of PRP preparations.

Keywords: biomaterials; bioprocessing; regeneration; tissue engineering; wounds

4.1 Introduction

Platelet-rich plasma (PRP) is defined as an autologous preparation from whole blood (WB), in which platelets are concentrated in to a small fraction of plasma. This broad definition is considered to be the consensus definition by the International Olympic Committee (IOC) in sports medicine.[1]

Platelets are rich in growth factors, which are critical for tissue regeneration.[2, 3] Specifically, growth factors are released from activated platelets at sites of injury; the amount and activity of the growth factors depend on the recovery and preservation of platelets during PRP preparation.[1]

In general, PRP preparation is a sequential 3-step process that involves blood collection, centrifugation to separate and concentrate the platelets, and activation of the platelets. Accordingly, PRP quality and efficiency is highly dependent on the

protocol used for its preparation.[1, 4-6] There are a multitude of PRP preparation protocols in the literature, which differ in terms of the conditions used in the preparation steps, such as centrifugal acceleration and time, the number of centrifugation steps, the type of anticoagulant, and the type of platelet agonist.[7-11]

Due to this variation, it is difficult to compare the biological effects that are reported in different studies, even for a specific use, which can lead to doubts that compromise the credibility of PRP-based therapies.[1]

For the preparation of PRP, blood collection must be performed without trauma to the vessel wall to ensure the integrity of the platelets. Centrifugation is the first step in PRP preparation, which requires the recovery of a large number of intact platelets. Thus, both platelet activation and the final properties of the PRP preparation are influenced by the centrifugation step.

Studies on centrifugation for the preparation of PRP are scarce in the literature. The authors attempt to determine the optimal centrifugation conditions for the recovery of platelets using experimental data from a limited number of experimental conditions. In general, the physical phenomena involved in centrifugation as well as the integrity of platelets are not considered in the interpretation of the experimental data.[12-15]

Adding to the complexity, one of the great challenges in studying an autologous product like PRP is to extract a maximum of information from experiments performed with raw material that is not abundant for each donor and exhibits variability among and per donors. Given this context, the prediction of the system behavior based on the phenomenological behavior becomes essential.

Accordingly, the objective of the current work was to study the separation of red blood cells (RBCs), platelets (Pt) and plasma (Pl) by discontinuous centrifugation (DC) of whole blood (WB), with the aim of determining centrifugation conditions that modulate and maximize the efficiency of the recovery of platelets in the supernatant, or upper layer (UP), from a well-established pellet of red blood cells (RBCs) in the

bottom layer (BL). Our approach was to develop a mathematical model to predict the platelet and plasma recovery efficiencies (PtPlRE) as function of the operating variables of the DC and the initial data from the WB samples. To our knowledge, there is no model in the literature that predicts the PtPlRE from DC for the preparation of PRP. In this study, we focused on the preparation of P-PRP (Pure PRP, or Platelet-Rich), a type of PRP in which the buffy coat (BC) is not included.

4.2 Material and Methods

4.2.1 Experimental

All experiments were approved by the Ethics Committee of the Medical Sciences School of the University of Campinas (UNICAMP), CAAE: 0972.0.146.000-11.

The centrifugation assays were conducted in a Rotina 380R centrifuge (Hettich Lab Technology). The concentration of the WB components was determined using a hematological counter, the Micros ES 60 (Horiba). Blood was collected into 3.5-mL vacuum tubes (Vacuette®) containing sodium citrate (3.2%) as an anticoagulant, in the volumetric proportion 9:1 blood:sodium citrate. After counting the RBCs and platelets, the WB was centrifuged for 10 minutes at 70, 100, 190, 280, 370, 460, 550, and 820xg. The supernatant (not including the buffy coat layer) was carefully pipetted to measure the volume and transferred to another tube to determine the platelet concentration. After that, the BC layer was also carefully collected and added to the UL fraction, and the new volume and platelet concentration were determined. The platelet concentration in the BC was determined by the difference in the platelet counts in the volumes with and without BC.

4.2.2 Recovery efficiencies of plasma and platelets

The plasma recovery efficiency in the UL, $E_{(Pl)UL}$, was calculated using equation (1).

$$E_{(\mathrm{Pl})\mathrm{UL}} = \left(\frac{V_{(\mathrm{Pl})\mathrm{UL}}}{V_{(\mathrm{Pl})\mathrm{WB}}}\right).100 \quad (1)$$

$V_{(Pl)WB}$ was estimated as V_{WB}.(1 - H), where V_{WB} is the volume of whole blood and H is the hematocrit. RBCs were defined here as the total blood cells (RBCs are 99% of the total cells in WB).

The platelet recovery efficiency, $E_{(Pt)UL}$, or the percentage of platelets in the UL was calculated using Equations 2-4.

$$E_{(\mathrm{Pt})\mathrm{UL}} = \frac{\mathrm{Pt}_{\mathrm{UL}}}{\mathrm{Pt}_{\mathrm{WB}}}.100 \quad (2)$$

$$\mathrm{Pt}_{\mathrm{UL}} = \mathrm{N}_{(\mathrm{Pt})\mathrm{UL}}.\mathrm{V}_{\mathrm{UL}} \quad (3)$$

$$\mathrm{Pt}_{\mathrm{WB}} = \mathrm{N}_{(\mathrm{Pt})\mathrm{WB}}.\,\mathrm{V}_{\mathrm{WB}} \quad (4)$$

4.2.3 Concentration factor of platelets

The concentration factor of platelets, $F_{CP,}$ defined by Equation 5, is the ratio between the concentrations of platelets in the UL and in the WB.

$$F_{\mathrm{CP}} = \frac{\mathrm{N}_{(\mathrm{Pt})\mathrm{UL}.}}{\mathrm{N}_{(\mathrm{Pt})\mathrm{WB}.}}.100 \quad (5)$$

4.2.4 The analytical model

The analytical model for the prediction of the PtPIRE in the UL was derived from a description of the separation of RBCs from WB under DC, as follows (Eqs. 6–18).

Initially, the separation of the components of WB under a centrifugal field was evaluated in terms of the settling velocities at infinite dilution (v_∞) in the Stokes regime (Equations 6 and 7).[16] Integration of Equation 6 yields Equation 8, which represents the displacement of a particle between two points, x_1 and x_2, in a centrifugal tube, with the settling velocities taken at infinite dilution.

$$\upsilon_\infty = \frac{dx}{dt} = \frac{2r_p^2\omega^2(\rho_p - \rho_f)}{9\mu_f} \tag{6}$$

$$\upsilon_x = GS \tag{7}$$

where G is the centrifugal acceleration, S is the sedimentation coefficient , and the subscripts p and f refer to the particle (blood component) and fluid (WB), respectively. For the calculations, we used the physical properties of various blood components as reported by Brown,[17] except for the blood viscosity[18] (0.03g.[cm.s]) and the platelet density[19] (1.06g/cm^3).

$$\ln\left(\frac{x_2}{x_1}\right) = \frac{2r_p^2\omega^2(\rho_p - \rho_f)}{9\mu_f}t \tag{8}$$

Equation 8 is the basic equation of DC. In equation 8, ω^2 must be written in terms of $G\ x\ g$, where $G\ x\ g = \omega^2 r_r$ and r_r is the radius of the axis of the rotor.

Next, to consider the backflow of the cell suspension, instead of only the backflow of plasma, the settling velocity of RBCs was corrected. Thus, in a second step, a correlation was obtained between the ratio of the actual setting velocity of RBCs to the predicted settling velocity at infinite dilution and a correction factor ((1-H_{BL})/H_{BL}), where H_{BL} is the RBC concentration in the BL (Eq. 9). The correction factor represents the fractional volume concentrations of plasma and RBCs in the centrifugal pellet, or BL. It also represents the packing of RBCs in the BL. To generate the correlation, the settling velocity of RBCs was determined experimentally by measuring the height of the UL in the centrifugation tube and dividing by the time of centrifugation.

$$\frac{\upsilon_x}{\upsilon_\infty} = 4.87\left(\frac{1-H_{BL}}{H_{BL}}\right), R^2 = 0.99 \quad (9)$$

Third, H_{BL}, the concentration of RBCs in the BL, was determined based on the conservation of RBCs from the WB to the BL and was written as function of V_{UL} (Eqs. 10-12). V_{UL} was calculated as a function of the operating variables (*G*) and time (*t*), using the basic equation of DC and including υ_∞ as corrected by the factor ((1-H_{BL})/H_{BL}). Therefore, H_{BL} and V_{UL} were calculated by an iterative process that determined x_2, which is the distance from the axis of the centrifugal head (or rotor), through Equations 10-15.

$$HV_{WB} = H_{BL}V_{BL} \quad (10)$$

$$V_{BL} = V_{WB} - V_{UL} \quad (11)$$

$$H_{BL} = \frac{HV_{WB}}{V_{WB} - V_{UL}} \quad (12)$$

$$V_{UL} = \pi(R)^2 \Delta h_{UL} \quad (13)$$

$$\Delta h_{UL} = x_2 - x_1 \quad (14)$$

$$\ln\left(\frac{x_2}{x_1}\right) = 0{,}416\left(\frac{1-H_{BL}}{H_{BL}}\right)\upsilon_\infty t \quad (15)$$

In a fourth step, the ratio of platelet and plasma recovery efficiencies also was correlated with the factor (1-H_{BL})/H_{BL} (Eq.16), and the PtPlRE were calculated using Equations 1-15. Finally, the model for the prediction of the ratio of platelet and plasma recovery efficiencies was written as a function of $V_{WB,}$ H and V_{UL} (Eqs. 17 and 18).

For the actual settling velocities:

$$\frac{E_{(Pt)UL}}{E_{(Pl)UL}} = 1.77\left(\frac{1-H_{BL}}{H_{BL}}\right), \quad R^2 = 0.94 \tag{16}$$

$$\frac{E_{(Pt)UL}}{E_{(Pl)UL}} = 1.77.\frac{V_{WB}(1-H)-V_{UL}}{V_{WB}H} \tag{17}$$

$$E_{(\mathbf{Pl})\mathbf{UL}} = \frac{V_{UL}}{(1-H)V_{WB}} \tag{18}$$

Note that to establish this model, WB was first collected from a single donor. The model was then validated using data from 10 healthy individuals who were in the age range of 25-30 years. The assumptions for the model are as follows: isothermal centrifugation (25°C); RBCs considered as spherical and rigid particles, range of G 50 to 820 g and time 1 to 10,000 sec (plausible conditions for preparation of PRP); discontinuous centrifugation with brake off, and sodium citrate as anticoagulant.

4.3 Results

4.3.1 Separation of the components of whole blood

We initially used the physical properties of WB to calculate the settling velocities at infinite dilution (υ_∞) as a function of *G* for the various WB components: RBCs, white blood cells (WBCs) and platelets. Figure 4.1a shows these settling velocities for WB cells as a function of G. The υ_∞ values increased with *G* for the types of blood cells considered, reaching different plateaus. Platelets, which are the smallest cells, moved more slowly than the other cells, allowing them to be separated from the RBCs. Figure 4.1b shows the positions of the cells in a centrifuge tube schematically; the positions reflect the theoretical cell separation after centrifugation,

without consideration of the interactions among particles.. We observed a supernatant, or UL, composed mainly of platelets plus some WBCs dispersed in the plasma; a pellet, or BL, in which all RBCs are settled, but which also contained platelets and WBCs and an intermediate thin layer, or BC, that was between the UL and the BL and was rich in WBCs.

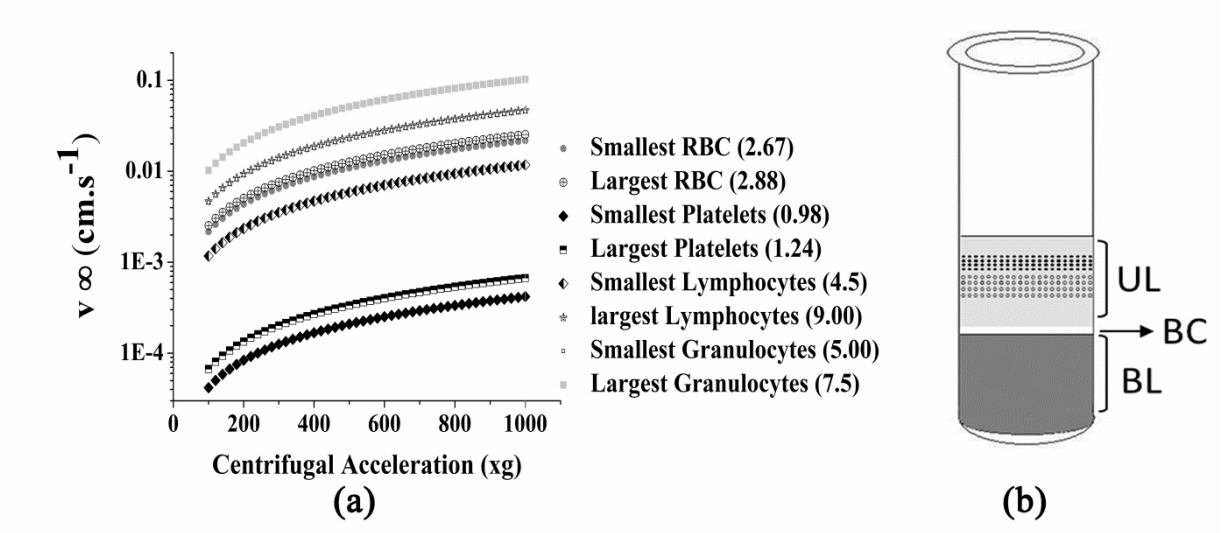

Figure 4.1(a) Settling velocities at infinite dilution, v_∞, as a function of the centrifugal acceleration (*G*), for the various cells in whole blood (size x 10^{-4} cm) and (b) relative positions of the blood cells inside the centrifuge tube after discontinuous centrifugation. Plasma (light gray), platelets (cells dispersed in plasma), buffy coat (BC; intermediate white blood cell layer), and concentrated red blood cells (RBCs) and other kinds of cells (dark gray) are positioned as shown.

4.3.2 Experimental parameters

Table 4.1 summarizes the experimental results (i.e., the UL and the UL+ BC volumes as well as the platelet concentrations and the factor of platelet concentration, F_{CP}, in the UL.

As expected, the UL volume increased with increasing *G*. At values of *G* ranging from 70 to 100 g, the platelet concentration in the UL was ~ 500 x 10^{-3} platelets/mm^3, while the platelet concentration decreased markedly at higher *G*.

Although the total BC volume was the same for all of the samples (0.6 mL), the platelet concentration in the UL+BC was lower at up to 460 g. However, it was higher in the UL+BC than in the UL at the highest values of G (550 and 820 g). These results show that at 550 and 820 g, the platelets stayed mainly in the BC. As a consequence, the F_{CP} had a maximum value of 2.0 in the UL at *G* up to 100xg, and it decreased at higher values of *G*.

Table 4.1 also shows the calculated values for H_{BL} and the recovery efficiencies of plasma ($E_{(Pl)UL}$) and platelets ($E_{(Pt)UL}$) in the UL as a function of *G*. From a hematocrit of ~ 0.4, H_{BL} increased up to 0.87, which shows the packing of the RBCs into the BL. $E_{(Pl)UL}$ increased with increasing *G* up to 90.5%, while $E_{(Pt)UL}$ increased from 60% to 70% for *G* up to 100 g and then decreased sharply to 8% as *G* rose toward 820 g.

Table 4.1 Experimental data and calculated parameters.

G (g)	$N_{(Pt)WB}$ ($Pt/mm^3 \times 10^{-3}$)	V_{UL} (mL)	$N_{(Pt)UL}$ ($Pt/mm^3 \times 10^{-3}$)	$N_{(Pt)UL+BC}$ ($Pt/mm^3 \times 10^{-3}$)	$F_{C(UL)}$	H_{BL}	$E_{(Pl)UL}$ (%)	$E_{(Pt)UL}$ (%)
50	230	1.0	481	361	2.1	0.52	45.3	60.0
70	264	1.2	540	396	2.0	0.59	55.9	70.1
100	245	1.3	467	379	1.9	0.63	62.0	70.8
190	246	1.4	350	174	1.4	0.66	66.7	56.9
280	241	1.7	178	117	0.7	0.77	81.0	35.9
370	230	1.8	117	57	0.5	0.82	85.7	26.2
460	235	1.8	92	82	0.4	0.82	85.7	20.1
550	260	1.9	114	128	0.4	0.87	90.5	23.8
820	247	1.9	36	109	0.1	0.87	90.5	7.9

Experimental data include platelet concentrations in the whole blood, upper layer, and upper layer plus buffy coat, as well as the volume of the upper layer. Calculated parameters include the platelet concentration factor, the packing of the red blood cells in the bottom layer, and the platelet and plasma recovery efficiencies as a function of centrifugal acceleration.

G, centrifugal acceleration; $N_{(Pt)WB}$, number of platelets per unit volume in whole blood; $N_{(Pt)UL}$, number of platelets per unit volume in the upper layer; $N_{(Pt)LP+BC}$, number of platelets per unit volume in the upper layer + buffy coat; V_{UL} , volume of the upper layer; $F_{C(UL)}$, platelet concentration factor; H_{BL}, packing of the red blood cells in the bottom layer; $E_{(Pl)UL}$ and $E_{(Pt)UL}$, plasma and platelet recovery efficiencies, respectively.

4.3.3 Recovery efficiencies of platelet and plasma

The analytical model (Eqs. 17 and 18) allowed us to predict the PtPIRE for a given volume of collected WB, V_{WB}, with hematocrit H, subjected to a given G for a defined time period. The model allows for the prediction of the PtPIRE.

Figure 4.2 shows the algorithm used for calculating the $E_{(Pt)UL}$ and $E_{(Pl)UL}$ using the derived model.

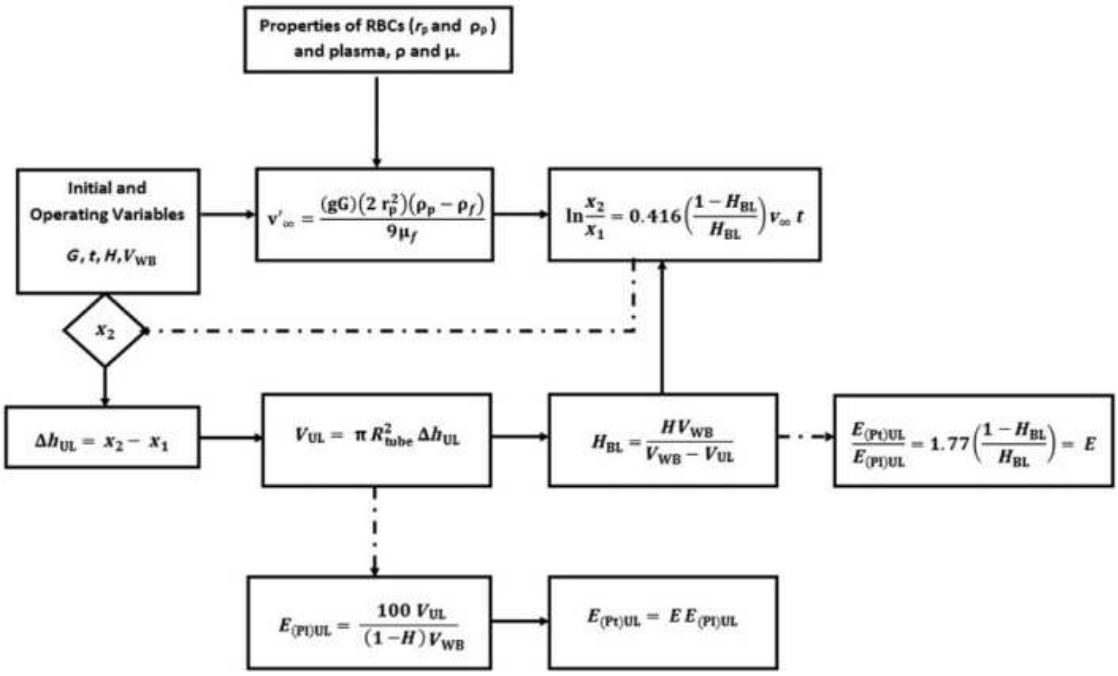

Figure 4.2 Algorithm for the calculation of plasma and platelet recovery efficiencies, E (Pt)UL and E (Pl)UL , respectively, using the derived model for the platelet and plasma recovery efficiencies (Equations 17 and 18).

4.3.4 Validation and performance of the model

Figure 4.3 shows the experimental data and the predicted values for the $E_{(Pt)UL}$ (Fig. 4.3a) and the $E_{(Pl)UL}$ (Fig. 4.3b). Notably, there were variations in the experimental data because there were several blood donors and because blood was collected on different days. The predicted $E_{(Pl)UL}$ fitted the experimental data better

than the predicted $E_{(Pt)UL}$ did. For the latter, the model underestimated the experimental data.

Figures 4.3c shows the performance of the model in terms of platelet concentration compared with the average of the experimental data. This graphical result is useful because it directly provides the platelet concentration for the preparer of PRP, and it also evaluates the performance of the centrifugation process.

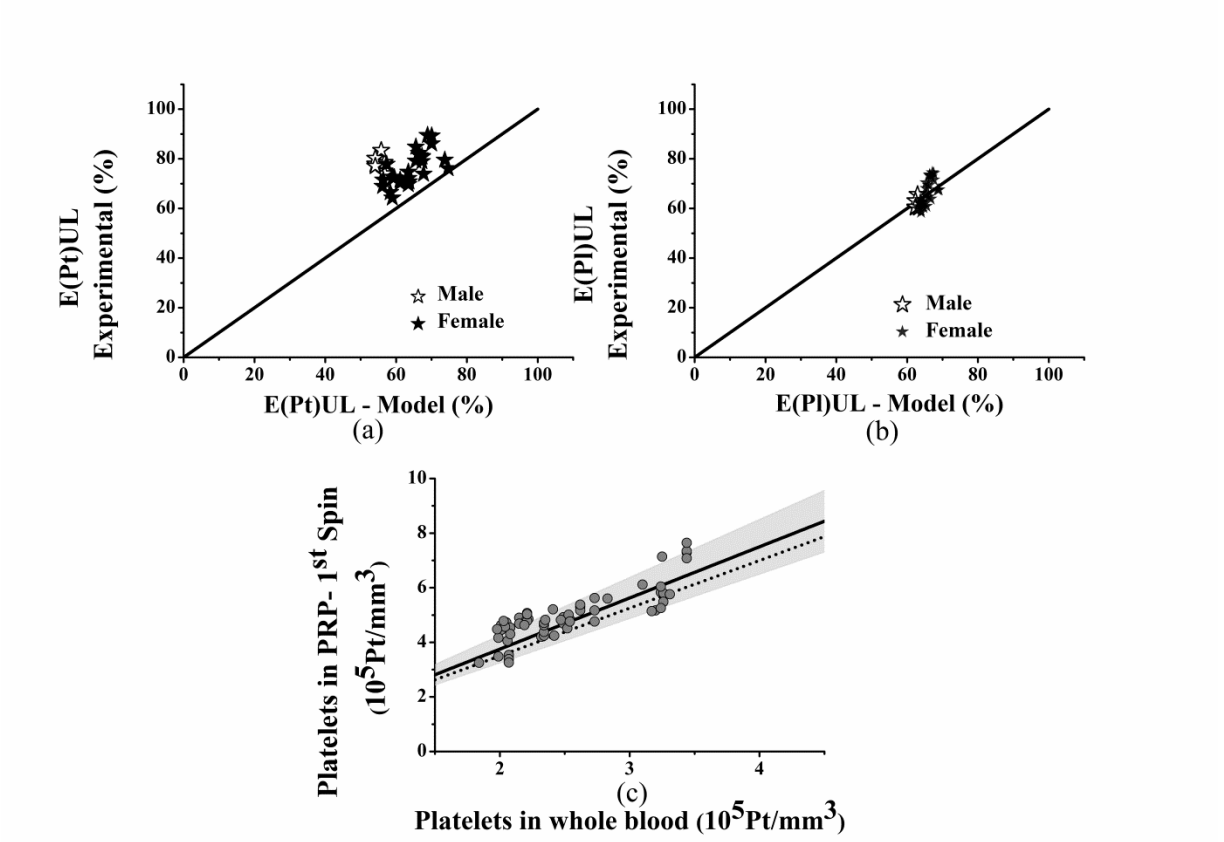

Figure 4.3 Validation and performance of the derived model with experimental data. The derived model was obtained from Equations 6–18. The experimental data were from 10 healthy individuals in the age range of 25–30 years, whose blood was centrifuged at 100 g for 600 sec. (a) Recovery efficiencies of platelets. (b) Recovery efficiencies of plasma. (c) Performance of the model in terms of the platelet concentrations before and after centrifugation. The solid line represents the experimental average of the platelets; the dashed line depicts the platelet

concentrations predicted by the model; and the grey zone is the dispersion of the experimental data.

4.3.5 Predicted behaviors

Figure 4.4 illustrates the behaviors for H_{BL}, $E_{(Pl)UL}$ and $E_{(Pt)UL}$, which were predicted using the model.

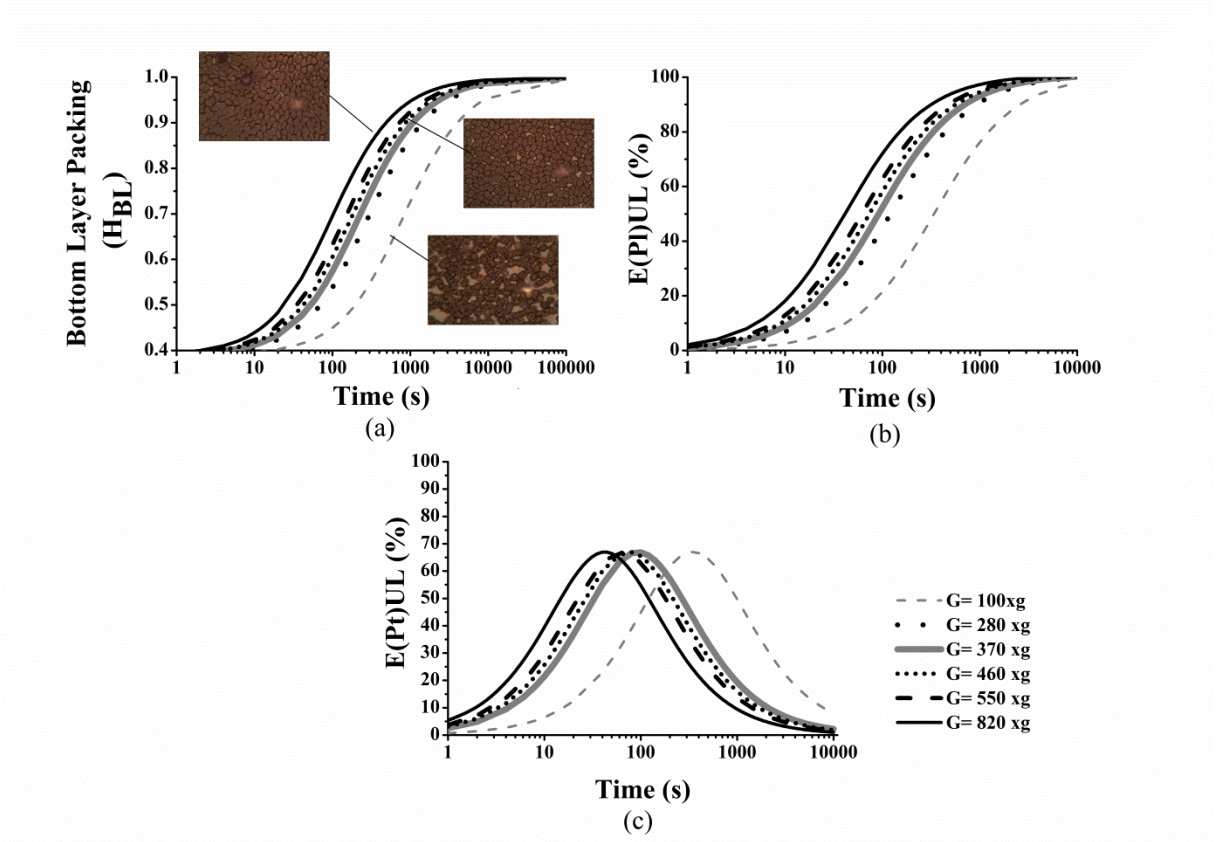

Figure 4.4 Influence of the operating variables G and time on (a) the packing of red blood cells in the bottom layer, (b) the recovery efficiency of plasma in the upper layer, and (c) the recovery efficiency of platelets on the upper layer.

The curves in Figure 4.4 show a sharp influence of both *G* and time on the separation behavior of RBCs, platelets and plasma. In Figure 4.4a, H_{BL} increases with *G* and time and asymptotically approaches 1, which is the maximum packing of RBCs, at a time of approximately 10,000 sec. The inset micrographs show the

differences in the RBC packing at 600 sec for values of *G* equal to 100, 280 and 820 g. A more porous BL was formed at 100 g, while at 820 g, a denser BL was obtained. In addition, it seems that at low values of *G*, the RBCs settle and pack in a configuration different from that of the individual elongated cells seen in the micrographs generated at higher *G*. This behavior recalls the effect of the natural rouleaux formation of RBCs at low shear rates. This is reflected by a rise in the RBC sedimentation rate, as previously reported.[18] This is consistent with the correlation described by Equation 9, in which at low *G* (low H_{BL}), the settling velocity v_x is higher than the terminal velocity determined for individual RBCs. Figure 4.4a also shows that at times less than 50 sec, the BL is still incipient, with an H_{BL} of $\sim$ 0.5. A well-established BL of RBCs can be defined as having an $H_{BL} \geq 0.6$ and facilitates the removal of the V_{UL} for the preparation of PRP.

Similarly, for the recovery of plasma (Fig. 4.4b), the curves increase with both G and time and reach the maximum (100% of plasma in the UL) at a time of ~10,000 s.

For platelets (Fig. 4.4c), the recovery efficiencies also increase with *G* and time, but they reach a maximum of 70% at times that are dependent on the value of *G*. The maxima of the curves correspond to times ranging from 50 to 400 sec, in which the packing of RBCs in the BL is approximately 60% (Fig. 4.4a).

Figure 4.5 shows the recovery efficiencies of platelets and plasma as predicted by the model (Eqs.17 and 18) at various *G*s and times for a V_{WB} of 3.5 mL and an average *H* equal to 0.4. It can be seen the overlapping of the curves at various *G*s and times. The figure also defines a point of maximum recovery of platelets, 70%, which corresponds to a recovery of 50% of the plasma. Therefore, the region around this point corresponds to the optimal condition for the recovery of platelets and plasma from WB by DC. Note that at $E_{(Pl)UL}$ <50%, the $E_{(Pt)UL}$ is higher than the $E_{(Pl)UL}$.

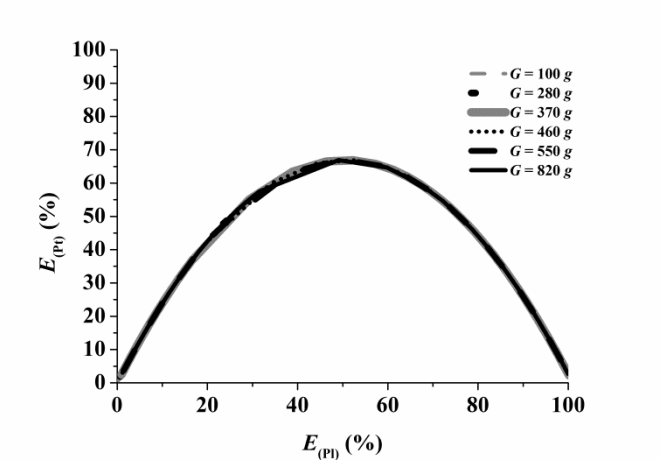

Figure 4.5 Behavior of the recovery efficiencies of platelets and plasma at centrifugal accelerations from 100 to 820 g and times from 1 to 10,000 sec for an average hematocrit 0.4. There is overlapping of the curves at the various Gs and times.

For a **G** of 100 g, the influence of the hematocrit on the recovery of platelets, as well as on the packing of RBCs and on the V_{UL}, is shown as a function of time in Figure 4.6. The recovery of the platelets decreases as the hematocrit increases, and this effect is most pronounced at the region of the maximum recovery of platelets.

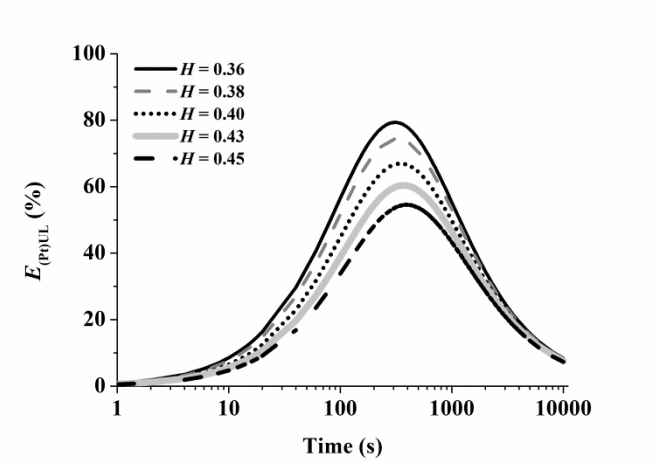

Figure 4.6 Influence of hematocrit and time on the recovery efficiency of platelets with centrifugal acceleration G = 100 g.

4.3.6 Modulation and Control

The modulation and control of the PtPIRE from centrifugation can be achieved through the operating variables *G*, time and hematocrit. Figure 4.4c shows that the maximum recovery of platelets can be obtained at higher *G*s and shorter times, or lower *G*s and longer times. However, high *G*s may affect the integrity of the platelets, a phenomenon which should be investigated. Therefore, low values of *G*, such as 100 g, provide a maximum recovery of platelets and should also preserve the integrity of the platelets. For 100 g, the times of maximum recovery of platelets are from 300 to 400 sec. These times should also determine the amount of WBCs such as lymphocytes, neutrophils and granulocytes in the UL, which must also be investigated. The control of the hematocrit can be achieved by dilution, which can be made with platelet-poor plasma. Such dilution enhances the recovery of Pts in the UL, as seen from the trend of the curves in Figure 4. 6.

4.4 Discussion

As expected, centrifugation separated the cells of WB based on their physical properties, which resulted in different settling velocities (Fig. 4.1a). However, the combined effects of density, viscosity and backflow of the suspension yielded Equation 9, which corrected the settling velocity of RBCs at infinite dilution by a factor that relates the concentration of voids to the concentration of RBCs in the BL. Since this factor took into account the partition of plasma between the BL and the UL, it also correlated well with the ratio of recovery efficiencies of the platelets and plasma. Surprisingly, at low *G*, the terminal velocity did not overestimate the actual speed of RBCs, a fact that we attribute to the effect of rouleaux formation, which increased the sedimentation rate, provided a more porous packing of RBCs in the BL and increased the recovery of platelets. Greater *G*s and times produced higher H_{BL} values, a decrease in the porosity of the BL and a sharp decrease in platelet recovery.

In discontinuous centrifugation, the cells are distributed in the tube in three phases: an UL, a BC fraction and a BL (Fig. 4.1b). The concentrations of platelets in the UL and in the UL+BC showed that the retention of platelets in the BC layer was

only ~ 10%, except when *G* was 820 *g*, which yielded a retention of 20% (Table 4.1). We used only the platelet concentration in the UL to derive the model for P-PRP. An important result from the experimental data was that a *G* equal to 100 *g* and a time of 600 sec resulted in the highest concentration of platelets in the UL, with an average concentration factor, F_{CP}, of 2.0. For other values of *G*, the F_{CP} was less than 1. The maximum F_{CP} corresponded to an H_{BL} of ~0.6, in which the fraction of plasma was 0.4 and the recovery efficiency of platelets was maximal, ~70% (Table 4.1). Therefore, lower *G* favored the recovery of platelets in the UL. In contrast, fast and dense packing of RBCs at higher *G* caused platelets losses of approximately 30–40% (Table 4.1). Therefore, the packing of the RBCs (H_{BL}) influenced the platelet separation from WB. As shown in Figure 4.3, the behavior predicted by the model was consistent with the trends in the experimental data. Therefore, although the model underestimated the recovery efficiency of platelets relative to the experimental data, we considered these predictions to be effective in light of the complexity and variability of an autologous product such as PRP. The advantage of the model is primarily its practicality because it includes the initial data of hematocrit and volume of WB, the upper volume generated as a function of the operating variables G and time, as well as the ease of the algorithm used to perform the calculations. In addition, the predictions from the model provide an understanding of the behavior of the separation and the modulation of the recovery of platelets using less blood as a raw material than could a solely experimental study.

A comparison of our results with those reported in the literature revealed that the recovery efficiencies of platelets and Pl in DC do not follow the 45° straight line that was described by Brown[17] for continuous centrifugation. With respect to the results reported for just one centrifugation by Kahn et al.[14] (100% recovery efficiency, *G* of 2300 to 3000 *g* and centrifugation time of 1 min) and Jo et al.[13] (92% recovery efficiency, *G* of 900 *g* and centrifugation time of 5 min), although the range of *G* they used is outside the range we studied, our experimental and predicted tendencies did not agree with theirs. Rather, our results indicate that for *G*s and times of this order of magnitude, the RBC packing still is incipient, the separation is not well

established, and it is difficult to assure reproducible data for the platelet recovery efficiency (Fig. 4.4).

Landesberg et al.[15] obtained an F_{CP} of 2 when centrifuging 5 mL of WB for 10 minutes at G = 100 g, and Araki et al.[12] obtained a platelet recovery efficiency of 70-80% using G = 70 g for 10 min. Both of these results are in agreement with our results.

Finally, the predictions of the behavior of separation of RBCs, platelets and plasma by DC allowed us to modulate and to control the recovery of platelets in terms of G, time and hematocrit.

These findings contribute to the preparation of PRP under a scientific basis and controlled conditions as well as the standardizing the PRP as an autologous product for specific applications. Studies to account for the effects of variations in the age range and the state of health of the individuals, as well as the integration of the centrifugation step with the activation step in the preparation of PRP, are ongoing in our group. These studies will allow a refinement of the model derived in this work for P-PRP.

4.5 Conclusions

This study showed that discontinuous centrifugation for the recovery of platelets, which is a crucial step in the preparation of PRP, can be described by a mathematical model that is based on a physical description of events. The model allowed us to predict the behavior of the separation of RBCs and to maximize, modulate and control the recovery efficiency of platelets through G, time and hematocrit by identification of the regions in which the efficiency of platelet recovery is maximal. Adopting these predicted conditions in P-PRP protocols will ensure that the composition of the P-PRP is controlled, reproducible and can even be modulated. These findings contribute to the standardization of the quality of P-PRP in a scientific basis for in vitro biological assays. The characterization and the interconnection

between the quality and biological properties of PRP form the basis for further clinical studies.

Acknowledgments

The authors appreciate the participation of the volunteer blood donors and thank the state financial agency, FAPESP (Fundação de Amparo a Pesquisa do Estado de São Paulo), Brazil, which supported this work.

Disclosure Statement

There are no competing financial interests to declare.

Abbreviations

BC: buffy coat

BL: bottom layer

DC: discontinuous centrifugation

$E_{(Pl)UL}$: recovery efficiency of plasma in the upper layer

$E_{(Pt)UL}$: recovery efficiency of platelets in the upper layer

F_{CP}: platelet concentration factor

G: centrifugal acceleration, defined as the number of times exceeding the acceleration due to gravity, g

H_{BL}: fraction of red blood cells in the BL

H_{WB}: hematocrit in whole blood (volume fraction of red blood cells in whole blood)

$N_{(Pt)WB}$: number of platelets per unit volume in whole blood

$N_{(Pt)UL}$: number of platelets per unit volume in the supernatant or upper layer

PRP: platelet-rich plasma

P-PRP: pure platelet-rich plasma (PRP rich in platelets only, where the buffy coat layer was not included)

Pt: platelets

Pl: plasma

Pt_{UL}: number of platelets in the supernatant or upper layer

Pt_{WB}: number of platelets in whole blood

RBCs: red blood cells

PtPlRE: recovery efficiency of platelets and plasma after centrifugation

UL: supernatant, or upper layer

V_{BL}: volume of the pellet, or bottom layer, after centrifugation

V_{UL}: volume of the supernatant, or upper layer,after centrifugation

$V_{(Pl)WB}$: volume of plasma in whole blood

V_{WB}: volume of whole blood

WB: whole blood

WBC: white blood cells or leukocytes

$v_{x:}$ actual or corrected settling velocity of red blood cells

v_{∞}: settling velocity of red blood cells at an infinite dilution

Δh_{UL}: height of the supernatant, or upper layer, after centrifugation

References

1. Engebretsen L, Steffen K, Alsousou J, et al. IOC consensus paper on the use of platelet-rich plasma in sports medicine. Br J Sports Med. 2010;44(15):1072-1081.

2. Harrison P, Cramer EM. Platelet alpha-granules. Blood Rev. 1993;7(1):52-62.

3. Werner S, Grose R. Regulation of wound healing by growth factors and cytokines. Physiological Reviews. 2003;83(3):835-870.

4. de Vos RJ, Weir A, van Schie HT, et al. Platelet-rich plasma injection for chronic Achilles tendinopathy: a randomized controlled trial. JAMA. 2010;303(2):144-149.

5. Mishra A, Pavelko T. Treatment of chronic elbow tendinosis with buffered platelet-rich plasma. Am J Sports Med. 2006;34(11):1774-1778.

6. Peerbooms JC, Sluimer J, Bruijn DJ, Gosens T. Positive effect of an autologous platelet concentrate in lateral epicondylitis in a double-blind randomized controlled trial: platelet-rich plasma versus corticosteroid injection with a 1-year follow-up. Am J Sports Med. 2010;38(2):255-262.

7. Anitua E, Sanchez M, Nurden AT, et al. Platelet-released growth factors enhance the secretion of hyaluronic acid and induce hepatocyte growth factor production by synovial fibroblasts from arthritic patients. Rheumatology (Oxford). 2007;46(12):1769-1772.

8. Crovetti G, Martinelli G, Issi M, et al. Platelet gel for healing cutaneous chronic wounds. Transfus Apher Sci. 2004;30(2):145-151.

9. El-Sharkawy H, Kantarci A, Deady J, et al. Platelet-rich plasma: growth factors and pro- and anti-inflammatory properties. J Periodontol. 2007;78(4):661-669.

10. Hom DB, Linzie BM, Huang TC. The healing effects of autologous platelet gel on acute human skin wounds. Arch Facial Plast Surg. 2007;9(3):174-183.

11. van den Dolder J, Mooren R, Vloon AP, Stoelinga PJ, Jansen JA. Platelet-rich plasma: quantification of growth factor levels and the effect on growth and differentiation of rat bone marrow cells. Tissue Eng. 2006;12(11):3067-3073.

12. Araki J, Jona M, Eto H, et al. Optimized preparation method of platelet-concentrated plasma and noncoagulating platelet-derived factor concentrates: maximization of platelet concentration and removal of fibrinogen. Tissue Eng Part C Methods. 2012;18(3):176-185.

13. Jo CH, Roh YH, Kim JE, Shin S, Yoon KS, Noh JH. Optimizing platelet-rich plasma gel formation by varying time and gravitational forces during centrifugation. Journal of Oral Implantology. 2011.

14. Kahn RA, Cossette I, Friedman LI. Optimum centrifugation conditions for the preparation of platelet and plasma products. Transfusion. 1976;16(2):162-165.

15. Landesberg R, Roy M, Glickman RS. Quantification of growth factor levels using a simplified method of platelet-rich plasma gel preparation. Journal of Oral and Maxillofacial Surgery. 2000;58(3):297-300.

16. Hunter RJ. *Foundations of Colloid Science*: Oxford University Press: USA, 2001.

17. Brown RI. The Physics of Continuous Flow Centrifugal Cell Separation. Artificial Organs. 1989;13(1):4-20.

18. Salsbury AJ. Effect of transfusion materials on rouleaux formation and sedimentation rate of erythrocytes. Br Med J. 1967;4.

19. Penington D, Lee N, Roxburgh A, McGready J. Platelet density and size: the interpretation of heterogeneity. British journal of haematology. 1976;34(3):365-376.

Capítulo 5. Fibrin Network Architectures in Pure Platelet-Rich Plasma as Characterized by Fiber Radius and Correlated with Clotting Time

Amanda G.M Perez[a], Ana A. Rodrigues[b], Angela C.M. Luzo[c], José F.S.D. Lana[a,b,d,] William D. Belangero[b] and Maria H. A. Santana[a*]

[a]Department of Engineering of Materials and Bioprocesses- School of Chemical Engineering, University of Campinas, Albert Einstein Av., 500, 13083-852, Campinas-SP, Brazil.

[b]Department of Orthopaedic and Traumatology - Faculty of Medical Sciences, University of Campinas, Cinco de Julho St., 350, 13083-970, Campinas-SP, Brazil.

[c]Haematology and Hemotherapy Center, Umbilical Cord Blood Bank, University of Campinas, Carlos Chagas St., 480, 13083-878, Campinas-SP, Brazil.

[d]Research Institute of Sports Medicine, Orthopedics and Regeneration - iMOR, Santos Dumont St., 2946, 38000-000, Uberaba-MG, Brazil.

*Correspondence to:

Maria Helena A Santana; e-mail: mariahelena.santana@gmail.com

Phone: +55-19-35213921

Abstract Fibrin networks are obtained through activation of platelet-rich plasma (PRP) for use in tissue regeneration. The importance of fibrin networks relies on mediation of release of growth factors, proliferation of tissue cells and rheological properties of the fibrin gels. Activation of PRP usually involves the decomposition of fibrinogen by agonists, in a wide range of, concentrations. Therefore fibrin networks with a large structural diversity are formed, making comparative evaluations difficult. In order to standardize the fibrin networks, we used the statistical techniques central

composite rotatable design and response-surface analysis, to correlate the radius of the fibers with the ratios between the agonists (autologous serum/calcium chloride) and agonist/PRP. From an individual and interactive analysis of the variables, architectures characterized by thick, medium and thin fibers were delineated on the response-surface. Furthermore, the architectures were correlated with coagulation time. This approach is valuable for standardizing the PRP preparation for clinical applications.

KEYWORDS platelet-rich plasma, fibrin networks, clotting time, response-surface analysis, central composite rotatable design

5.1 Introduction

Platelet-rich plasma (PRP) is an autologous preparation that concentrates platelets in a small volume of plasma [1]. Platelets are rich in growth factors (GFs), which play an important role in the healing process and tissue regeneration. PRP has the necessary biopolymers, such as fibrinogen and thrombin, and also calcium for the formation of fibrin networks whereby the GFs from platelets are released [2]. Among the various classifications of PRPs, the most current classifications consider networks from platelet concentrates in plasma that are low in leukocytes (pure PRP, or P-PRP); rich in leukocytes (L-PRP), including the leukocyte layer from the centrifugation of whole blood; rich in fibrin and platelets (P-PRF); and rich in leukocytes and fibrin (L-PRF) [3].

The preparation of P-PRP and L-PRP is a sequential process that involves two main steps: 1.the separation and concentration of platelets and 2. platelet activation and the formation of fibrin networks. The events in the second step are similar to those in the natural coagulation cascade: fibrinogen is cleaved by thrombin and is responsible for the processes of hemostasis, platelet adhesion and aggregation toward to form a fibrin network, the structural scaffold of blood clots [4]. The conversion of fibrinogen into networks of fibrin fibers occurs through a series of steps. After vessel injury, thrombin cleaves fibrinogen at four sites, catalyzing the hydrolytic removal of fibrinopeptides A and B, which exposes binding sites in fibrinogen's central

domain. These sites interact with complementary sites in the end domains of fibrin molecules. After the removal of fibrinopeptide A, monomer-monomer and monomer-fibrinogen interactions are favored, and the formation of protofibrils begins. These interactions are enhanced by the removal of fibrinopeptide B, leading to more rapid and longer protofibril formation. Fibrinopeptide B is responsible for the lateral aggregation of the protofibrils in slower reactions than the protofibrils' elongation. Lastly, the protofibrils assemble into fibers, yielding three-dimensional fibrin networks [5-7].

Other parameters such as pH, ionic strength and calcium ion concentration also affect the conversion of fibrinogen to fibrin [8-10]. Particularly, calcium stabilizes fibrinogen structure, accelerates fibrin formation by acting as a thrombin cofactor, can partially protect fibrinogen degradation and also inhibits the polymerization of fibrin fibers [9, 11, 12].

The formation of fibrin networks has been extensively studied in the literature [5, 13-19]. In general, purified human fibrinogen and bovine thrombin are used to evaluate the extension of the fibrinogen hydrolysis reaction, the formation of fibrin networks and the stability of the clots. Studies have also shown the relative kinetics of the release of fibrinopeptides A and B [20, 21] and the influence of the fibrinogen/thrombin ratio and the ionic strength on physical properties of the fibrin networks, such as fiber diameter, mass/length, density, porosity and permeability, which may lead to changes in cell adhesion and migration [21]. The fibrin networks are mainly controlled by the reactions of fibrin polymerization and fibrinogen decomposition [22-24].

Studies on the formation of fibrin networks from PRP still are scarce. The few reports in the literature aimed at general classification related to the presence of leukocytes and the richness of fibrin [3]. Calcium chloride and purified human thrombin are the most commonly used agonists in PRP activation [25]. More recently, clinical studies have used autologous purified thrombin [26, 27]. Autologous serum, containing thrombin and other proteins, obtained from centrifugation of the whole

blood in the absence of anticoagulant [28] as well as calcium alone [27, 28] have also been used. Other studies prepare fibrin networks in PRP without the addition of agonists but with blood collection in the absence of anticoagulants. In the last case, the activation of platelets occurs during the centrifugation step for red blood-cell separation, resulting in fibrin-rich (PRF) or Choukroun-type PRP [3].

Although the scarce studies, innumerous applications of PRPs in different therapies have been reported. Researchers and physicians desire a standardization of PRP to enable the comparison of clinical results. For the same class of PRP, different separation efficiencies and concentrations of platelets can be obtained, and several fibrin networks can be generated with different radii and mass/length, depending on the preparation conditions. Moreover, the autologous nature of PRP leads to significant variability among individuals. In addition to these factors, the autologous nature of PRP limits the amount of raw material available for studies, which must be performed using a reduced number of experiments. Therefore, studying PRP on a scientific basis is a challenge.

Aiming to standardize the fibrin networks in PRP preparation, this work used a central composite rotatable design (CCRD) and response-surface analysis as statistical techniques for the evaluation of the effects of activation variables in P-PRP on the radii of fibrin fibers. Our hypothesis was that numerous networks could be grouped in a smaller number of architectures, comprising ranges of radii of fibrin fibers, with a statistical rigor. The technique also was used for grouping clotting times in ranges which were correlated with the fibrin network architectures. The biological impact of these results is to contribute to the understanding the effects of the variables involved in PRP activation. They also are relevant by making further physicochemical and biological studies feasible towards PRP standardization in a scientific basis. To the best of our knowledge, the present work is the first report where the fibrin networks generated by PRP activation were characterized by architectures and correlated with the clotting time.

5.2 Materials and Methods

This study was approved by the Ethics Committee of the Medical Sciences School of the University of Campinas (UNICAMP), CAAE: 0972.0.146.000-11. All donors were healthy individuals aged between 20 and 30 years who were previously assessed by clinical examination.

5.2.1 Blood collection

P-PRP manipulation was performed with 3.15 mL of whole blood (WB), collected in 3.5 mL tubes (Vacuette, Ref. 454327; Greiner Bio-One GmbH, Frickenhausen, Germany) that containing 0.35 mL of 3.2% sodium citrate, as anticoagulant. Besides hemogram, fibrinogen was also dosed by coagulometric method.

5.2.2 P-PRP preparation

The WB was centrifuged at 100xg for 10 min in a Rotina 380R centrifuge (Hettich, Zentrifugen), with the run-up and run-down speeds set to shorter times. Those conditions were selected for maximum efficiency of platelet recovery, according to our previous work [29].

After the formation of three layers : a bottom layer composed of RBCs; an upper layer composed mainly of plasma and platelets but also containing low amounts of white blood cells (WBCs); and an intermediate layer, or buffy coat, primarily composed of WBCs, the upper layer was collected with a pipette to obtain P-PRP. This collection was performed carefully to avoid disturbing the bottom layer of RBCs and the buffy coat layer. The collected samples were then transferred to empty siliconized glass tubes to be homogenized. Afterward, blood cell counts were performed with cell counting equipment (Micros ES 60 Horiba®). The prepared P-PRP was characterized based on the platelet and WBC concentrations.

5.2.3 Autologous serum preparation

Autologous serum was prepared by collecting 5 mL of WB in tubes without anticoagulant[28]. After 30 min of clot formation, the WB was centrifuged at 2000 xg for 10 min. The upper phase was the autologous serum used to activate the PRP preparations.

5.2.4 P-PRP activation

P-PRP activation was performed in a 96-well microplate. Volumetric percentages of the agonist related to P-PRP (A/PRP) from 10 to 30% and volumetric serum/$CaCl_2$ (S/$CaCl_2$) ratios from 0.1 to 9.0 were used to adhere to the statistical technique of CCRD. The final volume of all preparations was 200 µL.

5.2.5 Radius and mass/length of fibrin fibers

Radius and mass/length were the parameters used for the characterization of the fibrin fibers in the networks. The parameters were calculated using the complete Carr equation [19] (Eq. 1):

$$\tau\lambda^5 = \frac{2\pi^3 Cn\mu\left(\frac{dn}{dC}^2\right)\frac{44}{15}\left(\lambda^2 - \frac{184}{154}\pi^2 r^2 n^2\right)}{N} \quad (1)$$

Where τ is the turbidity of the solutions; C is the initial fibrinogen concentration $(g.cm^3)^{-1}$; N is Avogadro's number; λ is the incident wavelength (cm); µ=mf/L, with mf being the protein mass in a fiber (Da) of length L (cm) and radius r (cm);n=1.33; and dn/dC= 0.17594 cm.

Next, $\tau\lambda^5$ was plotted against λ^2, resulting in a straight line whose slope yielded the mass/length ratio, and the ordinate at the origin gave the square of the average radius.

The turbidity was calculated from the optical density of the gelled fibrin networks using Eq. 2, where D is the optical density:

$$\tau = 1 - \exp(-D.\ln(10)) \quad (2)$$

5.2.6 Clotting time

The clotting time was determined by measurements of the optical density (OD) of the gelled fibrin networks at a 640 nm wavelength, 2 h after the activation of the P-PRP. From the kinetic profiles obtained, two straight lines were traced on the curves: one at the plateau of constant OD and the other as a tangent at the origin of the curves (t=0). The clotting time was determined from the interception of the two straight lines.

5.2.7 CCRD and response-surfaces

The effects of autologous serum, calcium and PRP composition on the fibrin networks were evaluated by the statistical techniques CCRD and response-surface analysis [30] . Various fibrin networks were generated through P-PRP activation under different conditions according to the CCRD. The CCRD was planned for two independent variables with three repetitions at the central level (0) in a total of 11 experiments. The software Statistica 7.0 (Statsoft Inc., USA) was used to analyze the results.

Two CCRDs were planned, with one in a calcium-rich region and the other in a serum-rich region, as detailed in Table 5.1. The surface responses were constructed from experimental data from a single healthy blood donor to ensure clear tendencies. Afterward, the statistical model was validated using data from additional healthy donors in the same range of ages.

Table 5.1 Central composite rotatable design (CCRD) for the variables serum/$CaCl_2$ (S/$CaCl_2$) and agonist/PRP (A/PRP) in regions rich in calcium and serum.

Coded variables		**Calcium-rich region – real variables**			**Serum-rich region – real variables**		
X1 S/$CaCl_2$	X2 A/PRP (%)	Assay Ca(E)	x1 S/$CaCl_2$	x2 A/PRP (%)	Assay S(E)	x1 S/$CaCl_2$	x2 A/PRP (%)
-1	-1	(E1)	0.23	13	(E1)	2.2	13
1	-1	(E2)	0.87	13	(E2)	7.8	13
-1	1	(E3)	0.23	27	(E3)	2.2	27
1	1	(E4)	0.87	27	(E4)	7.8	27
-1.41	0	(E5)	0.10	20	(E5)	1.0	20
1.41	0	(E6)	1.00	20	(E6)	9.0	20
0	-1.41	(E7)	0.55	10	(E7)	5	10
0	1.41	(E8)	0.55	30	(E8)	5	30
0	0	(E9)	0.55	20	(E9)	5	20
0	0	(E10)	0.55	20	(E10)	5	20
0	0	(E11)	0.55	20	(E11)	5	20

5.2.8 Independent variables

The independent variables were selected to represent the formation of the fibrin networks in terms of the polymerization of fibrin fibers (volumetric agonists ratio: autologous serum/$CaCl_2$) and the decomposition reaction of fibrinogen (volumetric percentage of agonist/PRP ratio). Volumetric ratios were chosen because these ratios are practical variables easily controlled, that are commonly used in clinical preparations of PRP [31-33].

5.2.9 Response variables

The radius (r) of the fibrin fibers and clotting time were the response variables for PRP activation study. Mass/length also was determined for the fibrin fibers by Eq

(1), but its response-surface could not be generated within the constraints of Statistica 7.0.

5.2.10 Characterization of fibrin network architectures

The fibrin network architectures were characterized by delineated ranges of radius in which the fibrin fibers were classified as thick, medium and thin. These ranges are shown in color gradients on the response-surface.

5.2.11 Images of the fibrin networks

Samples were fixed in a solution of 4% paraformaldehyde and 2.5% glutaraldehyde in phosphate buffer, pH 7.4, for 2 h. The samples were then dehydrated in ethanol for 15min intervals using the ethanol dilutions in water (50%, 70%, 95% and 100% (2x)) and dried at the critical point. After gold coating (Sputter Coater POLARON, SC7620, VG Microtech), the samples were visualized with a scanning electron microscope (Leo440iLEO) with an accelerating voltage of 20 kV.

5.3 Results and discussion

5.3.1 Characterization of P-PRP

Table 5.2 shows the platelet and WBC concentrations in WB and in P-PRP. The platelets in the P-PRP were concentrated approximately 2 to 3 times above baseline by only one centrifugation step at 100 xg for 10 min. Under these conditions, the average recovery efficiencies were approximately 80% for platelets and 10% for WBCs. The concentration of RBC in all P-PRP samples ranged from 0 to 0.03 x 10^6 cells/mm^3.

Table 5.2 Concentration of platelets (Pt) and white blood cells (WBCs) in whole blood (WB) and in pure platelet-rich plasma (P-PRP), and Fibrinogen in WB. FCPt is the platelet concentration factor.

	Donor	Ptx10^3/mm^3 (±SD)	WBCsx10^3/mm^3 (±SD)	FCPt [a]	E(Pt) (%)[b]	Fibrinogen (mg/dL)
Whole Blood	1	233 ±7.9	8.3 ±0.2	-	-	212
	2	208 ±7.9	5.6 ±0.1	-	-	276
	3	283	5.5	-	-	265
	4	142 ±2.5	5.8 ±0.1	-	-	341
	5	191 ±5.0	4.9 ±0.05	-	-	327
	6	326 ±1.5	6.1 ±0.1	-	-	350
	7	223 ±2.5	3.6 ±0.1	-	-	381
	8	247 ±12.5	5.7 ±0.1	-	-	305
	9	216 ±0.1	7.8 ±0	-	-	335
	10	210 ±2.5	6.1 ±0.1	-	-	283
P-PRP	1	565 ±18	1.9 ±0.3	2.4	62.4	-
	2	463 ±10	1.7 ±0.3	2.2	76.4	-
	3	560	1.2	2.0	84.8	-
	4	378 ±2.5	3.2 ±0	2.6	91.5 ±0.8	-
	5	418 ±3.5	2.0 ±0.05	2.2	87.7 ±1.3	-
	6	779 ±2.0	4.1 ±0.9	2.4	91.6 ±2.4	-
	7	496 ±24	2.4 ±0.1	2.2	76.3 ±2.3	-
	8	582 ±10	1.2 ±0.2	2.4	100.9 ±2.8	-
	9	542 ±1.5	1.1 ±0	2.5	100.5 ±0.5	-
	10	680 ±12	4.8 ±0.9	3.1	49.2	-

[a]*FCPt = Pt concentration in P-PRP/Pt concentration in WB*

[b]*Platelet recovery = [(Pt concentration in P-PRP x P-PRP volume) / (Pt concentration in WB x WB volume)] x 100*

5.3.2 CCRD analysis in the calcium-rich region

Although ODs were measured, only the conditions of the Ca assays (E1, E2, E6, E7) formed gels macroscopically during the first 2 h, most likely due to the high concentrations of $CaCl_2$. Carr et al (1986)[5] reported that at ionic strengths below 0.10, the presence of 5 $mMCa^{2+}$ caused the precipitation and macroscopic aggregation of fibrinogen. Because the gels were obtained from only four conditions, the surface response could not be drawn. The validation of these assays was performed by repeating the assays with four more donors (donors 2, 3, 8 and 9). The results for the parameters of radius and mass/length are shown in Table 5.3. Most of the radii of the fibers were between 75 and 85 nm. The mass/length ratio showed that an excess of calcium in relation to the serum produced short and dense fibrin fibers.

Table 5.3 Radius (r) and mass/length obtained from the assays (E1, E2, E6, E7) for the donors whose P-PRPs were characterized in Table 5.2.

Assay Ca(E)	S/ $CaCl_2$	A/PRP (%)	r(nm)[a]					mass/length x10^{12} (Da/cm)[a]				
			Donors					Donors				
			1	2	3	8	9	1	2	3	8	9
(E1)	0.23	13	78.4	84.8	77.3	85.5 -	83.7 ±1.4	5.1	9.3	8.6	8.3 -	7.7 ±0.9
(E2)	0.87	13	75.9	83.7	71.5	77.8 ±0.5	82.1 ±0.5	9.7	8.45	3.8	6.1 ±0.02	6.6 ±0.1
(E6)	1.00	20	80.1	75.5	-	85.6 ±1.0	84.1 ±0.7	5.2	7.8	-	5.0 ±0.5	7.5 ±0.2
(E7)	0.55	10	72.4	94.1	78.0	83.8 ±0.8	82.7 ±0.1	6.0	6.7	8.6	6.8 ±0.15	6.4 ±0.5

[a] *The values were determined using the Carr equation (Eq. 1).*

Indeed, calcium inhibits the elongation of the fibers (polymerization of fibrin) by neutralizing negative charges at the ends of the fibrinopeptides generated from the cleavage of fibrinogen. The difference in radius reflects lateral aggregation, which depends more on the A/PRP ratio (assays E6 and E7) because this parameter is associated with the fibrinogen concentration in the hydrolysis reaction.

The variability of the data was mainly due to the differences in the concentrations of platelets and fibrinogen from the donors, as shown in Table 5.2.

5.3.3 CCRD analysis in the serum-rich region

Table 5.4 shows the responses for radius, mass/length and clotting time for the CCRD performed in the serum-rich region.

Table 5.4 Mass/length, radius (r) and clotting time (Ct) for the fibrin fibers in the serum-rich region. The assays in the CCRD were described in Table 5.1. The data were from donor 1.

Assay S(E)	**S/ $CaCl_2$**	**A/PRP (%)**	**mass/length x 10^{12} (Da/cm)[a]**	**r (nm)[a]**	**Ct (s)**
(E1)	2.2	13	3,09	56.68	180
(E2)	7.8	13	2,00	52.29	500
(E3)	2.2	27	2,69	69.61	850
(E4)	7.8	27	1,51	38.93	0
(E5)	1.0	20	4,25	71.33	740
(E6)	9.0	20	1,69	40.72	0
(E7)	5	10	2,19	53.37	300
(E8)	5	30	4,58	68.41	130
(E9)	5	20	2,84	54.27	130
(E10)	5	20	1,96	53.36	125
(E11)	5	20	2,59	56.68	100

[a]*The values were determined using the Carr equation (Eq. 1).*

In the serum-rich region, the fibers were thinner and longer than in the region rich in calcium (Table 5.3). An increase in S/$CaCl_2$ reduced the mass/length ratio, leading to longer fibers. The clotting times were short and nearly instantaneous at high S/$CaCl_2$ and A/PRP ratios. These results are in agreement with the physicochemical phenomena because the thinner the fibers the higher is their entanglement favoring aggregation and gel formation, thus strongly reducing clotting time.

Regarding the reproducibility of the results based on repetition at the central point (assays 9 to 11), differences of less than 10% were observed for the radii and of approximately 30% were noted for the clotting times.

5.3.4 Significance of the effects of the independent variables

Figure 5.1 shows the Pareto diagrams for the statistical effects of the independent variables on the radius, mass/length and clotting time responses.

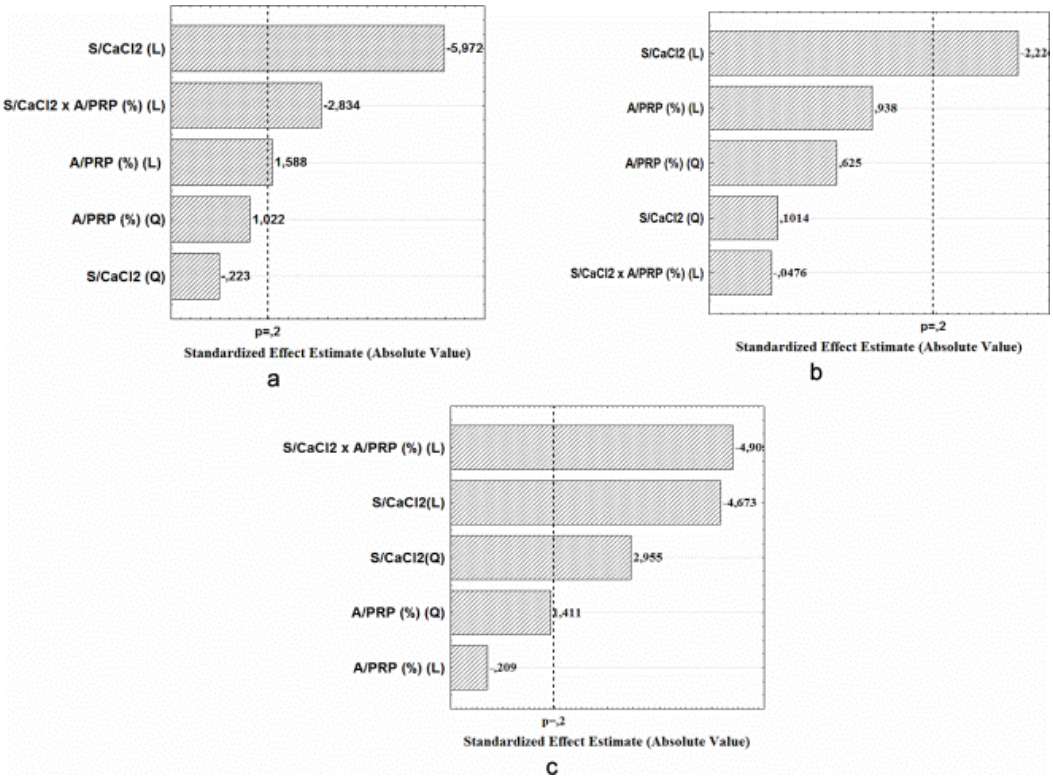

Figure 5.1 Pareto diagrams. Effects of the variables $S/CaCl_2$ and A/PRP and their interactions on (a) the radius of the fibers, (b) the mass/length of the fibers and (c) the clotting time.

The Pareto diagrams show that the effects of the individual variables and their interactions on the response radius were significant at a significance level of 80% (p-value of 0.2). However, for mass/length, only the variable $S/CaCl_2$ was significant. These results are physically coherent because the response in terms of mass/length

represents the polymerization of the fibrin fibers, whose elongation depends only on the S/$CaCl_2$ ratio, being independent of the fibrinogen decomposition.

In both cases, the linear effects of the variables were much greater than the quadratic effects.

The linear terms for the variable S/$CaCl_2$ and for its interaction with A/PRP had negative effects on the response radius. Therefore, increasing the S/$CaCl_2$ ratio decreased the radius of the fibers. The opposite effect occurred for the linear term for A/PRP. These results are consistent with the results presented in the literature for activation with purified thrombin and calcium chloride.[14, 34, 35] At higher thrombin concentrations, fibrinopeptide cleavage and protofibril formation are faster than lateral aggregation, leading to the formation of thin protofibrils. However, at low thrombin concentrations, the rate of fibrinopeptide cleavage is lower, and protofibrils form more slowly, while lateral aggregation increases the radius of the fibers [17].

Although lower (in absolute value) than for the radius, the linear term for the variable S/$CaCl_2$ also had a negative effect on the mass/length response: an increase in the S/$CaCl_2$ ratio decreased the mass/length. Therefore, longer fibers were formed at higher S/$CaCl_2$ ratios. Blomback [34] and Shah [16] observed the same tendency and observed that the mass/length values decreased much more slowly when the network was produced in plasma than in purified fibrinogen.

The linear terms, for the variable S/$CaCl_2$ and for the interaction between the variables, had negative effects on the response clotting time. For the linear effects, an increasing S/$CaCl_2$ and A/PRP decreased the clotting time.

In summary increasing S/$CaCl_2$ reduces radius, mass/length and clotting time. The interaction with A/PRP also reduced radius and clotting time, but it had no effect on mass/length.

5.3.5 Statistical analysis and models

The regression coefficients for the models that predict the radius of the fibrin fibers (r) and clotting time (Ct) as function of the studied variables are shown in Chart 1 (a).The linear terms for both variables and the interactions between the two independent variables were significant ($p<0.20$) for the response fiber radius (r).

The ANOVA is shown in Chart 1 (b). The correlation coefficients were 0.94 and 0.96 for the fiber radius and clotting time, respectively. The calculated F-value was approximately 8.0 times higher than the listed F for both responses. Therefore, the coded models were considered adequate to describe the response-surface for the radius of the fibers (Chart 1 (c)) and the clotting time (Chart 1(d)).

As expected from the effects results, the analysis of variance (ANOVA) for the response variable mass/length was not good enough to build a predictive model because the variable effects were very small in absolute values.

a

Factor	Regression coefficient		Standard error		t-value		p-value	
	r	*Ct*	*r*	*Ct*	*r*	*Ct*	*r*	*Ct*
Mean	54.86	118.33	2.68	68.85	20.48	1.72	0.0000*	0,1463**
$S/CaCl_2$ (L)	-9.79	-197.07	1.64	42.17	-5.97	-4.67	0.0019*	0,0055*
$S/CaCl_2$ (Q)	-0.43	148.33	1.95	50.19	-0.22	2.96	0.8323	0,0317*
A/PRP (%) (L)	2.60	-8.80	1.64	42.17	1.56	-0.21	0.1731**	0,8429
A/PRP (%) (Q)	1.99	70.83	1.95	50.19	1.02	1.41	0.3536	0,2172
$S/CaCl_2$ x A/PRP (%) (L)	-6.57	-292.50	2.32	59.63	-2.83	-4.91	0.0365*	0,0043*

**p <0.05 and **p<0.2*

b

Source of variation	Sum of squares		Degrees of freedom		Mean squares		F-test[a]	
	r	*Ct*	*r*	*Ct*	*r*	*Ct*	*r*	*Ct*
Regression	994.45	805485.45	3	4	331.48	201371.36	17.00	16.84
Residual	136.50	71740.53	7	6	19.50	11956.75		
Lack of fit	129.53	71223.86	5	4				
Pure Error	6.98	516.67	2	2				
Total	1130.96	877225.98	-	-				

Regression coefficients: R_r = 0.94 and R_{Ct}=0.96; [a]F(0.80;3:7) = 2.02 and F(0.80;4:6)= 2.10

c

$$r = 56.0 - 9.8.\frac{S}{CaCl_2} + 2.6.\frac{A}{PRP} - 6.6.\left(\frac{S}{CaCl_2}.\frac{A}{PRP}\right)$$

d

$$Ct = 118.3 - 197.1\frac{S}{CaCl_2} + 148.3\left(\frac{S}{CaCl_2}\right)^2 + 70.8\left(\frac{A}{PRP}\right)^2 - 292.5\left(\frac{S}{CaCl_2}.\frac{A}{PRP}\right)$$

Chart 5.1 Statistical parameters and model equations for radius (r) and clotting time (Ct). Regression coefficients (a), ANOVA with full factorial design in the region rich in serum (b), model equations for radius (c) and the clotting time (d).

5.3.6 Responses surfaces

Figure 5.2 represents the response-surface for the radius predicted by the model. Increasing the $S/CaCl_2$ ratio caused a decrease in the fiber radius, which was more pronounced for higher proportions of A/PRP. The assays detailed in Table 5.4 clearly delineated three regions that represent the architectures of the networks (A1-A3) on

the response surface (Figure 5.2b). From the gradient of colors, we can observe that the architecture A1 (thick fibers) included networks with fiber radii between 70 and 80 nm, whereas in architecture A2 (medium fibers) the radii ranged between 60 and 70 nm, and in architecture A3 (thin fibers) the radii were between 40 and 50 nm.

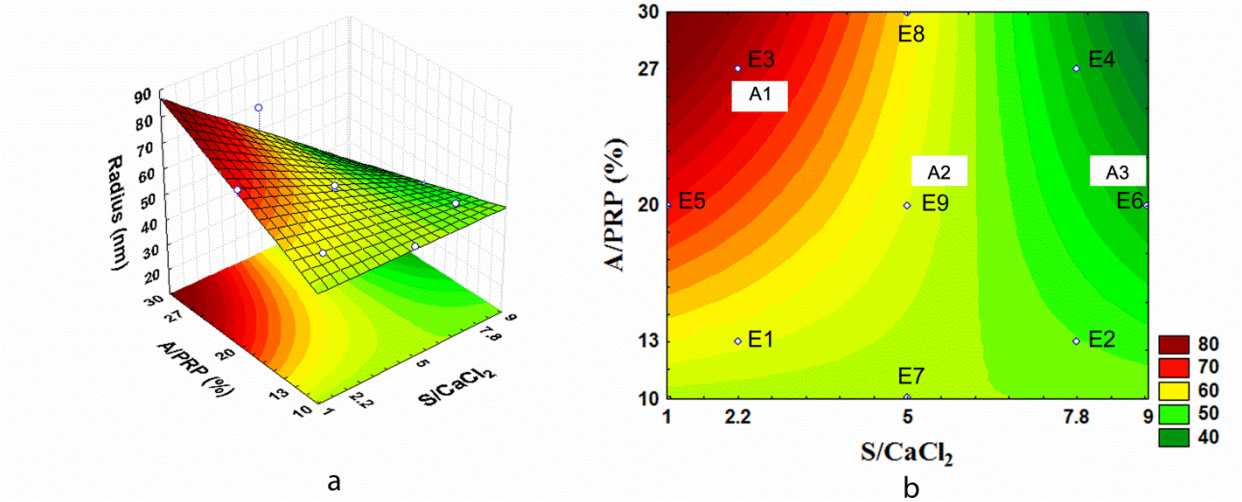

Figure 5.2 Response surface for the fibrin fiber radius. The three-dimensional response surface (a), and the projection of the surface in two dimensions (b). A1, A2 and A3 on the response-surface are the characterized architectures. E1 to E9 correspond to the experimental conditions in CCRD. The response surface was constructed with data from donor 1.

The response surfaces for clotting time, constructed for the same levels of the variables are shown in Figure 5.3.

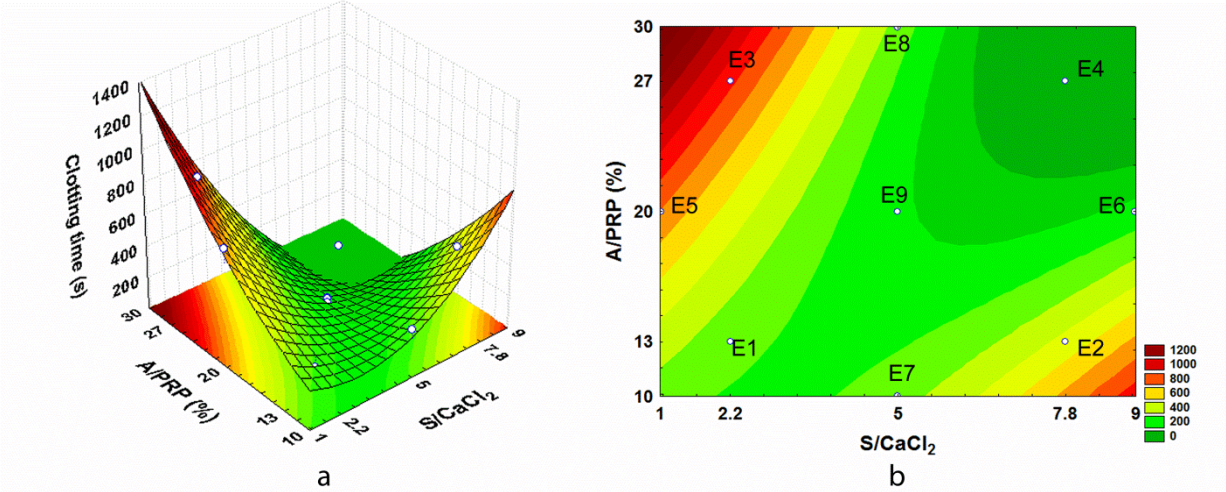

Figure 5.3 Response surface for clotting time. The three-dimensional response surface (a) and the projection of the response surface in two dimensions (b). The response surface was constructed with data from donor 1.

The variation of the clotting time was in the range of 200 to 1400s (3 to 24 min). Comparing the response surfaces for the radius (Figure 5.2) and clotting times (Figure 5.3), we could observe overlaps in regions of thicker and thinner fibers that compose architectures A1 and A3, respectively. In the intermediate region the overlap was partial because of the increase in the clotting times at the highest $S/CaCl_2$ and lowest A/PRP ratios. Therefore, we may correlate the highest clotting times (800 to 1400s) with the networks of thicker fibers in architecture A1 and the lowest clotting times (< 800 s) to the networks of thinner fibers in architectures A2 and likely also in A3.

5.3.7 Response surface validation

The surface response for the radius was constructed from data from donor 1, and the architectures were validated using data from eight more donors. The validation of the model was performed by comparing the radius predicted by the statistical model with the values calculated using the complete Carr equation (Table 5.5).

Table 5.5 Predicted and experimental fibrin radii in the characterized network architectures for validation of the statistical model

Arch[a] Assay (E)	**S/ $CaCl_2$**	**A/PRP (%)**	**r(nm)[b]**	**Donors**							
				1	2	4	5	6	7	8	9
A1 (E3)	2.2	27	75.0	69.6	76.1	84.1 ±0.1	84.0 ±0.3	86.0 ±0.4	88.0 ±5.5	85.1 ±2.3	84.2 ±1.6
A2 (E9)	5.0	20	56.0	54.3	76.4	73.9 ±0.3	73.4 ±1.2	65.2 ±0.4	75.8 ±0.1	71.1 ±3.3	71.3 ±0.3
A3 (E6)	9.0	20	42.1	40.7	66.5	67.8 ±0.1	66.7 ±0.5	63.0 ±3.0	68.7 ±0.1	64.2 ±2.9	65.8 ±0.8

[a] *Architectures according to response surface presented in Figure 5.2*

The data show the same tendency indicated by the statistical model for all donors. When the S/$CaCl_2$ ratio increased, the fiber radius tended to decrease. The thinnest fibers were observed for a S/$CaCl_2$ ratio equal to 9. Therefore, we believe that the architectures generated by the statistical model for the radius were validated by the experimental data.

Table 5.6 shows the validation of the clotting time generated by the statistical model for the same selected architectures.

Table 5.6 Data from eight donors for validation of the clotting time of the architectures of the fibrin networks.

Arch[a] Assay S(E)	S/ **$CaCl_2$**	**A/PRP (%)**	**Ct(s)[b]**	**Donors**							
				1	**2**	**4**	**5**	**6**	**7**	**8**	**9**
A1 (E3)	2.2	27	827	850	360	189 ±30	1650 ±30	3000 ±0	640 ±140	360 ±60	-
A2 (E9)	5.0	20	118	130	-	-	-	180 ±0	-	-	-
A3 (E6)	9.0	20	136	-	-	-	-	-	-	-	-

[a]Architectures according to response surface presented in Figure 5.2; [b]Predicted by the model

- clot formation almost immediately

Despite having the same tendency, large variation was observed in the clotting times of the various donors. We believe that this variation is due to the absorbance measurements and the indirect determination of clotting time.

5.3.8 Images of the fibrin networks

Figures 5.4 and 5.5 show the images from scanning electron microscopy (SEM) performed with activated P-PRP samples in the serum-rich and calcium-rich regions, respectively. The P-PRPs were from the donors 7 and 10. The images clearly reveal the networks formed from innumerous fibers. Despite the interference of the samples' drying with the fiber radius, the images show thinner fibers for architecture 3 (A3, E(6)) compared with architectures 2 and 1 (A2 and A1, E(3) and E(9)),in agreement with the response surface obtained for the radius (Figure 5.2).Thicker fibers were obtained in the calcium-rich region in the E(2) and E(7) assays (Table 5.3). These same tendencies were observed for samples prepared with PRP from two other donors.

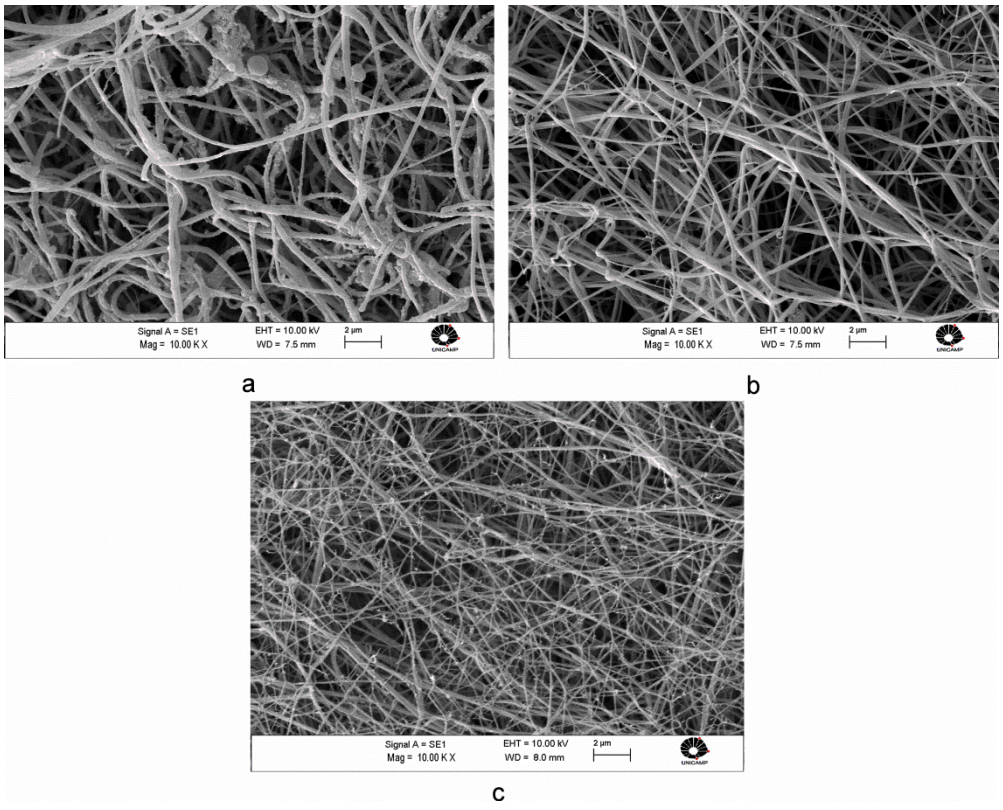

Figure 5.4 Scanning electron microscopy for the fibrin network architectures A1 (a), A2 (b) and A3 (c), which were formed under the conditions of assays E(3), E(9) and E(6), respectively, in the serum-rich region (Table 5.4). x10,000.

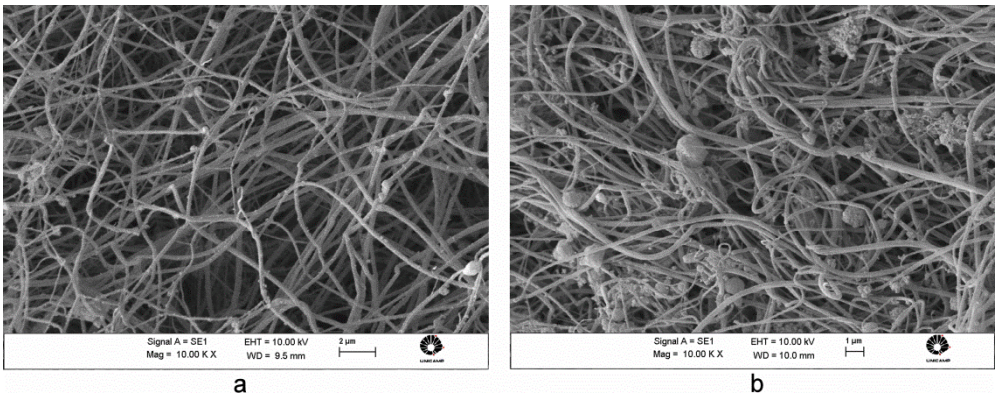

Figure 5.5 Scanning electron microscopy for the fibrin network architectures formed under the conditions of assays E(2) (a) and E(7) (b) in the calcium-rich region (Table 5.3), x10,000.

5.4 Conclusions

The effects of the variables S/$CaCl_2$ and A/PRP ratios and their interactions on the fiber radius characterized three fibrin network architectures, which were composed by thick, medium and thin fibers. The CCRD and response-surface analysis were valuable strategies for delineating the architectures of the fibrin networks with statistical reliability, and requiring a minimum number of experiments. The architectures and clotting time were correlated toward reduction of clotting time from the architectures with thicker to thinner fibrin fibers. Future studies might evaluate the influence of the architectures on the release of GFs, cell proliferation and differentiation and also to characterize the rheological behavior of the architectures, towards modulation and standardization of PRP for clinical applications.

Acknowledgment The authors acknowledge the Fundação de Amparo à Pesquisa do Estado de São Paulo.

References

1. Engebretsen L, Steffen K, Alsousou J, Anitua E, Bachl N, Devilee R et al. IOC consensus paper on the use of platelet-rich plasma in sports medicine. Br J Sports Med. 2010;44(15):1072-81. doi:10.1136/bjsm.2010.079822.

2. Cole BJ, Seroyer ST, Filardo G, Bajaj S, Fortier LA. Platelet-Rich Plasma: Where Are We Now and Where Are We Going? Sports Health. 2010;2(3):203.

3. Dohan Ehrenfest DM, Rasmusson L, Albrektsson T. Classification of platelet concentrates: from pure platelet-rich plasma (P-PRP) to leucocyte- and platelet-rich fibrin (L-PRF). Trends Biotechnol. 2009;27(3):158-67. doi:10.1016/j.tibtech.2008.11.009.

4. Zhao H, Ma L, Zhou J, Mao Z, Gao C, Shen J. Fabrication and physical and biological properties of fibrin gel derived from human plasma. Biomed Mater. 2008;3(1):015001. doi:10.1088/1748-6041/3/1/015001.

5. Carr ME, Jr., Gabriel DA, McDonagh J. Influence of Ca2+ on the structure of reptilase-derived and thrombin-derived fibrin gels. Biochem J. 1986;239(3):513-6.

6. Falvo MR, Gorkun OV, Lord ST. The molecular origins of the mechanical properties of fibrin. Biophys Chem. 2010;152(1-3):15-20. doi:10.1016/j.bpc.2010.08.009.

7. Ryan EA, Mockros LF, Weisel JW, Lorand L. Structural origins of fibrin clot rheology. Biophysical Journal. 1999;77(5):2813-26.

8. Henschen A. On the structure of functional sites in fibrinogen. Thrombosis research. 1983;29:27-39.

9. Mihalyi E. Clotting of bovine fibrinogen. Calcium binding to fibrin during clotting and its dependence on release of fibrinopeptide B. Biochemistry. 1988;27(3):967-76.

10. Weisel JW. Fibrinogen and fibrin. Advances in protein chemistry. 2005;70:247-99.

11. Hardy JJ, Carrell NA, McDonagh J. Calcium ion functions in fibrinogen conversion to fibrin. Ann N Y Acad Sci. 1983;408:279-87.

12. Procyk R, Blomback B. Disulfide bond reduction in fibrinogen: calcium protection and effect on clottability. Biochemistry. 1990;29(6):1501-7.

13. Carr ME, Gabriel DA. Dextran-induced changes in fibrin fiber size and density based on wavelength dependence of gel turbidity. Macromolecules. 1980;13(6):1473-7.

14. Carr ME, Jr., Hermans J. Size and density of fibrin fibers from turbidity. Macromolecules. 1978;11(1):46-50.

15. Shah J, Janmey P. Strain hardening of fibrin gels and plasma clots. Rheologica Acta. 1997;36(3):262-8.

16. Shah GA, Nair CH, Dhall DP. Comparison of fibrin networks in plasma and fibrinogen solution. Thromb Res. 1987;45(3):257-64.

17. Weisel J, Nagaswami C. Computer modeling of fibrin polymerization kinetics correlated with electron microscope and turbidity observations: clot structure and assembly are kinetically controlled. Biophysical Journal. 1992;63(1):111.

18. Weisel J. Structure of fibrin: impact on clot stability. Journal of Thrombosis and Haemostasis. 2007;5(s1):116-24.

19. Yeromonahos C, Polack B, Caton F. Nanostructure of the fibrin clot. Biophys J. 2010;99(7):2018-27. doi:10.1016/j.bpj.2010.04.059.

20. Doolittle RF. Fibrinogen and Fibrin. Annual Review of Biochemistry. 1984;53(1):195-229. doi:doi:10.1146/annurev.bi.53.070184.001211.

21. Davis HE, Miller SL, Case EM, Leach JK. Supplementation of fibrin gels with sodium chloride enhances physical properties and ensuing osteogenic response. Acta Biomater. 2011;7(2):691-9. doi:10.1016/j.actbio.2010.09.007.

22. Ferry JD, Morrison PR. Preparation and Properties of Serum and Plasma Proteins. VIII. The Conversion of Human Fibrinogen to Fibrin under Various Conditions1,2. Journal of the American Chemical Society. 1947;69(2):388-400. doi:10.1021/ja01194a066.

23. Wolberg A. Thrombin generation and fibrin clot structure. Blood reviews. 2007;21(3):131.

24. Janmey P, Winer J, Weisel J. Fibrin gels and their clinical and bioengineering applications. Journal of the Royal Society Interface. 2009;6(30):9.

25. El-Sharkawy H, Kantarci A, Deady J, Hasturk H, Liu H, Alshahat M et al. Platelet-rich plasma: growth factors and pro- and anti-inflammatory properties. J Periodontol. 2007;78(4):661-9. doi:10.1902/jop.2007.060302.

26. Everts PA, Overdevest EP, Jakimowicz JJ, Oosterbos CJ, Schonberger JP, Knape JT et al. The use of autologous platelet-leukocyte gels to enhance the healing

process in surgery, a review. Surg Endosc. 2007;21(11):2063-8. doi:10.1007/s00464-007-9293-x.

27. Hom DB, Linzie BM, Huang TC. The healing effects of autologous platelet gel on acute human skin wounds. Arch Facial Plast Surg. 2007;9(3):174-83. doi:10.1001/archfaci.9.3.174.

28. Obata S, Akeda K, Imanishi T, Masuda K, Bae W, Morimoto R et al. Effect of autologous platelet-rich plasma-releasate on intervertebral disc degeneration in the rabbit anular puncture model: a preclinical study. Arthritis research & therapy. 2012;14(6):R241.

29. Perez AG, Lichy R, Lana JFS, Rodrigues AA, Luzo ÂCM, Belangero WD et al. Prediction and Modulation of Platelet Recovery by Discontinuous Centrifugation of Whole Blood for the Preparation of Pure Platelet-Rich Plasma. BioResearch Open Access. 2013;2(4):307-14. doi:10.1089/biores.2013.0015. .

30. Neto BdB, Scarminio IS, Bruns RE. Planejamento e otimização de experimentos. 2nd. ed. Campinas,SP, Brazil: Editora Unicamp; 2001.

31. Filardo G, Kon E, Ruiz MTP, Vaccaro F, Guitaldi R, Di Martino A et al. Platelet-rich plasma intra-articular injections for cartilage degeneration and osteoarthritis: single-versus double-spinning approach. Knee Surgery, Sports Traumatology, Arthroscopy. 2012;20(10):2082-91.

32. Sánchez M, Guadilla J, Fiz N, Andia I. Ultrasound-guided platelet-rich plasma injections for the treatment of osteoarthritis of the hip. Rheumatology. 2012;51(1):144-50.

33. Crovetti G, Martinelli G, Issi M, Barone M, Guizzardi M, Campanati B et al. Platelet gel for healing cutaneous chronic wounds. Transfusion and Apheresis Science. 2004;30(2):145-51. doi:http://dx.doi.org/10.1016/j.transci.2004.01.004.

34. Blomback B, Carlsson K, Hessel B, Liljeborg A, Procyk R, Aslund N. Native fibrin gel networks observed by 3D microscopy, permeation and turbidity. Biochim Biophys Acta. 1989;997(1-2):96-110.

35. Shah GA, Nair CH, Dhall DP. Physiological studies on fibrin network structure. Thromb Res. 1985;40(2):181-8.

Capítulo 6. Assessment of the Effects of the Architectures of Fibrin Scaffolds on the Quality of Pure Platelet-Rich Plasma

A.G.M. Perez[a], A.A. Rodrigues[b], A.A.M. Shimojo[a], A.C.M. Luzo[c], J. F. S.D. Lana[a,b,d], W.D. Belangero[b] and M. H. A. Santana[a,*].

[a]Department of Engineering of Materials and Bioprocesses, School of Chemical Engineering, University of Campinas, Campinas-SP, Brazil, Phone: 55-19-35213921, FAX: 55-19-35213890, E-mail: mariahelena.santana@gmail.com

[b]Department of Orthopaedic and Traumatology, Faculty of Medical Sciences, University of Campinas, Campinas-SP, Brazil, Phone: 55-19-35217498. E-mail: belangerowd@gmail.com

[c]Haematology and Hemotherapy Center, Umbilical Cord Blood Bank, University of Campinas, Campinas-SP, Brazil. E-mail: angela.luzo@gmail.com

[d]Research Institute of Sports Medicine, Orthopedics and Regeneration - iMOR, Uberaba- MG, Brazil, Phone: 55-34-33317777, Fax: 55-34-33317777, E-mail: josefabiolana@gmail.com

*Corresponding author

Abstract Platelet-rich plasma (PRP) is an autologous preparation that has been widely used in regenerative medicine. Considering the importance of the activation step on the quality of PRP, this study extends our previous findings by investigating the effects of the architectures of fibrin scaffolds on their mechanical properties, release of growth factors (GFs) and proliferation of human adipose-derived mesenchymal stem cells (hAdMSCs). The architectures were characterized based on the radius of the fibrin fibers as 85.8 nm (thicker), 70.85 nm and 65.4 nm (thinner). P-PRP (pure PRP), a type of PRP without the leukocyte layer, was obtained from the first centrifugation of whole blood (platelet concentrations 2-3 times above baseline). The analyzed GFs were TGF-β1 (transforming growth factor) and PDGF-AB (platelet

derived growth factor). The results showed that the architectures formed physical and viscoelastic gels. At the platelet concentrations used, strain hardening of the gels was observed above 2 rad.s^{-1}. The best balance of the viscous/viscoelastic moduli was obtained for the architectures with the thinnest fibers. GFs were released from the gels over a period of 24 h. The release profiles were diffusive for the three architectures, with no significant differences between the GF fluxes even at higher platelet concentrations. The growth of hAMSCs was higher for the architecture composed of the thinnest fibers. Thinner fiber architectures therefore appear to be more promising, but the association of specific architectures with higher platelet concentrations must be further investigated. These findings contribute to the standardization of P-PRP for clinical applications.

Keywords: platelet rich plasma, fibrin networks, thrombin and calcium agonists, growth factors, mesenchymal stem cells

6.1 Introduction

Platelet-rich plasma (PRP, the plasma of autologous blood containing a platelet concentration above baseline) has been widely used in various regenerative medicine therapies (Engebretsen*, et al.*, 2010). Pure PRP (P-PRP) is a type of PRP that is free of or contains small concentrations of leukocytes (Dohan Ehrenfest*, et al.*, 2009).

Tissue regeneration therapy is based on three fundamental elements: scaffolds, cells and growth factors. Figure 6.1 highlights these elements and their capabilities in the triangle of cell proliferation (Crane and Everts, 2008).

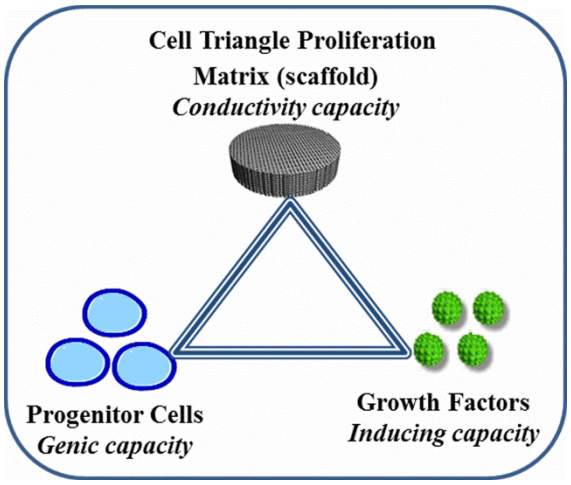

Figure 6.1 The triangle of cell proliferation, highlighting the capacities and the close relationships between progenitor cells, growth factors and the conducting matrix or scaffolds.

Platelets are rich in growth factors (GFs) and other bioactive molecules, which, upon activation, are released into the surrounding environment to stimulate wound healing and tissue regeneration (Anitua, 1999, Anitua*, et al.*, 2012, Foster*, et al.*, 2009). Platelet activation, which follows the separation and concentration of platelets during PRP preparation, is generally performed by agonists. Calcium, thrombin and autologous serum (containing thrombin and other proteins) are the natural agonists in the coagulation cascade and are also the most used agonists in PRP preparations (El-Sharkawy*, et al.*, 2007, Everts*, et al.*, 2007, Hom*, et al.*, 2007). Thrombin cleaves peptide fragments from the soluble plasma protein fibrinogen, yielding insoluble fibrin peptides that aggregate to form fibrils. A fibrin network is then formed, which entraps platelets and other blood components to form the scaffolds required for cell growth and differentiation (Bensaıd*, et al.*, 2003, Weisel and Nagaswami, 1992). Calcium acts as a cofactor of thrombin and modulates the elongation of fibers during polymerization by promoting lateral branching and functions in clot stability *in vitro* and *in vivo* (Falvo*, et al.*, 2010, Ryan*, et al.*, 1999).

The structural flexibility of fibrin fibers makes them a key material with different requirements depending on whether homeostasis, pathology or regenerative

medicine is the main focus. Fibrin polymerizes to form clots with a great diversity of structural, biological, physical and chemical properties, all of which depend on the conditions of formation. The mechanical properties, release of GFs and growth of cells in the architectures of fibrin scaffolds are of primary importance for developing the most effective system (Bensaıd*, et al.*, 2003, Dohan Ehrenfest*, et al.*, 2012).

In the two decades since the milestone discoveries of the potential of PRP in tissue regeneration, research on PRP has evolved to focus primarily on clinical applications. Basic science research remains scarce, and the following two types of studies are common: reports of a large number of clinical cases treated successfully, and studies that only attempt to optimize individual steps in the preparation of PRP without considering the overall process. The methods used for platelet activation vary in many of these studies, with different serum or autologous thrombin and calcium proportions, resulting in PRPs with different qualities. These differences make the results of these studies difficult to compare. PRP preparations are generally characterized by the platelet and leukocytes concentrations (Araki*, et al.*, 2012, Cho*, et al.*, 2011, Ito*, et al.*, 2013, Zimmermann*, et al.*, 2001) and, more recently, in terms of the cytokines and GFs (Amable*, et al.*, 2013). In addition to efficacy and safety, the standardization of PRP preparation has become an extremely important issue for translating preparation methods to tissue engineering strategies and clinical studies.

To address these issues, we previously investigated PRP preparation as an integrated process of platelet concentration and activation. Initially, we developed a phenomenological mathematical model to predict platelet and plasma recovery efficiencies, using operating variables associated with discontinuous centrifugation and initial data from whole blood samples (Perez*, et al.*, 2013). Our predictive approach to PRP activation involved a surface response statistical model in which the radii of fibrin fibers could be modulated by variables that are easy to manipulate in clinical practice, such as the ratios between autologous serum/calcium and agonist/PRP. This approach allowed for variation in the architecture networks according to radius, with fibrin fibers classified as thick (>80 nm), medium and thin (approximately 60 nm). The fibrin fiber thickness was altered by combining the

interactions between serum/calcium chloride in a range of (1 to 9) and agonist/PRP (10 to 30 %). These architectures were formed in PRP with low platelet concentration 2-3 times, obtained from the first centrifugation, and used mainly to investigate the role of the fibrin network architectures. P-PRP was used to minimize the effects of white blood cells.

Accordingly, the objective of the current work was to advance these previous findings by studying the influence of various architectures on the mechanical properties of the fibrin gels, the release of TGF-β1 and PDGF-AB and the proliferation of hAdMSCs.

6.2 Materials and Methods

All experiments were approved by the Ethics Committee of the Medical Sciences School of the University of Campinas (UNICAMP; CAAE: 0972.0.146.000-11). The donors were healthy individuals between 20 and 30 years of age who had previously been assessed by clinical examination.

6.2.1 Blood collection

P-PRP manipulation was performed with 3.15 mL of whole blood (WB), which was collected in 3.5 mL tubes (Vacuette, Ref. 454327; Greiner Bio-One GmbH, Frickenhausen, Germany) that contained 0.35 mL of 3.2% sodium citrate as an anticoagulant. In addition to hemogram, fibrinogen was also dosed using the coagulometric method.

6.2.2 P-PRP preparation

The concentration of whole blood (WB) and PRP cells was determined using a Micros ES 60 hematological counter (Horiba, Montpellier, France). Centrifugation assays were conducted in a Rotina 380R centrifuge (Hettich Lab Technology, Tuttlingen, Germany).

After WB centrifugation at 100 xg for 10 min at 25°C, the supernatant (not including the BC layer) was carefully pipetted to avoid disturbing the bottom layer of

the red blood cells (RBCs) and the buffy coat (BC) layer. The collected samples were then transferred to empty siliconized glass tubes and homogenized. The prepared P-PRP was characterized by determining the platelet and WBC concentrations. Subsequent platelet concentrations were obtained by centrifuging P-PRP at 400 xg for 10 min to sediment the platelets, followed by the removal of different volumes of the supernatant platelet-poor plasma (PPP). To obtain concentrations of platelets that were approximately 3x and 5x above baseline, 1/2 and 1/3 of the PPP volume, respectively, was removed after the second centrifugation.

6.2.3 Autologous serum preparation

Autologous serum was prepared by collecting 5 mL of whole blood in tubes without anticoagulant (Obata*, et al.*, 2012). After incubation for 30 min to permit clot formation, WB was centrifuged at 2000 xg for 10 min. Serum containing thrombin and other proteins was used to activate the PRP preparations.

6.2.4 P-PRP activation

P-PRP activation was performed using autologous serum and a 10% (w/v) $CaCl_2$ solution as agonists. The volumetric percentages of the agonist related to P-PRP (A/PRP) and different volumetric ratios of the serum to calcium chloride (S/$CaCl_2$), as described in Table 6.1, were selected from our previous studies to form the different fibrin architectures.

Table 6.1. Volumetric ratios of autologous serum to calcium chloride ($S/CaCl_2$) and agonist to PRP (A/PRP [%]) used to activate the PRP.

Assay	$S/CaCl_2$	A/PRP (%)	Ca (mM)
1	0.55	10	58.1
2	0.87	13	62.5
3	1.0	20	90.0
4	2.2	27	76.1
5	5	20	30.2
6	9	20	18.0

6.2.5 Architectures of the fibrin scaffolds

The architectures of the fibrin scaffolds formed from P-PRP, according to the conditions described in Table 6.1, were characterized based on the radius, mass/length and the viscous and viscoelastic moduli of their fiber networks.

The radius and mass/length were calculated using the complete Carr equation (Eq. 1) (Yeromonahos, et al., 2007).

$$\tau\lambda^5 = \frac{2\pi^3 Cn\mu\left(\frac{dn}{dC}^2\right)\frac{44}{15}\left(\lambda^2 - \frac{184}{154}\pi^2 r^2 n^2\right)}{N} \qquad \text{Eq.1}$$

where τ is the turbidity of the solutions, C the initial fibrinogen concentration $(g.cm3)^{-1}$, N is Avogadro's number, λ is the incident wavelength (cm), and μ=mf/L, where mf is the protein mass in a fiber (Da) of length L (cm) and radius r (cm). The values of n and dn/dC were 1.33 and 0.17594 cm, respectively.

$\tau\lambda^5$ was plotted against λ^2, resulting in a straight line whose slope yielded the mass/length ratio and whose ordinate at the origin yielded the square of the average radius.

The turbidity was calculated from the optical density of the gelled fibrin networks using Eq. 2, where D is the optical density.

$$\tau = 1 - \exp(-D.\ln(10)) \qquad \text{Eq. 2}$$

6.2.6 Rheological Studies

The viscous and viscoelastic moduli of the gels were obtained from assays conducted using a Haake model RheoStress 1 rheometer (Haake, Germany). The measurements were performed in steady and oscillatory regimes at 25°C, using parallel plate geometry of 20 mm. Oscillatory measurements were conducted in the linear region, at a stress of 1.188 Pa and in the frequency range of 0.01 to 10 Hz.

6.2.7 Growth factor release

P-PRP was activated in 24-well microplates with autologous serum and a $CaCl_2$ solution (10% w/v) at different volumetric ratios, using the S/$CaCl_2$ ratio and A/PRP (%), as described in Table 6.1. P-PRP was incubated with the agonists for 45 min, after which 1.5 mL of Dulbecco's Modified Eagle's Medium with low glucose (DMEM-LG, Gibco) was added to the gelled fibrin networks containing the activated platelets. The microplates were maintained in an incubator (Sanyo Scientific, USA) with 5% CO_2. Samples (1.5 mL) were withdrawn from the medium outside the gels at various time points over 72 hours without removing the gels from the wells. The aspirated volume was replaced with an equal volume of fresh medium. The samples were stored at -80°C for further characterization. The concentrations of the released GFs PDGF-AB and TGF-β1 were measured using enzyme-linked immunosorbent assay (ELISA) kits (R&D Systems), according to the manufacturer's instructions and specifications.

6.2.8 Cell preparation/isolation for in vitro assays

The protocol for the isolation of hADSCs was approved by the Ethics Committee of the Medical Sciences School of the University of Campinas (UNICAMP), process number: CEP 0226.0146.000-08.

Human subcutaneous adipose tissue that was initially acquired from liposuction surgery was washed with sterile PBS, separated into 10 g fractions, digested with 20 mg of collagenase type 1A and maintained in 20 mL of DMEM-LG containing 10% BSA (bovine serum albumin) and 10 µL of gentamicin for 30 min in a bath at 37°C. After complete digestion, the reaction was quenched with 10 mL of fetal bovine serum (FBS) and immediately centrifuged for 15 min at 1500 rpm. The supernatant was discarded, and the pellet was suspended in 10 mL of DMEM-LG with 10% FBS.

After cultivation for 24 h, the culture medium was changed every 3 days. After the fourth passage, the cells were characterized by immunophenotyping using flow cytometry and by adipogenic, osteogenic and chondrogenic differentiation and then used in the subsequent experiments.

6.2.9 Culture of hADSC-seeded fibrin scaffolds

The cell-seeded fibrin scaffolds had a final hADSC density of $2x10^4$ cells/mL. The platelet concentration was approximately 560 $x10^6$ platelets/mL (2x above baseline). The cells were dispersed in P-PRP before activation and were inoculated in a 48-well microplate. After the addition of the agonists at $S/CaCl_2$ ratios of 2.2, 5.0 and 9.0, as described in Table 6.1, a fibrin gel formed, containing platelets and hAdMSCs. These gels or scaffolds were maintained at room temperature for 45 min before adding 0.75 mL of the culture medium (DMEM). The seeded gels were maintained at 37°C for 14 days.

6.2.10 Cell viability

Cell viability was quantified using the thiazolyl blue tetrazolium bromide (MTT) assay. At 3, 7, 10, 12 and 14 days, the gels were removed and transferred to 24-well plates; 0.5 mL of 1 mg/ml MTT was then added, and the plates were cultured at 37°C for 4 hours. The MTT solution was then discarded, and 1 mL of DMSO was added to dissolve the purple formazan crystals. The samples were shaken at 120 rpm for 30 min to ensure homogeneous dissolution of the formazan dye, and then 200 µL of each sample was transferred to a 96-well plate in triplicate. The optical density was measured at 595 nm using a microplate reader (FilterMax F5 Molecular Devices).

6.2.11 Images of the cell-seeded fibrin scaffolds

The cell-seeded fibrin scaffolds were characterized by scanning electron microscopy. Gels were fixed in a solution of 4% paraformaldehyde and 2.5% glutaraldehyde in phosphate buffer, pH 7.4, for 2 hours. The samples were then dehydrated in ethanol for 15-min intervals in aqueous 50%, 70%, 95% and 100% ethanol solutions (2x) and dried at the critical point. After gold coating (Sputter Coater POLARON, SC7620, VG Microtech), the samples were observed using a scanning electron microscope (Leo440iLEO) with an accelerating voltage of 20 kV.

6.3 Results

6.3.1 Characterization of P-PRP

Table 6.2 shows the platelet and white blood cell concentrations in the whole blood and in P-PRP obtained from the first centrifugation step from four healthy donors aged 25-30 years who were selected after their clinical exams. Based on the centrifugation conditions for whole blood, platelets in P-PRP were concentrated approximately 2-3-fold above baseline. The recovery efficiencies of the platelets ranged from 76% to 100%. The maximum recovery of WBCs was 25.4%, with concentrations as low as 1.1 to 4.1 $x10^3$ cells/mm^3, thereby characterizing a P-PRP.

Table 6.2 Concentration of platelets (Pt) and white blood cells (WBCs) in whole blood and in P-PRP. (FCPt) is the platelet concentration factor.

	Whole Blood					***P-PRP***				
Donors	***1***	***2***	***3***	***4***	***5***	***1***	***2***	***3***	***4***	***5***
Ptx10^3/mm^3 (±SD)	326 ±1.5	223 ±2.5	248 ±12.5	216 ±1.0	210 ±2.5	779 ±2.0	496 ±24	582 ±10	542.5 ±15	680 ±12
WBC Recovery (%)	-	-	-	-	-	25.4 ±6.2	22.7 ±0.8	8.7 ±1.3	5.64 ±0.0	12.5 ±2.2
WBCx10^3/mm^3 (±SD)	6.1 ±0.1	3.6 ±0.1	5.7 ±0.1	7.8 ±0.0	6.1 ±0.1	4.1 ±0.9	2.4 ±0.1	1.2 ±0.15	1.1 ±0.0	4.8 ±0.9
FC_{Pt} *	-	-	-	-	-	2.4 ±0.01	2.2 ±0.10	2.4 ±0.04	2.5 ±0.01	3.1 ±0.04
Pt Recovery (%)**	-	-	-	-	-	91.6 ±2.4	76.3 ±2.3	100.0 ±0.75	100.5 ±0.15	49.2 ±0.09
Fibrinogen (mg/dL)	350	381	305	335	283	-	-	-	-	-

**FC_{Pt} = Pt concentration in P-PRP /Pt concentration in WB; **Platelet Recovery = [(Pt centration in P-PRP x P-PRP volume) / (Pt concentration in WB x WB volume)] x 100*

Table 6.3 presents the characterization of P-PRP used in the study on the effect of the platelet concentration on the release profiles of GFs.

Table 6.3 Concentration of platelets (Pt) in whole blood and in P-PRP prepared with different platelet concentration factors (FC_{Pt}).

	Whole Blood		***P-PRP*** ***(FC_{Pt} 2x)***		***P-PRP*** ***(FC_{Pt} 3x)***		***P-PRP*** ***(FC_{Pt} 5x)***	
Donors	***6***	***7***	***6***	***7***	***6***	***7***	***6***	***7***
$Ptx10^3/mm^3$	206	234	464	441	713	630	1,109	1,030
FC_{Pt}	-	-	2.2	1.9	3.5	2.7	5.4	4.4

6.3.2 Architectures of the fibrin scaffolds

The architectures of the fibrin scaffolds, which were modulated by the activation of P-PRP by the $S/CaCl_2$ ratios of 2.0, 5.0, and 9.0, were characterized by the radius and mass /length of the fibrin fibers (Table 6.4).

Table 6.4. Radius and mass/length of fibrin fibers in the architectures formed after P-PRP activation with the specified volumetric ratios of autologous serum to calcium chloride ($S/CaCl_2$) and an agonist to PRP (agonist/P-PRP(%)).

Assay	**S/ $CaCl_2$**	**A/PRP (%)**	***Radius (nm)***				***Mass/length x 10^{12} (Da/cm)***			
			1	***2***	***3***	***4***	***1***	***2***	***3***	***4***
4	2.2	27	86.0 ±0.4	88.0 ±5.5	85.1 ±2.3	84.2 ±1.6	6.8 ±0.4	6.6 ±0.3	12.6 ±0.1	9.2 ±1.6
5	5.0	20	65.2 ±0.4	75.8 ±0.1	71.1 ±3.3	71.3 ±0.3	2.6 ±0.1	6.1 ±0.1	4.4 ±0.54	5.0 ±0.25
6	9.0	20	63.0 ±3.0	68.7 ±0.1	64.2 ±2.9	65.8 ±0.8	2.5 ±0.4	4.0 ±0.1	2.6 ±0.68	3.1 ±0.06

As expected, the values in Table 6.4 indicate larger fibers with an average radius of 85.8 nm for the S/$CaCl_2$ 2.2 and A/PRP 2.7% ratios, whereas for the higher ratios (5.0 and 9.0) and A/PRP (20%), the average radii decreased to 70.85 nm and 65.4 nm, respectively. In all cases, the architectures of thick and thin fibers were generated for further assays.

The same tendency, although less pronounced, was observed for mass/length. Increasing the S/$CaCl_2$ ratios from 2.2 to 9.0 resulted in a decrease in the mass/length values.

6.3.3 Mechanical properties

The mechanical properties of the fibrin gels determine whether the tensions at the location of PRP application cause deformation that is reversible or irreversible or results in breakage. The viscoelastic behavior of fibrin gels has been well studied since the 40s, mainly using purified fibrinogen and human or bovine thrombin. The results have shown unusual rheology for the fibrin gels, which is different compared to most polymers. A very large degree of strain hardening was observed, which was determined using plots of stress vs. shear strain and that showed a distinct upward curvature for strains above 10% (Roberts*, et al.*, 1973).

Studies that were more similar to PRP preparations added gel-filtered platelets to plasma containing glucose and albumin. The strain hardening of fibrin gels was eliminated by adding a high concentration of platelets (number not specified), which caused a large increase in the shear storage modulus in the low strain linear viscoelastic limit. The reduction in strain hardening may have resulted from fibrin strand retraction, which occurs when the platelets become activated. This interpretation is consistent with recent theoretical treatments of semi-flexible polymer network viscoelasticity (Shah and Janmey, 1997). Therefore, much of the elastic resistance to deformation of the platelet-rich plasma clots, and, presumably, for the clots formed *in vivo*, depends on the presence of platelets.

Figure 6.2 shows the mechanical behavior of the gels containing the studied architectures in terms of the viscous (G'') and viscoelastic (G') moduli and by their complex (η*) and shear (η) viscosities.

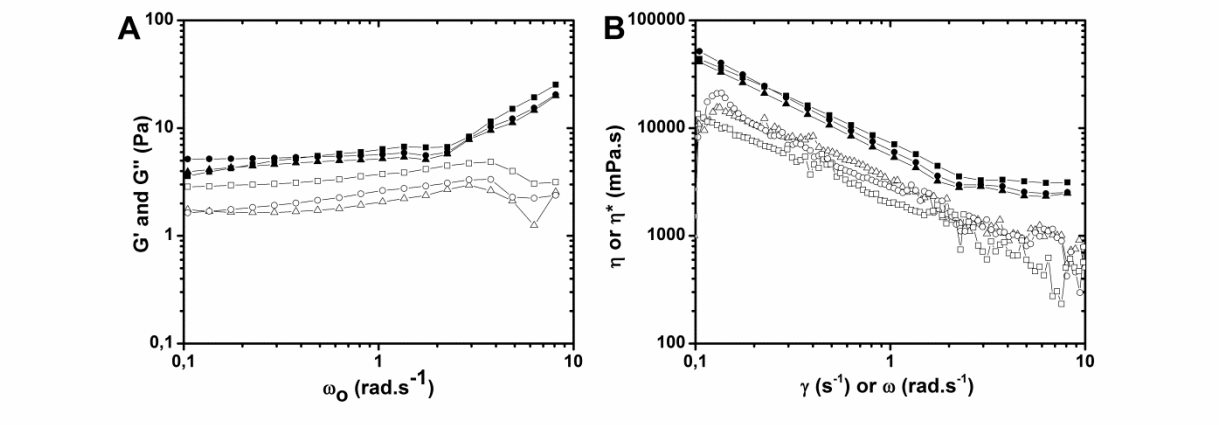

Figure 6.2 (a) Storage G' (closed symbol) and loss G" (open symbol) shear moduli as a function of frequency and (b) Complex viscosity (η*) versus angular frequency (ωo) (closed symbol) and apparent viscosity (η) versus shear rate (γ) (open symbol): (■) and (□) (assay 4); (●) and (○) (assay 5) and (▲) and (Δ) (assay 6). S/$CaCl_2$ and A/PRP(%) in the assays are 4 (2.2 and 27); 5 (5 and 20) and 6 (9 and 20).

The profiles shown in Figure 6.2 were similar for the studied architectures. In Figure 6.2A, at the low range of frequencies up to 2 rad.s^{-1}, the curves exhibited typical gel-type mechanical spectra with little frequency dependence in either moduli. Additionally, G' is higher than G" in all studied frequency ranges. However, above 2 rad.s^{-1}, a significant increment of G' indicates strain hardening behavior.

The well-known power law parameters A and B ($G' = A.\omega^B$) also determine the degree of oscillation frequency (ω) dependence, as described by (Ramkumar*, et al.*, 1996). The B values define the mechanical strength of the gels. It is known that B=0 for covalent gels and B> 0 for physical gels (Khondkar*, et al.*, 2007). The tan δ ($=G'/G''$), parameter, where δ is the phase shift or phase angle, which is also a function of frequency, also describes the viscoelastic behavior of gels. Values of tan δ

< 0.1 indicate predominantly elastic gels, while for tan δ>0.1, the gels are classified as weak (Ikeda and Nishinari, 2001).

Table 6.5 shows the power law parameters for the architectures and the values of tan δ (=G'/G''). Based on these criteria, the gels from the studied architectures are physical gels; the lowest B values of assays 5 and 6 show that although non-covalent, they have considerable strength. The value of tan δ<0.1 for assay 6 (thinner fibers) confirms those tendencies by suggesting a non-weak elastic gel.

The viscosity profiles show a steep linear decrease for both complex and shear viscosities with γ or ω_0 (Figure 6.2B). However, above 2 rad.s^{-1}, the behavior of the complex viscosity η* tends to be frequency independent, as a reflex of the G' and G'' behavior. For the shear viscosity (η) a strong shear thinning is observed at higher shear rates, indicating non-Newtonian pseudoplastic behavior.

The fibrin clots also did not obey the Cox-Merz rule, defined by η*(ω) = η(γ) (for γ= ω), for homogeneous structures. In the current case, the complex viscosity η* in the range of small deformations is higher than the shear viscosity η at equivalent rates of deformation.

Table 6.5 The power law parameters A and B ($G' = A.\omega^B$) and values of tan δ (=G'/G'') at 1 Hz for architectures of the fibrin scaffolds.

Assay	S/$CaCl_2$	A/PRP (%)	A (Pas)	B	tan δ
4	2.2	27	6.427	0.269	0.158
5	5.0	20	5.623	0.041	0.146
6	9.0	20	5.200	0.123	0.086

6.3.4 Release of growth factors

The normalized release profiles of these GFs from the PRPs gels are shown in Figure 3(a) and (b). Additional architectures were added (from assays 1, 2 and 3 – Table 6.1) to confirm this behavior.

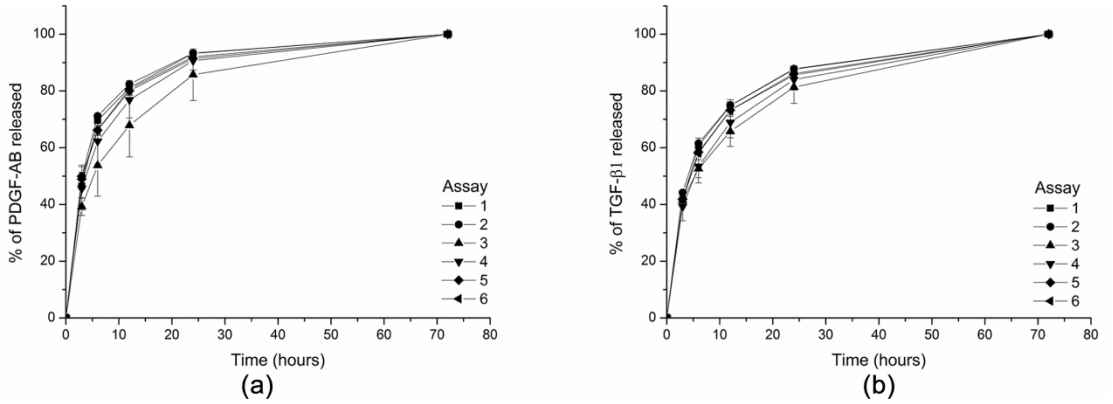

Figure 6.3 Growth Factor release profile from P-PRPs activated with different ratios of S/$CaCl_2$ and A/PRP (%) for assay conditions described in Table 6.1 for assays 1 to 6. PDGF-AB (a) and TGF-β1 (b). S/$CaCl_2$ and A/PRP (%) in the assays were: 1 (0.55 and 10); 2 (0.87 and 10); 3 (1.0 and 20); 4 (2.2 and 27); 5 (5 and 20) and 6 (9 and 20).

The curves show diffusive profiles, indicating no collapse of the architectures throughout the assay. For all conditions studied, approximately 70% of TGF-β1 and 80% of PDGF-AB were released during the 12 first hours. The initial velocities were approximately 9.5 (±0.7) %GF and 10.8 (±1.1) %GF released/h for TGF-β1 and PDGF-AB, respectively.

The GF release profiles were similar in networks with architectures formed by thinner fibers and networks of thicker fibers. The difference in the GF release profiles in these networks was not significant according to *Tukey's* test ($p<0.05$).

Figure 6.4 shows a comparison of the release profiles with increased platelet concentrations of 2x, 3x and 5x above baseline. The curves also showed diffusive

profiles, and the initial rate and total levels of the released GFs were proportional to the platelet concentration.

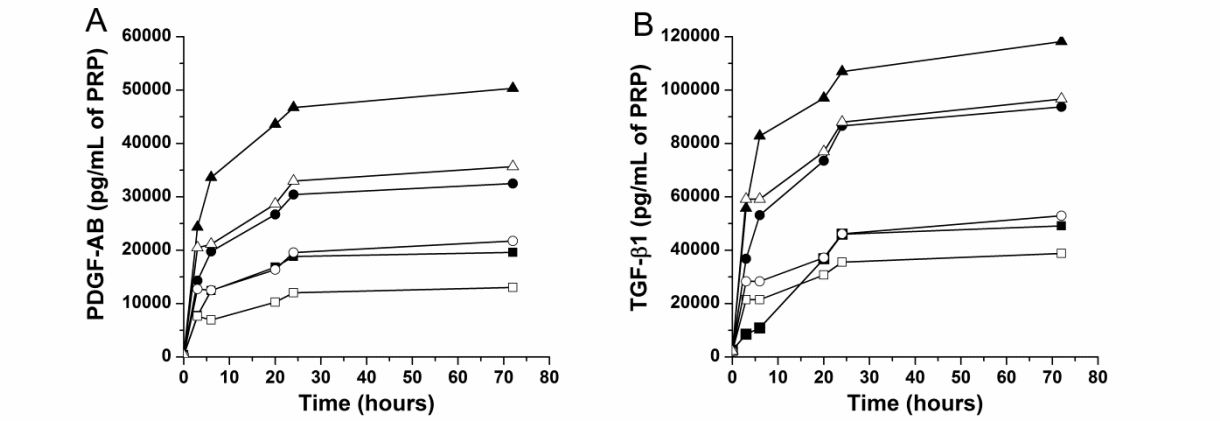

Figure 6.4 Release profiles for the GFs and PDGF-AB (a) and TGF-β1 (b) from PRPs prepared with a platelet concentration factor (FCPt) 2x (■ and □); 3x (● and ○) and 5x (▲and Δ) above baseline from donor 6 (closed symbols) and donor 7 (open symbols).

6.3.5 Cell Proliferation

Figures 6.5 show the growth profiles of the hAdDSC-seeded fibrin scaffolds derived from 2 donors.

Cell growth was higher in the fibrin scaffolds composed of the thinnest fibers, with a higher S/$CaCl_2$ ratio (9.0), and the agonist/PRP (20%) used for PRP activation (Table 6.1).

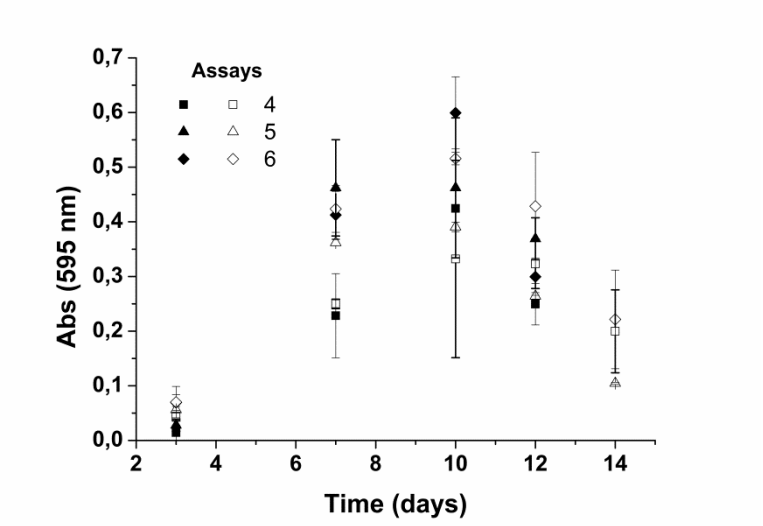

Figure 6.5 Growth profiles of hAdDSC-seeded fibrin scaffolds with different architectures derived from donors 3 (closed symbols) and 4 (open symbols), for the assay conditions described in Table 6.1.

6.3.6 Images of the networks after cell growth

The images obtained by SEM show the cell growth in the fibrin scaffolds at days 7 and 10 (Figure 6.6). Higher cell density can be observed in images from the 10^{th} day when compared to those taken on the 7^{th} day, which is consistent with the cell viability results. The cells appear more dispersed on the thinnest fibers, which correspond to activation with 20% agonist/PRP and 9.0 S/$CaCl_2$ ratio. Larger clusters are formed on the surface of the thickest fiber scaffolds, which may be associated with poor migration to the inner domains of the scaffolds.

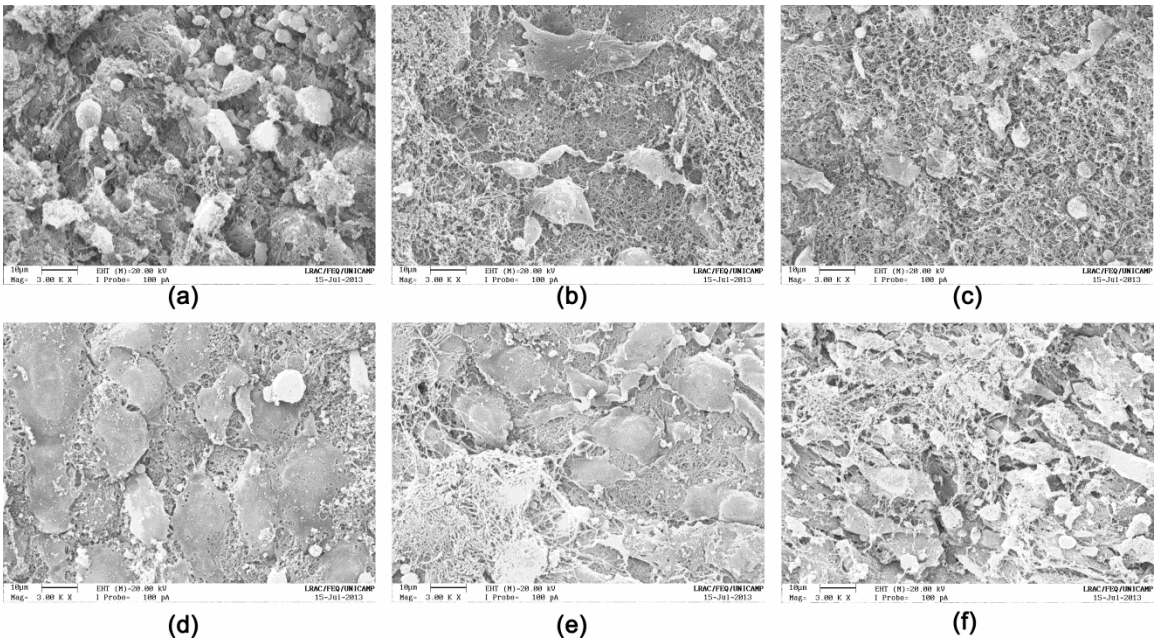

Figure 6.6 Scanning electron microscopy images of hAdMSCs seeded scaffolds at the 7th day (first line) and 10th day (second line) of growth. S/$CaCl_2$ and A/PRP (%): (a), (d) 2.2 and 27; (b), (e) 5 and 20; (c), (f) 9 and 20.

6.4 Discussion

In the present study, we produced fibrin scaffolds composed of fiber networks of radii in the range of 65.4 to 85.8 nm and a mass/length of 2.5 to 12.6 x10^{12} Da/cm, with architectures modulated by the ratio of S/$CaCl_2$ (2, 5 and 9) and A/PRP (20 and 27%) used for PRP activation. Our results are consistent with the literature, which describe increased calcium concentration promoting the lateral and lengthwise growth of protofibrils, enabling the formation of thicker fibers. Lower calcium concentrations result in thinner fibers with smaller pores (Laudano and Doolittle, 1981, Rowe*, et al.*, 2007, Ryan*, et al.*, 1999). Architectures of thick, medium and thin fibers were formed, according our previous classification.

Although the gels are viscoelastic, strain hardening (increment of the viscoelastic modulus G' with deformation) was observed above 2 rad.s^{-1}, despite the presence of platelets concentrated 2-3 times above baseline. However, despite the similar behavior of the viscous and viscoelastic moduli of the architectures of the

formed physical gels, the B and tan δ values suggest non-weak gels for the thinner fibers. The thinner fibers also show the best G''/G' ratio, as described by tan δ (Table 6.5). These effects are due to the bundle-like structure, suggested by (Piechocka*, et al.*, 2010), in which the tight packing of the thinnest fibers promotes more lateral interactions. The failure of the Cox-Merz rule can also be explained by heterogeneities in the lateral interactions of the bundle of fibers, which are susceptible to deformations. However, the loss of similar behavior of the curves above 2 rad.s^{-1} observed in Figure 2B does not necessarily mean that such structures are permanently lost under large deformations, which must be further investigated.

While the elasticity modulus is a property of the material, hardening is a property of the structure. Gels that are very stiff deform less, while those that are softer or plastic might deform to a new shape with the same applied stress. Despite the incredible resilience of fibrin fibers against large deformations (Piechocka*, et al.*, 2010), hardening should be modulated or avoided, especially in applications subject to large strains. If the presence of gel-filtered platelets added to plasma eliminated strain hardening in previous experiments, (Shah and Janmey, 1997), strain hardening behavior in PRP should be investigated for higher platelet concentrations.

According to the literature, the levels of platelet concentrations in PRP also have striking effects on fibrinolysis. The fibers adjacent to the platelet aggregates were both thinner and denser with a lower lysis velocity (fibrinolysis) than those in platelet-poor areas or in the absence of platelets (Weisel, 2007).

Hardening also affects the interactions of cells with fibrin architectures. In wound healing, the associations between cells are likely to be different after stress is applied to fibrin by platelet retraction (Weisel, 2007). In the absence of platelets, the balance of the branching and thickness of the fibers controlled the rigidity of the fibers. Thus, the clots with thinner fibers had more branching, leading to higher rigidity. A high degree of inelasticity during deformation appeared to be more common in clots with thicker fibers. In addition to the activation conditions, thinner fibers and branch point densities were also obtained with higher fibrinogen concentrations. The

thinner fibers also dissolved at a slower rate than those with a coarse fibrin structure composed of thicker fibers, but thin fibers were cleaved at a faster rate than the thick fibers. Thus, the conditions that lead to thinner fibrin fibers should benefit the mechanical properties of the fibrin gels.

The release profiles of TGF-β1 and PDGF-AB GFs from fibrin scaffolds were similar for the architectures studied in this experiment, with no significant differences according to *Tukey's* test ($p<0.05$) (Figure 3). The results were analyzed in terms of the % of GF released to minimize the influence of individual variations in GF concentrations on the analysis of the results (Cho*, et al.*, 2011, Roussy*, et al.*, 2007). The results showed a more prolonged release, with a plateau at 24 h after gel formation (Figures 3 and 4).

Comparison with results from the literature is difficult, both because there are few comparable studies and because other studies used different or non-specified conditions of PRP preparation. Martineau et al. (Martineau*, et al.*, 2004) studied the effect of different thrombin and calcium concentrations for PRP activation on the release of GFs and demonstrated that there was no influence on the release profile of TGF-β1, consistent with the results of our study. Su et al. (Su*, et al.*, 2008) activated platelet gel with only $CaCl_2$ (final concentration, 23 mM) and observed a plateau in the release of TGF-β1 at approximately 60 min. Harrison et al. (Harrison*, et al.*, 2011) studied the activation of PRP with a defined amount of bovine thrombin and 10% $CaCl_2$ (ratio 50:1) and obtained almost immediate release (within 2 h) of PDGF-AB and TGF-β1.

With respect to cell growth, the proliferation of hADSCs cultured in the fibrin scaffold composed of the thinnest fibers was higher than that in the other two architectures (Figure 4). This effect may be attributed to the increased surface area, which should provide greater adhesion, growth, and cell migration. Previous works (Cox*, et al.*, 2004, Ho*, et al.*, 2006) have demonstrated that structural properties in the fibrin scaffold are important parameters for cell proliferation. Ho et al. (Ho*, et al.*, 2006) demonstrated that the fibrinogen concentration affects hMSC proliferation more

than the thrombin concentration and that the structural properties of the fibrin networks may also be an important parameter to consider. The lowest fibrinogen concentrations studied by Ho et al., 5 mg/mL and 500 mg/mL, were more effective for cell growth. This concentration is closer to the physiological fibrinogen concentrations used in the present study, which were approximately 200 to 380 mg/dL. Cox et al. have demonstrated that the proliferation of human dermal fibroblasts was highest in formulations containing a low concentration of fibrinogen (5–17 mg/mL) and a low to medium concentration of thrombin (1–167 U/mL).

The SEM images illustrated cell proliferation in the fibrin scaffolds at days 7 and 10, with a higher apparent cell density on the 10^{th} day.

The study indicates a trend of architectures with thinner fibers favoring the mechanical behavior of gels and the proliferation of cells. However, the modulation of the concentration of platelets is of fundamental importance in the quality of PRP, not only by the amount of GFs provided, which is directly proportional to the amount of platelets, but also by the mechanical properties of fibrin gels.

6.5 Conclusion

The architectures provided by thinner fibers in fibrin gels associated with platelet concentration are the main factors in determining the quality of PRP, providing mechanical resistance to stress and serving as scaffolds for the proliferation of mesenchymal cells. These architectures also promote gradual release of GFs over 24 h and may ensure the stability of the scaffolds *in vivo*. These findings are important for the standardization of PRP preparation for clinical applications.

Competing interests

The authors declare that they have no competing interests.

Acknowledgments

The authors appreciate the participation of the volunteer blood donors and thank the state financial agency FAPESP (Fundação de Amparo a Pesquisa do Estado de São Paulo), Brazil, which supported this work.

References

Amable P, Carias R, Teixeira M, Pacheco I, do Amaral R, Granjeiro J, Borojevic R. 2013, Platelet-rich plasma preparation for regenerative medicine: optimization and quantification of cytokines and growth factors**.** *Stem cell research & therapy*, **4:**67.

Anitua E. 1999, Plasma rich in growth factors: preliminary results of use in the preparation of future sites for implants**.** *Int J Oral Maxillofac Implants*, **14:**529-535.

Anitua E, Alkhraisat MH, Orive G. 2012, Perspectives and challenges in regenerative medicine using plasma rich in growth factors**.** *Journal of Controlled Release*, **157:**29-38.

Araki J, Jona M, Eto H, Aoi N, Kato H, Suga H, Doi K, Yatomi Y, Yoshimura K. 2012, Optimized preparation method of platelet-concentrated plasma and noncoagulating platelet-derived factor concentrates: maximization of platelet concentration and removal of fibrinogen**.** *Tissue Eng Part C Methods*, **18:**176-185.

Bensaıd W, Triffitt J, Blanchat C, Oudina K, Sedel L, Petite H. 2003, A biodegradable fibrin scaffold for mesenchymal stem cell transplantation**.** *Biomaterials*, **24:**2497-2502.

Cho HS, Song IH, Park S-Y, Sung MC, Ahn M-W, Song KE. 2011, Individual variation in growth factor concentrations in platelet-rich plasma and its influence on human mesenchymal stem cells**.** *The Korean journal of laboratory medicine*, **31:**212-218.

Cox S, Cole M, Tawil B. 2004, Behavior of human dermal fibroblasts in three-dimensional fibrin clots: dependence on fibrinogen and thrombin concentration**.** *Tissue engineering*, **10:**942-954.

Crane D, Everts PA. 2008, Platelet rich plasma (PRP) matrix grafts**.** *Practical Pain Management*, **8:**12-26.

Dohan Ehrenfest DM, Bielecki T, Jimbo R, Barbe G, Del Corso M, Inchingolo F, Sammartino G. 2012, Do the fibrin architecture and leukocyte content influence the growth factor release of platelet concentrates? An evidence-based answer comparing a pure platelet-rich plasma (P-PRP) gel and a leukocyte- and platelet-rich fibrin (L-PRF)**.** *Curr Pharm Biotechnol*, **13:**1145-1152.

Dohan Ehrenfest DM, Rasmusson L, Albrektsson T. 2009, Classification of platelet concentrates: from pure platelet-rich plasma (P-PRP) to leucocyte- and platelet-rich fibrin (L-PRF)**.** *Trends Biotechnol*, **27:**158-167.

El-Sharkawy H, Kantarci A, Deady J, Hasturk H, Liu H, Alshahat M, Van Dyke TE. 2007, Platelet-rich plasma: growth factors and pro- and anti-inflammatory properties**.** *J Periodontol*, **78:**661-669.

Engebretsen L, Steffen K, Alsousou J, Anitua E, Bachl N, Devilee R, Everts P, Hamilton B, Huard J, Jenoure P. 2010, IOC consensus paper on the use of platelet-rich plasma in sports medicine**.** *British Journal of Sports Medicine*, **44:**1072-1081.

Everts PA, Devilee RJ, Oosterbos CJ, Mahoney CB, Schattenkerk ME, Knape JT, van Zundert A. 2007, Autologous platelet gel and fibrin sealant enhance the efficacy of total knee arthroplasty: improved range of motion, decreased length of stay and a reduced incidence of arthrofibrosis**.** *Knee Surg Sports Traumatol Arthrosc*, **15:**888-894.

Falvo MR, Gorkun OV, Lord ST. 2010, The molecular origins of the mechanical properties of fibrin**.** *Biophys Chem*, **152:**15-20.

Foster TE, Puskas BL, Mandelbaum BR, Gerhardt MB, Rodeo SA. 2009, Platelet-rich plasma from basic science to clinical applications**.** *The American Journal of Sports Medicine*, **37:**2259-2272.

Harrison S, Vavken P, Kevy S, Jacobson M, Zurakowski D, Murray MM. 2011, Platelet activation by collagen provides sustained release of anabolic cytokines**.** *Am J Sports Med*, **39:**729-734.

Ho W, Tawil B, Dunn JC, Wu BM. 2006, The behavior of human mesenchymal stem cells in 3D fibrin clots: dependence on fibrinogen concentration and clot structure**.** *Tissue Engineering*, **12:**1587-1595.

Hom DB, Linzie BM, Huang TC. 2007, The healing effects of autologous platelet gel on acute human skin wounds**.** *Arch Facial Plast Surg*, **9:**174-183.

Ikeda S, Nishinari K. 2001, "Weak Gel"-Type Rheological Properties of Aqueous Dispersions of Nonaggregated κ-Carrageenan Helices**.** *Journal of Agricultural and Food Chemistry*, **49:**4436-4441.

Ito R, Morimoto N, Pham LH, Taira T, Kawai K, Suzuki S. 2013, Efficacy of the Controlled Release of Concentrated Platelet Lysate from a Collagen/Gelatin Scaffold for Dermis-Like Tissue Regeneration**.** *Tissue Engineering*.

Khondkar D, Tester RF, Hudson N, Karkalas J, Morrow J. 2007, Rheological behaviour of uncross-linked and cross-linked gelatinised waxy maize starch with pectin gels**.** *Food hydrocolloids*, **21:**1296-1301.

Laudano AP, Doolittle RF. 1981, Influence of calcium ion on the binding of fibrin amino terminal peptides to fibrinogen**.** *Science*, **212:**457-459.

Martineau I, Lacoste E, Gagnon G. 2004, Effects of calcium and thrombin on growth factor release from platelet concentrates: kinetics and regulation of endothelial cell proliferation**.** *Biomaterials*, **25:**4489-4502.

Obata S, Akeda K, Imanishi T, Masuda K, Bae W, Morimoto R, Asanuma Y, Kasai Y, Uchida A, Sudo A. 2012, Effect of autologous platelet-rich plasma-releasate on intervertebral disc degeneration in the rabbit anular puncture model: a preclinical study**.** *Arthritis research & therapy*, **14:**R241.

Perez AG, Lichy R, Lana JFS, Rodrigues AA, Luzo ÂCM, Belangero WD, Santana MHA. 2013, Prediction and Modulation of Platelet Recovery by Discontinuous Centrifugation of Whole Blood for the Preparation of Pure Platelet-Rich Plasma**.** *BioResearch Open Access*, **2:**307-314.

Piechocka IK, Bacabac RG, Potters M, MacKintosh FC, Koenderink GH. 2010, Structural hierarchy governs fibrin gel mechanics**.** *Biophysical Journal*, **98:**2281-2289.

Ramkumar D, Bhattacharya M, MENJIVAR JA, Huang T. 1996, Relaxation behavior and the application of integral constitutive equations to wheat dough**.** *Journal of texture studies*, **27:**517-544.

Roberts WW, Lorand L, Mockros LF. 1973, Viscoelastic properties of fibrin clots**.** *Biorheology*, **10:**29-42.

Roussy Y, Bertrand Duchesne MP, Gagnon G. 2007, Activation of human platelet-rich plasmas: effect on growth factors release, cell division and in vivo bone formation**.** *Clinical oral implants research*, **18:**639-648.

Rowe SL, Lee S, Stegemann JP. 2007, Influence of thrombin concentration on the mechanical and morphological properties of cell-seeded fibrin hydrogels**.** *Acta biomaterialia*, **3:**59-67.

Ryan EA, Mockros LF, Weisel JW, Lorand L. 1999, Structural Origins of Fibrin Clot Rheology**.** *Biophysical Journal*, **77:**2813-2826.

Shah J, Janmey P. 1997, Strain hardening of fibrin gels and plasma clots**.** *Rheologica Acta*, **36:**262-268.

Su CY, Kuo YP, Nieh H-L, Tseng YH, Burnouf T. 2008, Quantitative assessment of the kinetics of growth factors release from platelet gel**.** *Transfusion*, **48:**2414-2420.

Weisel JW. 2007, Structure of fibrin: impact on clot stability**.** *Journal of Thrombosis and Haemostasis*, **5:**116-124.

Weisel JW, Nagaswami C. 1992, Computer modeling of fibrin polymerization kinetics correlated with electron microscope and turbidity observations: clot structure and assembly are kinetically controlled**.** *Biophysical Journal*, **63:**111-128.

Yeromonahos C, Polack B, Caton F. 2007, Nanostructure of the FibrinClot**.** *Biophysical Journal* **99:**2018-2027.

Zimmermann R, Jakubietz R, Jakubietz M, Strasser E, Schlegel A, Wiltfang J, Eckstein R. 2001, Different preparation methods to obtain platelet components as a source of growth factors for local application**.** *Transfusion*, **41:**1217-1224.

Capítulo 7. Impact of Hyaluronic Acid Microparticles on the Quality of a Cell-Seeded Fibrin Scaffold derived from Pure Platelet-Rich Plasma

A.G.M. Perez[a], A.A. Rodrigues[b], A.A.M. Shimojo[a] A.C.M. Luzo[c], J. F. S.D. Lana[a,b,d], W.D. Belangero[b] and M. H. A. Santana[a,*].

[a]Department of Engineering of Materials and Bioprocesses - School of Chemical Engineering, University of Campinas, Campinas-SP, Brazil, Phone: 55-19-35213921, FAX: 55-19-35213890, E-mail: mariahelena.santana@gmail.com

[b]Department of Orthopedic and Traumatology - Faculty of Medical Sciences, University of Campinas, Campinas-SP, Brazil, Phone: 55-19-35217498. E-mail: belangerowd@gmail.com

[c]Hematology and Hemotherapy Center, Umbilical Cord Blood Bank, University of Campinas, Campinas-SP, Brazil. E-mail: angela.luzo@gmail.com

[d]Research Institute of Sports Medicine, Orthopedics and Regeneration - iMOR, Uberaba- MG, Brazil, Phone: 55-34-33317777, Fax: 55-34-33317777, E-mail: josefabiolana@gmail.com

*Corresponding author

Abstract Platelet-rich plasma (PRP) has been widely used as an autologous product in regenerative medicine. In addition to the concentrations of platelets and leukocytes, the fibrin scaffold, formed from fibrinogen polymerization during PRP activation, also defines the quality of PRP for clinical applications. The architecture of the fibrin fibers provides the mechanical properties of the scaffold, the barrier to releasing growth factors (GFs) and the environment for proliferation and migration of cells for tissue regeneration. In previous studies, we found that gels with thin fibrin fiber architectures (around 60 nm) had more promising viscoelastic properties and increased growth of human adipose-derived mesenchymal stem cells (hAdMSCs). However, for platelet concentrations 2-3 fold higher than the baseline, strain hardening of the gels was still observed, and the release of GFs was around 80% in the first 12 hours. In order to enhance the viscoelastic properties as well the growth of hAdMSCs, the present study investigated the impact of hyaluronic acid microparticles (HAM) on the fibrin scaffolds. HAM were added to cell-seeded PRP before activation, and the rheological parameters, the release of transforming growth factor- β1 (TGF-β1) and platelet derived growth factor-AB (PDGF-AB) and the growth of hAdMSCs were characterized. Fluid HA and pure fibrin gels were used as controls. The results demonstrated that HAM improved the quality of the fibrin scaffold by suppressing the strain hardening and prolonging the release of the GFs compared with pure fibrin gels. Additionally, HAM scaffolds improved the growth of hAdMSCs compared with fluid HA scaffolds in a HAM/PRP volumetric ratio-dependent manner. These results are important for basic science studies and also for the standardization of PRP for use in clinical applications.

Keywords: hyaluronic acid microparticles, platelet-rich plasma, fibrin scaffolds, growth factors, human adipose-derived mesenchymal stem cells

7.1 Introduction

The tissue regeneration process is based on three fundamental elements: scaffolds, cells, and growth factors [1]. The use of exogenous growth factors (GFs), natural or recombinant, accelerates the normal healing. However, they are not widely used due to the high cost, the potential immunological response and also because only a few of them are approved for clinical use [2-4]. In addition, the direct injection of exogenous GFs in their soluble form is not effective because of their short half-life and their fast dispersion at the injection site [4,5].

Platelet-rich plasma (PRP) was first used as an autologous source of GFs that combined GFs with other bioactive substances in physiological proportions. Nowadays, PRP is an autologous therapy widely used in regenerative medicine [6-8]. The applications of PRP in tissue healing and bone regeneration had its beginning in the '90s [9]. Since then, there have been numerous publications using PRP with remarkable results in many different areas, such as dentistry [7], maxillofacial facial surgery [10,11], plastic surgery [12], orthopedics [13] and rheumatology [14], and in the treatment of different types of injuries, chronic wounds [15-17] and muscle injuries [18]. An overview of the current progress, as well as a discussion of the technical aspects of preparation and therapeutic use of PRP has been described recently [19].

Regarding the fundamental element of scaffolds, the activation of PRP with thrombin and calcium exploits the final step of the coagulation cascade in which fibrinogen molecules are cleaved by thrombin, converted into fibrin monomers and assembled into fibrils, which are packed into fibers forming a three-dimensional network that entraps GFs [20-22].

The prolonged release of GFs increases their half-lives and cell growth, thus benefiting tissue regeneration. With this aim, various studies have investigated the incorporation of PRP in polymeric matrices. The most used polymers are: collagen [23], gelatin [2-4,22,24,25], chitosan [1,26] and hyaluronic acid [26-28].

Mesenchymal stem cells (MSCs) have been applied to tissue regeneration because of their remarkable features of replication and differentiation, and thus, the ability to replenish the supply of tissue-forming cells. Moreover, MSCs play an important role in wound healing by contributing to collagen deposition and supporting the regeneration of vascular, epithelial and dermal structures [29-31].

Hyaluronic acid (HA) is a non-sulfated, linear polysaccharide found mainly in the skin and connective tissue. It is composed of a repeating disaccharide, β-1,4-D-glucuronic acid–β-1,3-N-acetyl-D-glucosamine, linked alternately by glycosidic linkages [28,32,33]. HA plays a relevant role in many biological processes such as the modulation of cell migration, cell differentiation and wound healing. The mechanisms behind the beneficial action of HA in healing have been studied but are not yet fully elucidated. However, studies have shown that hyaluronic acid mediates cell activation by specific surface receptors such as CD44, RHAMM and toll like receptors. Moreover, the HA molecule is highly hydrated, a property that favors tissue hydration and has a beneficial effect on healing. HA and fibrin degradation products are seen as important molecules for controlling cellular functions involved in the inflammatory response and induction of angiogenesis in wound healing [34].

However, HA is easily degraded *in vivo*, compromising its integrity as a scaffold. Conversely, the short chains from degradation contribute to the interaction with the cell receptors. To overcome the instability of HA *in vivo*, chemical crosslinking or delivery with other biomolecules becomes essential for medical applications. HA cross-linked with divinyl sulfone (DVS) is currently used in products for viscosupplementation [35].

In recent years, HA has been applied as an adjuvant in combination with PRP and MSCs for tissue engineering and regenerative medicine applications [27,36-39]. Most of the reported results are from clinical studies and compare the effects of HA alone with the combination of HA and PRP or HA, PRP and MSCs on the healing process [28]. Although combinations of HA and PRP or HA and MSCs were found to be more effective at speeding the healing process than HA alone, there have been no

prior reports on the influence of HA on the quality of the fibrin scaffold derived from PRP to support the understanding of these results. Furthermore, the type of HA applied in clinical studies is not always specified with respect to its molecular weight or degree of crosslinking, and the information is often restricted to referencing the manufacturer.

Taking these findings into account, the aim of this study is to evaluate the impact of HA microparticles (HAM) cross-linked with DVS on the quality of the fibrin scaffolds derived from PRP *in vitro*. The behavior of the viscoelastic and viscous parameters, the release of transforming growth factor (TGF-β1) and platelet derived growth factor (PDGF-AB) and the proliferation of human adipose-derived mesenchymal stem cells (hAdMSCs) was analyzed in pure fibrin scaffolds and in scaffolds with HAM cross-linked with DVS and with fluid non-cross-linked HA.

One reason to investigate HAM is based on the properties of their dispersions, which could improve the properties of pure fibrin scaffolds such as viscoelasticity, suppression of strain hardening, prolonging the release of GFs and favoring cell growth and migration. Our previous studies have shown that HAM with mean diameters in the range of 75–100 µm exhibit typical gel behaviors: 1) they have viscoelastic and viscous moduli that are independent of the applied frequency; 2) they exhibit pseudoplastic behavior with shear thinning; and 3) although classified as weak gels, they have the ability to undergo deformation without breaking [35]. Moreover, the addition of HAM to PRP could interfere with the architecture of the fibrin scaffolds (i.e. filling the pores), while also having the advantage of suppressing the strain hardening and balancing the viscoelasticity and viscosity. HAM could also increase the stability of fibrin scaffolds and provide a sustained release of GFs and an additional surface area for cell adhesion. On the other hand, the crosslinking of HAM reduces hydration compared with fluid HA and could interfere with the interaction with the cell receptors.

Based on these observations, this study was conducted with pure PRP (P-PRP), a type of PRP without the leukocyte layer that was obtained from the first

centrifugation of whole blood (with a platelet concentration 2-3 times above baseline). HAM were prepared from fluid HA previously cross-linked with divinyl sulphone and were 75–100 µm in diameter. After preparation, HAM were added to cell-seeded P-PRP before activation, so as to be incorporated into the fibrin network during the activation of platelets with thrombin and calcium chloride. Similar experiments were conducted with fluid HA and with cell-seeded P-PRP only. Thus, the formed scaffolds were analyzed for their rheological properties, the release of GFs and the growth of human adipose-derived mesenchymal stem cells (hAdMSCs).

7.2 Material and Methods

All experiments were approved by the Ethics Committee of the Medical Sciences School of the University of Campinas (UNICAMP; CAAE: 0972.0.146.000-11). The blood donors were healthy individuals between 20 and 30 years of age who were previously assessed by clinical examination.

7.2.1 Blood Collection

Blood was collected into 3.5 mL vacuum tubes (Vacuette®, Greiner bio-one, USA) containing sodium citrate (3.2%) as an anticoagulant in the volumetric proportion of 9:1 blood:sodium citrate.

7.2.2 PRP preparation

The concentration of whole blood (WB) and PRP cells was determined using a Micros ES 60 hematological counter (Horiba, Montpellier, France). Centrifugation assays were conducted in a Rotina 380R centrifuge (Hettich Lab Technology, Tuttlingen, Germany).

The protocol for preparation of P-PRP applied in the present work was previously reported by our group [40]. After WB centrifugation at 100xg for 10 min at 25°C, the supernatant (not including the BC layer) was carefully pipetted to avoid disturbing the bottom layer of red blood cells (RBCs) and the buffy coat layer (BC). The collected samples were then transferred to empty siliconized glass tubes and

homogenized. The prepared P-PRP was characterized by determining the platelet and WBC concentrations. These samples were used to prepare the P-PRP scaffolds.

A second centrifugation step (400xg for 10 min) was performed to further concentrate the platelets. The half superior volume was discarded (PPP), and the half inferior volume, containing platelets, was used to prepare the PRP/HA scaffolds.

7.2.3 Autologous serum preparation

Autologous serum was prepared by collecting 5 mL of whole blood in tubes without anticoagulant [41]. After incubation for 30 min to permit clot formation, the WB was centrifuged at 2000xg for 10 min. Serum containing thrombin and other proteins was used to activate the P-PRP preparations.

7.2.4 Preparation of cross-linked HA hydrogel microparticles

Hyaluronic acid (HA) with a high molecular weight, an average of 1.8×10^6 Da, was obtained from Galena®. A 1% solution of HA was freeze-dried to obtain pure HA. Divinyl sulfone and phosphate buffered saline (PBS) solutions were purchased from Sigma–Aldrich.

Cross-linked hydrogels were prepared in a 1:1 ratio of HA:DVS (w:w) and sheared in an Ultra-Turrax T25 disperser (IKA, Germany) at 24,000 rpm to obtain the 130 µm hydrogel particles using a methodology reported by Shimojo (34). Particle size measurements were performed by laser scattering in a Horiba LA-900 particle analyzer (Horiba Instruments Incorporated, USA). The morphology of the HAM was verified through optical microscopy using a Reichert Jung—Series 150 Microscope (USA).

7.2.5 Preparation of the HA/fibrin or fibrin only scaffolds

Cell-seeded P-PRP and fluid HA or HAM were mixed in a 48-well microplate in different volumetric proportions as indicated in Table 7.1. The concentrations of HAM and fluid HA were 1.4% (w/w). According to our previous studies with pure fibrin scaffolds, activation of the P-PRP/HAM or the P-PRP/fluid HA mixture with

autologous serum and a 10% calcium chloride solution in the volumetric ratios of 5:1 serum/(calcium chloride) and 20% agonists/P-PRP would generate fibers with a width of approximately 60 nm. The total volume in the wells was 250 µL. The cell-seeded pure fibrin scaffolds were prepared with P-PRP from the 1st centrifugation step, and the fibrin/HA scaffolds were prepared with P-PRP from the 2nd centrifugation step. These gels or scaffolds were maintained at room temperature for 45 min before the cell cultivation procedure.

Table 7.1Types of scaffolds produced

Scaffold Type	**Volumetric ratio Fibrin/HA**
Fibrin/HAM (1/1)	1:1
Fibrin/HAM (3/1)	3:1
Fibrin/HAM (1/2)	1:2
Fibrin/HA fluid (1/1)	1:1
Pure Fibrin	1:0

7.2.6 Imaging the cell-seeded fibrin scaffolds

The cell-seeded scaffolds were fixed in a solution of 4% paraformaldehyde and 2.5% glutaraldehyde in phosphate buffer, pH 7.4, for 2 hours. The samples were than dehydrated in ethanol for 15 min intervals in aqueous 50%, 70%, 95% and 100% ethanol solutions (2x) and dried at the critical point. After gold coating (Sputter Coater POLARON, SC7620, VG Microtech), the samples were visualized with a scanning electron microscope (Leo440iLEO) with an accelerating voltage of 20 kV.

7.2.7 Rheological Studies

Rheological measurements were performed on a Haake RheoStress 1 rheometer (Haake, Germany). The properties of the scaffolds were characterized in both steady and oscillatory regimes at 25°C using a parallel plate geometry of 20 mm. Oscillatory measurements were conducted in the linear region at a stress of 1.19 Pa and in the frequency range of 0.01 to 10 Hz.

7.2.8 Growth factor release

The assays for GF release were conducted in the same microplates in which the gels were previously formed. A volume of 1.5 mL of Dulbecco's Modified Eagle Medium with low glucose (DMEM-LG, Gibco) was added to the gelled fibrin scaffolds containing the activated platelets. The microplates were maintained in an incubator (Sanyo Scientific, USA) with 5% CO_2. Samples (1.5 mL) were withdrawn from the medium with which the gels were incubated at various time points over 72 hours without removing the gels from the wells. The aspirated volume was replaced with an equal volume of fresh medium. The samples were stored at -80°C for further characterization. The concentrations of the released GFs PDGF-AB and TGF-β1 were measured using enzyme-linked immunosorbent assay (ELISA) kits (R&D Systems) according to the manufacturer's instructions and specifications.

7.2.9 Cell preparation/isolation for *in vitro* assays

The protocol for the isolation of hAdMSCs (process number: CEP 0226.0146.000-08) was approved by the Ethics Committee of the Medical Sciences School of the University of Campinas (UNICAMP).

Human subcutaneous adipose tissue that was initially acquired from liposuction surgery was washed with sterile PBS, separated into 10 g fractions, digested with 20 mg of collagenase type 1A and maintained in 20 mL of DMEM-LG containing 10% BSA (bovine serum albumin) and 10 µL of gentamicin for 30 min in a bath at 37°C. After complete digestion, the reaction was quenched with 10 mL of fetal bovine serum (FBS) and immediately centrifuged for 15 min at 1500 rpm. The

supernatant was discarded, and the pellet was suspended in 10 mL of DMEM-LG with 10% FBS.

After cultivation for 24 h, the culture medium was changed every 3 days. After the fourth passage, the cells were characterized by immunophenotyping using flow cytometry and by adipogenic, osteogenic and chondrogenic differentiation and then used in the subsequent experiments.

7.2.10 Culture of hAdMSC-seeded fibrin scaffolds

The culture of hAdMSCs-seeded fibrin scaffolds with or without HA or HAM was started by adding 0.75 mL of the culture medium (DMEM) to the 24-well microplates. The seeded gels were maintained at 37°C for 14 days.

7.2.11 Cell viability

Cell viability was quantified using the thiazolyl blue tetrazolium bromide (MTT) assay. At 3, 7, 10, 12 and 14 days post-activation, the gels were removed and transferred to 24-well microplates. Five hundred microliters of 1 mg/ml MTT was then added, and the plates were cultured at 37°C for 4 hours. The MTT solution was then discarded, and 1 mL of DMSO was added to dissolve the purple formazan crystals. The samples were shaken at 120 rpm for 30 min to ensure homogeneous dissolution of the formazan dye, and then 200 µL of each sample was transferred to a 96-well plate in triplicate. The optical density was measured at 595 nm using a microplate reader (FilterMax F5 Molecular Devices).

7.2.12 Imaging of the cell-seeded fibrin scaffolds

The cell-seeded fibrin scaffolds were characterized by scanning electron microscopy. Gels were fixed in a solution of 4% paraformaldehyde and 2.5% glutaraldehyde in phosphate buffer, pH 7.4, for 2 hours. The samples were then dehydrated in ethanol for 15 min intervals in aqueous 50%, 70%, 95% and 100% ethanol solutions (2x) and dried at the critical point. After gold coating (Sputter Coater

POLARON, SC7620, VG Microtech), the samples were observed using a scanning electron microscope (Leo440iLEO) with an accelerating voltage of 20 kV**.**

7.3 Results

7.3.1 P-PRP Composition

Table 7.2 shows the platelet and white blood cell concentrations in the whole blood (WB) and in the P-PRP for the three donors. Differences in platelet and WBC concentrations (what characterizes the autologous product) were observed among the donors. The platelets in the P-PRP were 2-3 times more concentrated than baseline after the 1st centrifugation step, and 2.5-4 times more concentrated after the 2nd centrifugation step.

Table 7.2 Concentration of platelets (Pt) and white blood cells (WBC) in whole blood (WB) and in platelet-rich plasma (PRP). FCPt is the platelet concentration factor.

Donor	Whole Blood		PRP (1st Centrifugation)			PRP (2nd Centrifugation)		
	Ptx10^3/mm^3	WBCx 10^3/mm^3	Ptx10^3/mm^3	WBCx 10^3/mm^3	FCPt*	Ptx10^3/mm^3	WBCx 10^3/mm^3	FCPt*
1	284 ±2.5	6.6 ±0.0	531 ±6.5	0.9 ±0.05	1.9 ±0.0	693 ±35.0	3.9 ±1.0	2.5 ±0.12
2	210 ±2.5	6.4 ±0.0	420 ±3.0	1.1 ±0.05	2.0 ±0.01	636 ±2.6	3.3 ±0.5	3.0 ±0.12
3	208 ±3.5	8.2 ±0.1	550 ±4.5	1.5 ±0.05	2.7 ±0.02	811 ±5.0	6.3 ±1.1	3.8 ±0.02

*FCPt = Pt concentration in P-PRP/Pt concentration in WB.

7.3.2 Scaffold Composition

The final composition of platelets in the scaffolds and the volumes of P-PRP and HA used are presented in Table 7.3. The concentration of platelets in the P-PRP obtained from the 2nd centrifugation was approximately 3 times higher than baseline in the scaffolds containing fluid HA or HAM. For the assays using pure fibrin scaffolds, the platelets were 2 times more concentrated than baseline from the 1st centrifugation.

Table 7.3 – Final composition of the fibrin scaffolds.

Scaffold type	Approximate FCPt	Volume of activated PRP (µL)	Volume of HA particles or fluid (µL)	Platelets/m^3 in the scaffolds Donor 1	Platelets/m^3 in the scaffolds Donor 2
Fibrin/HAM (1/1)	3x	125.0	125.0	277200	253200
Fibrin/HAM (3/1)	3x	187.8	62.5	415800	379800
Fibrin/HAM (1/2)	3x	83.4	166.7	184892	168884
Fibrin/fluid HA (1/1)	3x	125.0	125.0	277200	253200
Pure Fibrin	2x	250	0	424800	336000

7.3.3 Characterization of the cross-linked HA microparticles

The cross-linked HAM were approximately spherical, with an average size around 130 µm as measured by laser light scattering and observations with an optical microscope. The crosslinking degree (ICP) was 90%.

7.3.4 Characterization of the fibrin scaffolds Imaging

The images in Figure 7.1 show the fibrin scaffolds derived from PRP which were composed of fibrin fibers forming 3D networks. Although HAM or the seeded cells could not be observed in the images, the differences in the architecture of the scaffolds are clear. The pore size and the density of the fibers appear to decrease in the following order: pure fibrin scaffolds > HAM/fibrin (3/1, 1/1) scaffolds > fluid HA scaffolds. The fibers formed in the presence of HA (fluid or HAM) appear thinner than when HA is absent (pure fibrin scaffold).

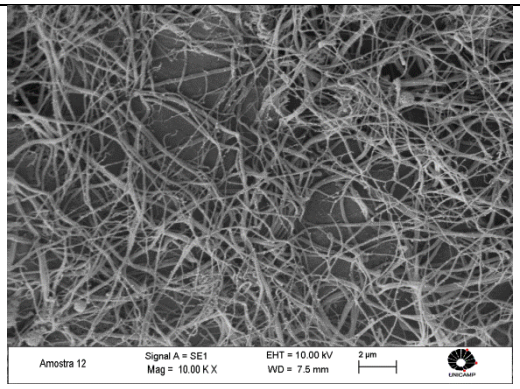

(a) Fibrin/HAM (1/1)

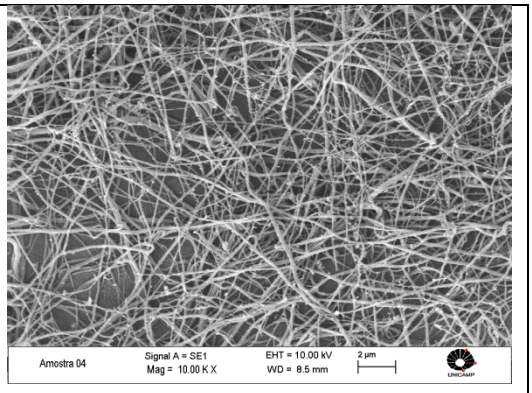

(b) Fibrin/HAM (3/1)

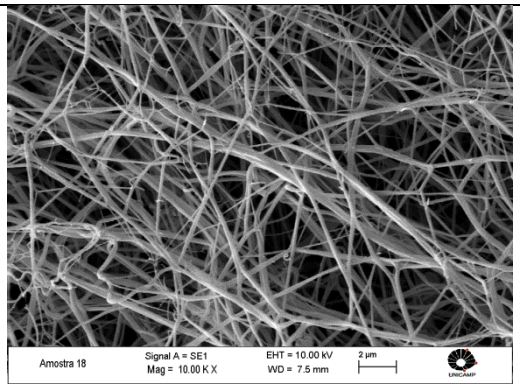

(c) Fibrin

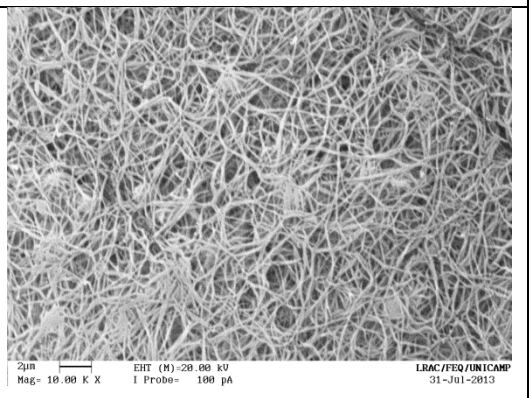

(d) Fibrin/fluid HA (1/1)

Figure 7.1 Scanning electron microscopy images of the fibrin scaffolds: (a) Fibrin/HAM (1/1); (b) Fibrin/HAM (3/1); (c) pure Fibrin; and (d) Fibrin/fluid HA (1/1).

7.3.5 Rheology

The rheological measurements were generated with PRP from donors 3, 4 and 5. First, we compared the oscillation spectra of the fibrin/HAM scaffolds with different particle proportions (1/1, 1/2 and 3/1 fibrin/HAM) between the two donors (Figure 7.2 and Table 7.3). Next, we compared the fibrin/HAM scaffolds with the fibrin/fluid HA scaffolds, both at a 1/1 proportion, for a single donor (Figure 7.3 and Table 7.4). In both cases, the pure fibrin scaffold was used as a control.

The curves for both donors illustrated in Figure 7.2 (a) and (b) exhibited a typical gel-like mechanical spectra with an elastic moduli G' slightly higher than the loss moduli G"; however, the differences between the absolute values were likely due to differences in fibrinogen concentrations. We observed an increase in both moduli, elastic and loss, in the fibrin/HAM scaffolds at all proportions studied compared with those for pure fibrin scaffolds. Additionally, the strain hardening behavior of the pure fibrin scaffolds was suppressed with the presence of HAM.

The data shown in Figure 7.2 (c) and (d) indicate that the gels do not obey the Cox-Merz rule defined by h*(w)| = h (g = w) for homogeneous structures. Although there are deviations, the curves remain parallel in the oscillatory spectra, indicating the gels are able to undergo deformation. Moreover, the curves of apparent viscosity (η) versus shear rate (γ) show strong shear thinning at the shear rates studied, indicating a non-Newtonian pseudoplastic behavior. Differences between the donors show the curves are more similar to donor 1 than donor 2, but in both cases the curves show a similar behavior and are in the same range of viscosities.

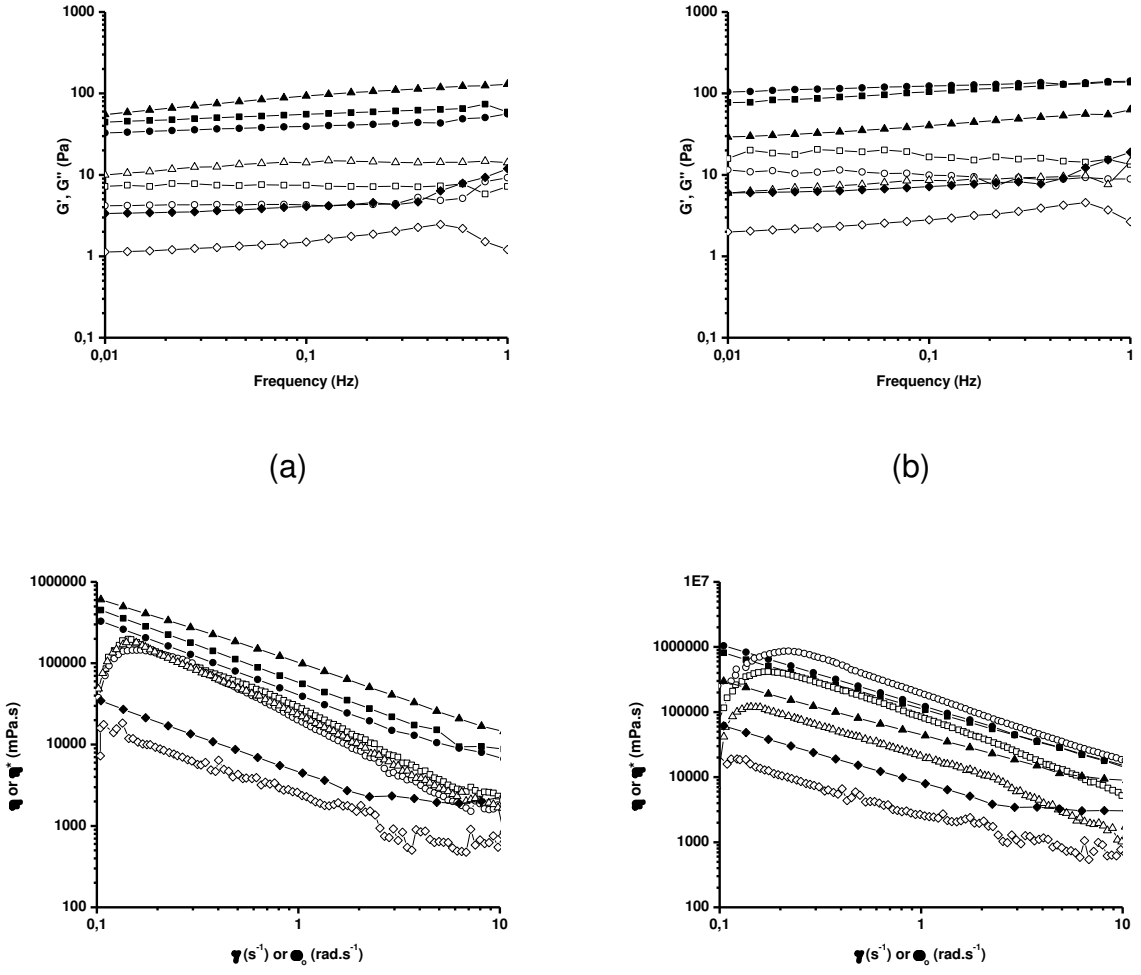

Figure 7.2 Storage G' (closed symbol) and loss G" (open symbol) moduli as a function of frequency for the fibrin/HAM scaffolds and for two donors: (a) donor 1 and (b) donor 2. Complex viscosity (η*) versus oscillatory frequency (ωo) and apparent viscosity (η) versus shear rate (γ) for fibrin/HAM scaffolds and for two donors: (c) donor 1 and (d) donor 2. (■) and (□) fibrin/HAM 1/1; (●) and (○) fibrin/HAM 1/2; (▲) and (Δ) fibrin/HAM 3/1; (♦) and (◊) pure fibrin. Characterization of the whole blood from the donors in Table 7. 2.

The degree of frequency dependence can also be determined by the power law parameters $G' = A.\omega^B$ described by Ramkumar and Bhattacharya [42]. In the power law relationship, G' is the storage modulus, ω is the oscillation frequency in rad.s^{-1}, A is a constant, and the exponent B is the slope of a log–log plot of G' versus ω. The parameter B defines the mechanical strength of the gels. It is known that B = 0 for a covalent gel or stronger gels, whereas B > 0 for physical or weak gels [43].

Table 7.4 The Power Law parameters ($G' = A.\omega^B$) and values of tan δ (at 0.1 Hz) for the different scaffolds.

Scaffold	donor	A (Pas)	B	tan δ
Fibrin/HAM 1/1	1	57.8	0.095	0.134
Fibrin/HAM 1/2	1	40.9	0.079	0.108
Fibrin/HAM 3/1	1	102.1	0.218	0.151
Fibrin	1	4.3	0.099	0.366
Fibrin/HAM 1/1	2	110.9	0.136	0.158
Fibrin/HAM 1/2	2	127.1	0.069	0.081
Fibrin/HAM 3/1	2	43.4	0.156	0.214
Fibrin	2	7.6	0.098	0.390

tan δ = G''/G'

The results show that the B values characterize the scaffolds as physical gels. The tan δ is a measure of the relative contribution of the viscous and viscoelastic components to the mechanical properties of the scaffolds. We observed that the presence of HAM decreased tan δ, indicating a higher viscoelastic contribution, which increases with the proportion of HAM in the fibrin scaffolds.

Figure 7.3 illustrates a comparison of the viscoelastic and viscous performances of the pure fibrin, pure HAM, fibrin/fluid HA and fibrin/HAM (1/1) scaffolds. As expected, the oscillation spectra show a typical gel-like mechanical spectra. The effects of strain hardening can be observed for the pure fibrin and fibrin/fluid HA scaffolds. The rheological behavior of HAM and fibrin/HAM (1/1) scaffolds are similar, demonstrating the effect of HAM on the fibrin scaffold. Moreover, fibrin/HAM (1/1) scaffolds have a higher G' modulus than HAM scaffolds, indicating an interactive contribution of HAM with the fibrin fibers. The HAM and fibrin/fluid HA gels also do not obey the Cox-Merz rule, but they are able to undergo deformation and they also present a non-Newtonian pseudoplastic behavior.

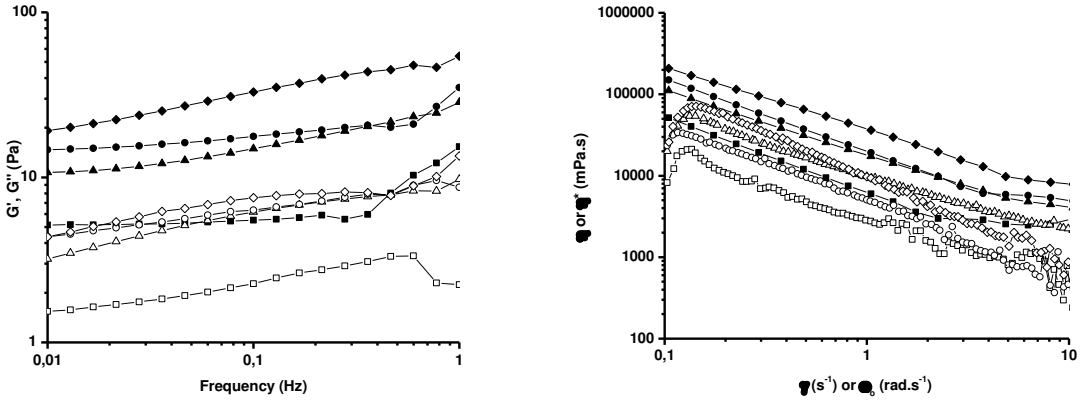

(a) (b)

Figure 7.3 (a) Storage G' (closed symbol) and loss G" (open symbol) moduli as a function of frequency. (b) Complex viscosity (η*) (closed symbol) versus oscillatory frequency (ωo) and apparent viscosity (η) (open symbol) versus shear rate (γ) for the fibrin scaffolds derived from: (■) and (□) pure fibrin; (▲) and (Δ) HAM; (●) and (○) fibrin/fluid HA 1:1; (♦) and (◊) fibrin/HAM 1:1. The data were obtained from analysis of the whole blood of donor 3.

Table 7. 5 shows a comparison of the power law parameters and values of tan δ. Like pure fibrin and fibrin/HAM (1/1) scaffolds, the PRP/fluid HA (1/1) and HAM scaffolds are also classified as physical and weak gels (B > 0). The values of tan δ

demonstrate that the addition of HA (fluid or HAM) to fibrin scaffolds decreases the tan δ values compared with HAM and pure fibrin scaffolds. Moreover, the values show a good interaction between fibrin and HA, mainly evidenced in the fibrin/HAM scaffolds.

Table 7.5 The Power Law Parameters ($G' = A.\omega^B$) and values of tan δ (at 0.1 Hz) for Fibrin/HAM (1/1), Fibrin/fluid HA (1/1), pure fibrin and HAM scaffolds.

Scaffold	**donor**	**A (Pas)**	**B**	**tan δ**
Fibrin/HAM 1/1	3	36.6	0.240	0.229
Fibrin/fluid HA 1/1	3	18.6	0.096	0.358
HAM	5	16.4	0.180	0.413
Pure Fibrin	3	5.6	0.037	0.412

7.3.6 Release of growth factors

The GF release profiles from the scaffolds are shown in Figure 7.4 (a) and (b). Due to the variations of GF concentrations among donors and of the platelet concentration in the scaffolds, the concentrations of PDGF-AB and TGF-β1 were normalized and presented as % released.

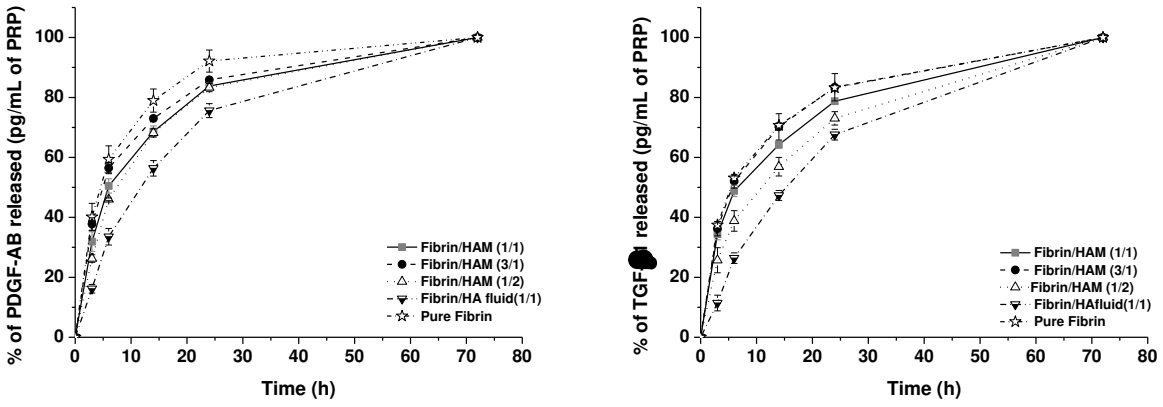

(a) (b)

Figure 7.4 Growth factor release profiles from the fibrin scaffolds. (a) PDGF-AB and (b) TGF-β1. The data were obtained from the PRP of donors 1 and 2.

Figure 7.4 (a) and (b) show that the release of GFs was faster from the pure fibrin than from the fibrin/HAM scaffolds. The presence of HA reduced the release rate of both GFs, mainly for the fibrin/fluid HA scaffold, which was likely due to the higher hydration provided by the fluid HA. All release profiles were a diffusive type, in which the release rate is proportional to the concentration gradient of the GFs. Considering the direct proportionality between the platelet concentration and initial concentration of the GFs, Table 7.3 shows lower platelet concentrations, due to dilution, for the HAM or fluid HA scaffolds (40% fibrin/HAM (1/1) fibrin/fluid HA) compared with the pure fibrin scaffolds. Therefore, the release rate delay in HA scaffolds is due to the lesser concentration gradients.

However, the normalized curves do not allow for identification of other effects. In order to complete the release information, the absolute values of the cumulative concentrations of the released GFs also were measured. The data illustrated in Tables 7.6 and 7.7 show the concentrations of released GFs slowed according to the following order: fibrin/HAM > pure fibrin > fibrin/fluid HA. From these results, we could infer that either HAM stimulates platelet activation and the release of GFs from their α-granules and/or that the interactions of the GFs with the HAM were weaker than

with pure fibrin. The slowest release with fluid HA is due to the resistance imparted to the water layer provided by the fluid HA.

Table 7.6 Cumulative concentrations of PDGF-AB [ng/mL of PRP] released from the studied scaffolds.

Time (h)	PDGF-AB released [ng/mL of PRP] for the scaffolds				
	Fibrin/HAM (1/1)	Fibrin/HAM (3/1)	Fibrin/HAM (1/2)	Fibrin/fluid HA (1/1)	Pure Fibrin
3	7.0±0.7	8.7±0.9	4.9±0.6	1.5±0.2	6.8±0.8
6	11.1±0.8	13.0±1.1	8.5±0.7	3.2±0.5	10.0±0.8
12	15.1±0.6	16.8±1.1	12.6±1.2	5.3±0.6	13.4±0.9
24	18.4±0.7	19.7±1.2	15.4±1.4	7.1±0.8	15.6±0.9
72	22.0±1.1	22.9±1.3	18.4±1.6	9.4±0.8	16.9±0.7

Table 7.7 Cumulative concentrations of TGF-β1 [ng/mL of PRP] released from the studied scaffolds

Time (h)	TGF-β1 released [ng/mL of PRP] for the scaffolds				
	Fibrin/HAM (1/1)	Fibrin/HAM (3/1)	Fibrin/HAM (1/2)	Fibrin/fluid HA (1/1)	Pure Fibrin
3	27.0±2.1	24.4±1.2	18.3±3.6	4.1±0.9	18.7±1.0
6	38.3±2.8	35.0±1.6	27.5±3,9	9.4±1.2	26.5±1.1
12	50.4±2.6	47.2±1.4	40.2±4.2	16.9±1.6	35.2±1.5
24	61.8±2.7	56.1±1.5	51.5±4.2	24.1±2.1	41.5±1.8
72	78.4±3.8	67.3±3.6	70.6±5.1	35.7±2.6	49.9±2.0

7.3.7 Cell growth

Figure 7.5 shows the growth hAdMSCs seeded in the studied scaffolds. We observed a more intense cell growth in the pure fibrin scaffolds, and the fibrin/HAM scaffolds had more efficient cell growth than the fibrin/fluid HA scaffolds. The cell growth was also proportional to the relative amount of fibrin and HAM in the scaffolds (1/1 or 3/1). However, the cell growth was stimulated by the GFs, and there was a direct proportionality between the concentrations of platelets and GFs. Table 7.3 shows the platelet concentration in pure fibrin scaffolds was approximately 40% higher than in the fibrin/HAM (1/1) scaffolds. Therefore, from these results we can conclude that HAM stimulate the growth of the seeded hAdMSCs.

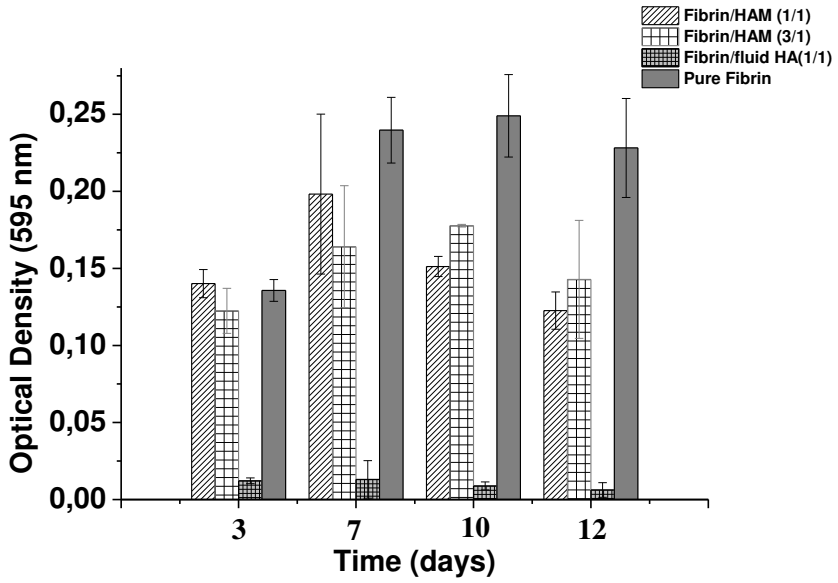

Figure 7.5 hAdMSC cell growth in the fibrin scaffolds as evaluated by optical density. The data were obtained from the PRP of donors 1 and 2.

7.4 Discussion

In this study, we generated different scaffolds using PRP, HAM and fluid HA. The architectures of the fibrin networks in the various scaffolds displayed differences

in pore size and fiber density. These differences were confirmed with an analysis of the rheological properties, the release of GFs and the cell growth in the scaffolds. The results were well correlated and show the superiority of the fibrin/HAM scaffolds in terms of viscoelasticity, mechanical resistance, stimulation for gradual release of GFs and seeded cell growth.

According to the mechanisms that explain the rheological behavior of the fibrin networks, the strain hardening observed in the pure fibrin scaffolds is mainly due to the branching of the fibrin fibers, as a consequence of the polymerization of the protofibrils [44-46]. The presence of HAM probably filled the empty spaces between the branches, thus mediating the interactions between the fibers and forming a more cohesive structure that was able to deform reversibly in the range of 0.1 to 1.0 Hz. The degree of hydration appears to be a key component in this feature because the filling of pores with fluid HA did not suppress the strain hardening. Moreover, the crosslinking of the HAM produced enough stability for the sustained release of GFs and cell growth over 12 days. The increased level of viscoelasticity provided by the HAM in the fibrin scaffold makes this an attractive material. Further studies will be conducted with the fibrin/HAM scaffolds as a new material for tissue engineering and regenerative medicine applications in orthopedics.

The fibrin/HAM scaffolds also promoted a prolonged release of the studied GFs compared with the pure fibrin scaffolds. HAM provided an effective barrier to delay the release of the GFs, but it was not as efficient as that provided by the fluid HA. Our scaffolds released the GFs more slowly than the collagen or the fibrin scaffolds studied by Harrison et al. [47], from which the same GFs were completely released in 24 h and instantaneously from the collagen and pure fibrin scaffolds, respectively. Other anionic polymers like gelatin can interact electrostatically with some GFs, prompting their controlled release and improving the healing process [2,22,48]. Controlled release is beneficial in tissue engineering for preserving the activity of the GFs over the period of cellular growth, thereby enhancing healing. Furthermore, the fibrin/HAM scaffolds induced an elevation in the release of GFs, as indicated by elevated GF concentrations; these results suggest that the electrostatic

interactions with the GFs are different in fibrin/HAM scaffolds compared with fluid HA scaffolds and could also indicate that fibrin/HAM scaffolds stimulate platelet activation. These observations indicate the importance of the fibrin/HAM scaffold, which deserves further study.

Our results also demonstrate that cell growth was stimulated in the fibrin/HAM scaffolds. This effect can be seen in both the acceleration of growth and in the maximum cell concentration reached. The cell concentrations in the fibrin/HAM scaffolds were comparable to those obtained in the pure fibrin scaffold, even though the initial concentration of platelets was lower. These effects were proportional to the HAM concentrations (3/1 or 1/1 fibrin/HAM; shown in Figure 7.3), and indicate a better performance of the proportion 1/2 fibrin/HAM scaffolds.

These results were not observed when the fibrin/fluid HA scaffolds were used. This observation is likely due to the hindrance to cell adhesion provided by the water or to the high negative charge density [49], as well as by the high molecular weight of the HA used (average of 10^6 Da). As previously reported [50], high molecular weight HA at high concentrations is a potent inhibitor of cell division, whereas at lower molecular weights or at lower concentrations it is less inhibitory and, in some cases, is even stimulatory.

These findings confirm our initial hypothesis of the fibrin/HAM scaffolds, and classifies them as promising scaffolds for use in regenerative medicine. To the best of our knowledge, this is the first report on fibrin/HA scaffolds. Further studies are required to better evaluate the effects of the molecular weight of HA (fluid or in HAM), cell differentiation, and the *in vivo* performance of the fibrin/HAM scaffolds.

7.5 Conclusions

From the analyzed results, we conclude that the fibrin/HAM scaffolds meet the requirements of an efficient scaffold and have the advantages of a high viscoelasticity, a prolonged and stimulated release of GFs, and an acceleration and stimulation of seeded cell growth. Therefore, the fibrin/HAM scaffolds represent a

novel and promising biomaterial for tissue engineering and regenerative medicine applications.

Acknowledgments

The authors appreciate the participation of the volunteer blood donors and thank the state financial agency FAPESP (Fundação de Amparo a Pesquisa do Estado de São Paulo, Brazil), which supported this work, and Prof. Dr. Edvaldo Sabadini for the use of the rheometer.

Disclosure Statement

There are no competing financial interests to declare.

References

1. Kutlu B, T Aydın, R Seda, AC Akman, M Gümüşderelioglu and RM Nohutcu. (2013). Platelet-rich plasma-loaded chitosan scaffolds: Preparation and growth factor release kinetics. Journal of Biomedical Materials Research Part B: Applied Biomaterials 101:28-35.

2. Shuko Suzuki NM, Yoshito Ikada. (2013). Gelatin gel as a carrier of platelet-derived growth factors Journal of Biomaterials Applications 27.

3. Sawamura K, T Ikeda, M Nagae, S-i Okamoto, Y Mikami, H Hase, K Ikoma, T Yamada, H Sakamoto and K-i Matsuda. (2009). Characterization of in vivo effects of platelet-rich plasma and biodegradable gelatin hydrogel microspheres on degenerated intervertebral discs. Tissue Engineering Part A 15:3719-3727.

4. Ito R, N Morimoto, LH Pham, T Taira, K Kawai and S Suzuki. (2013). Efficacy of the Controlled Release of Concentrated Platelet Lysate from a Collagen/Gelatin Scaffold for Dermis-Like Tissue Regeneration. Tissue Engineering.

5. Tabata Y. (2003). Tissue regeneration based on growth factor release. Tissue engineering 9 Suppl 1:S5-15.

6. Anitua E, MH Alkhraisat and G Orive. (2012). Perspectives and challenges in regenerative medicine using plasma rich in growth factors. Journal of Controlled Release 157:29-38.

7. Anitua E. (1999). Plasma rich in growth factors: preliminary results of use in the preparation of future sites for implants. Int J Oral Maxillofac Implants 14:529-35.

8. Foster TE, BL Puskas, BR Mandelbaum, MB Gerhardt and SA Rodeo. (2009). Platelet-rich plasma from basic science to clinical applications. The American Journal of Sports Medicine 37:2259-2272.

9. Everts PA, JT Knape, G Weibrich, JP Schonberger, J Hoffmann, EP Overdevest, HA Box and A van Zundert. (2006). Platelet-rich plasma and platelet gel: a review. J Extra Corpor Technol 38:174-87.

10. Gentile P, DJ Bottini, D Spallone, BC Curcio and V Cervelli. (2010). Application of platelet-rich plasma in maxillofacial surgery: clinical evaluation. In: *J Craniofac Surg*. United States. pp 900-4.

11. Bhanot S and JC Alex. (2002). Current applications of platelet gels in facial plastic surgery. Facial plastic surgery 18:27-34.

12. Cervelli V, P Gentile, MG Scioli, M Grimaldi, CU Casciani, LG Spagnoli and A Orlandi. (2009). Application of platelet-rich plasma in plastic surgery: clinical and in vitro evaluation. Tissue Eng Part C Methods 15:625-34.

13. Dallari D, L Savarino, C Stagni, E Cenni, A Cenacchi, PM Fornasari, U Albisinni, E Rimondi, N Baldini and A Giunti. (2007). Enhanced tibial osteotomy healing with use of bone grafts supplemented with platelet gel or platelet gel and bone marrow stromal cells. In: *J Bone Joint Surg Am*. United States. pp 2413-20.

14. Filardo G, E Kon, MT Pereira Ruiz, F Vaccaro, R Guitaldi, A Di Martino, A Cenacchi, PM Fornasari and M Marcacci. (2012). Platelet-rich plasma intra-articular injections for cartilage degeneration and osteoarthritis: single- versus double-spinning approach. Knee Surg Sports Traumatol Arthrosc 20:2078-87.

15. Rozman P and Z Bolta. (2007). Use of platelet growth factors in treating wounds and soft-tissue injuries. In: *Acta Dermatovenerol Alp Panonica Adriat*. Slovenia. pp 156-65.

16. Cieslik-Bielecka A, T Bielecki, TS Gazdzik, J Arendt, W Krol and T Szczepanski. (2009). Autologous platelets and leukocytes can improve healing of infected high-energy soft tissue injury. In: *Transfus Apher Sci*. England. pp 9-12.

17. Margolis DJ, J Kantor, J Santanna, BL Strom and JA Berlin. (2001). Effectiveness of platelet releasate for the treatment of diabetic neuropathic foot ulcers. Diabetes care 24:483-488.

18. Hammond JW, RY Hinton, LA Curl, JM Muriel and RM Lovering. (2009). Use of autologous platelet-rich plasma to treat muscle strain injuries. In: *Am J Sports Med*. United States. pp 1135-42.

19. Lana JFSDAS, M.H.; Dias Belangero, W.; Malheiros Luzo, A.C. (Eds.). *Platelet-Rich Plasma Regenerative Medicine: Sports Medicine, Orthopedic, and Recovery of Musculoskeletal Injuries*. (2014).

20. Sánchez-González DJ, E Méndez-Bolaina and NI Trejo-Bahena. (2012). Platelet-rich plasma peptides: key for regeneration. International Journal of Peptides 2012.

21. Ishida K, R Kuroda, M Miwa, Y Tabata, A Hokugo, T Kawamoto, K Sasaki, M Doita and M Kurosaka. (2007). The regenerative effects of platelet-rich plasma on meniscal cells in vitro and its in vivo application with biodegradable gelatin hydrogel. Tissue engineering 13:1103-1112.

22. Hokugo A, Y Sawada, R Hokugo, H Iwamura, M Kobuchi, T Kambara, S Morita and Y Tabata. (2007). Controlled release of platelet growth factors enhances bone regeneration at rabbit calvaria. Oral Surgery, Oral Medicine, Oral Pathology, Oral Radiology, and Endodontology 104:44-48.

23. Murray MM, KP Spindler, E Abreu, JA Muller, A Nedder, M Kelly, J Frino, D Zurakowski, M Valenza and BD Snyder. (2007). Collagen-platelet rich plasma hydrogel enhances primary repair of the porcine anterior cruciate ligament. Journal of orthopaedic research 25:81-91.

24. Matsui M and Y Tabata. (2012). Enhanced angiogenesis by multiple release of platelet-rich plasma contents and basic fibroblast growth factor from gelatin hydrogels. Acta biomaterialia 8:1792-1801.

25. Okamoto S-i, T Ikeda, K Sawamura, M Nagae, H Hase, Y Mikami, Y Tabata, K-i Matsuda, M Kawata and T Kubo. (2011). Positive Effect on Bone Fusion by the Combination of Platelet-Rich Plasma and a Gelatin β-Tricalcium Phosphate Sponge: A Study Using a Posterolateral Fusion Model of Lumbar Vertebrae in Rats. Tissue Engineering Part A 18:157-166.

26. Rossi S, A Faccendini, MC Bonferoni, F Ferrari, G Sandri, C Del Fante, C Perotti and CM Caramella. (2013). “Sponge-like” dressings based on biopolymers for the delivery of platelet lysate to skin chronic wounds. International Journal of Pharmaceutics 440:207-215.

27. Cervelli V, L Lucarini, D Spallone, L Palla, GM Colicchia, P Gentile and B De Angelis. (2011). Use of platelet-rich plasma and hyaluronic acid in the loss of substance with bone exposure. Advances in skin & wound care 24:176-181.

28. Okabe K, Y Yamada, K Ito, T Kohgo, R Yoshimi and M Ueda. (2009). Injectable soft-tissue augmentation by tissue engineering and regenerative medicine with human mesenchymal stromal cells, platelet-rich plasma and hyaluronic acid scaffolds. Cytotherapy 11:307-316.

29. Yamada Y, M Ueda, T Naiki, M Takahashi, K-I Hata and T Nagasaka. (2004). Autogenous injectable bone for regeneration with mesenchymal stem cells and platelet-rich plasma: tissue-engineered bone regeneration. Tissue engineering 10:955-964.

30. Lee J-C, HJ Min, HJ Park, S Lee, SC Seong and MC Lee. (2013). Synovial Membrane–Derived Mesenchymal Stem Cells Supported by Platelet-Rich Plasma Can Repair Osteochondral Defects in a Rabbit Model. Arthroscopy: The Journal of Arthroscopic & Related Surgery 29:1034-1046.

31. Bensaıd W, J Triffitt, C Blanchat, K Oudina, L Sedel and H Petite. (2003). A biodegradable fibrin scaffold for mesenchymal stem cell transplantation. Biomaterials 24:2497-2502.

32. Toole BP. (2004). Hyaluronan: from extracellular glue to pericellular cue. Nature Reviews Cancer 4:528-539.

33. Prestwich GD. (2011). Hyaluronic acid-based clinical biomaterials derived for cell and molecule delivery in regenerative medicine. Journal of Controlled Release 155:193-199.

34. Garg HG and CA Hales. *Chemistry and biology of hyaluronan*. (2004). Access Online via Elsevier.

35. Shimojo AAM, AMB Pires, LG de la Torre and MHA Santana. (2012). Influence of particle size and fluid fraction on rheological and extrusion properties of crosslinked hyaluronic acid hydrogel dispersions. Journal of Applied Polymer Science.

36. Park SH, JH Cui, SR Park and BH Min. (2009). Potential of fortified fibrin/hyaluronic acid composite gel as a cell delivery vehicle for chondrocytes. Artificial organs 33:439-447.

37. Rampichova M, E Filova, F Varga, A Lytvynets, E Prosecka, L Kolacna, J Motlik, A Necas, L Vajner, J Uhlik and E Amler. (2010). Fibrin/hyaluronic acid

composite hydrogels as appropriate scaffolds for in vivo artificial cartilage implantation. ASAIO J 56:563-8.

38. Yang CL, HW Chen, TC Wang and YJ Wang. (2011). A novel fibrin gel derived from hyaluronic acid-grafted fibrinogen. Biomedical Materials 6:025009.

39. Fathi WK. (2013). The Effect of Hyaluronic Acid and Platelet-Rich Plasma on Soft Tissue Wound Healing: An Experimental Studyon Rabbits. Al-Rafidain Dental Journal 12.

40. Perez AG, R Lichy, JFS Lana, AA Rodrigues, ÂCM Luzo, WD Belangero and MHA Santana. (2013). Prediction and Modulation of Platelet Recovery by Discontinuous Centrifugation of Whole Blood for the Preparation of Pure Platelet-Rich Plasma. BioResearch Open Access 2:307-314.

41. Obata S, K Akeda, T Imanishi, K Masuda, W Bae, R Morimoto, Y Asanuma, Y Kasai, A Uchida and A Sudo. (2012). Effect of autologous platelet-rich plasma-releasate on intervertebral disc degeneration in the rabbit anular puncture model: a preclinical study. Arthritis research & therapy 14:R241.

42. Ramkumar D, M Bhattacharya, JA MENJIVAR and T Huang. (1996). Relaxation behavior and the application of integral constitutive equations to wheat dough. Journal of texture studies 27:517-544.

43. Khondkar D, RF Tester, N Hudson, J Karkalas and J Morrow. (2007). Rheological behaviour of uncross-linked and cross-linked gelatinised waxy maize starch with pectin gels. Food hydrocolloids 21:1296-1301.

44. Shah J and P Janmey. (1997). Strain hardening of fibrin gels and plasma clots. Rheologica Acta 36:262-268.

45. Weisel JW. (2007). Structure of fibrin: impact on clot stability. Journal of Thrombosis and Haemostasis 5:116-124.

46. Piechocka IK, RG Bacabac, M Potters, FC MacKintosh and GH Koenderink. (2010). Structural hierarchy governs fibrin gel mechanics. Biophysical Journal 98:2281-2289.

47. Harrison S, P Vavken, S Kevy, M Jacobson, D Zurakowski and MM Murray. (2011). Platelet activation by collagen provides sustained release of anabolic cytokines. Am J Sports Med 39:729-34.

48. Yamamoto M, Y Tabata, L Hong, S Miyamoto, N Hashimoto and Y Ikada. (2000). Bone regeneration by transforming growth factor β1 released from a biodegradable hydrogel. Journal of controlled release 64:133-142.

49. Dillon PW, K Keefer, JH Blackburn, PE Houghton and TM Krummel. (1994). The extracellular matrix of the fetal wound: hyaluronic acid controls lymphocyte adhesion. Journal of Surgical Research 57:170-173.

50. Goldberg RL and BP Toole. (1987). Hyaluronate inhibition of cell proliferation. Arthritis & Rheumatism 30:769-778.

Capítulo 8. Conclusõe Finais

8.1 Conclusões

Os resultados apresentados mostraram que o Plasma Rico em Plaquetas, apesar de ser um produto autólogo, pode ter a sua preparação padronizada. Os resultados obtidos neste trabalho contribuem para a padronização do P-PRP.

A estratégia experimental, de análise integrada dos resultados, e de padronização do P-PRP, estabelecida neste trabalho, mostrou-se eficiente por considerar não somente condições operacionais otimizadas, mas também o controle da qualidade do PRP durante a sua preparação.

A centrifugação descontínua para a recuperação de plaquetas, etapa crucial na preparação do PRP, pode ser descrita por um modelo matemático que é baseado na descrição física dos eventos. O modelo permitiu predizer o comportamento da separação das células vermelhas e maximizar, modular e controlar a eficiência de recuperação das plaquetas através da aceleração centrífuga, do tempo e do hematócrito, pela identificação de regiões nas quais a eficiência de recuperação de plaquetas é máxima. A adoção dessas condições nos protocolos de preparação do PRP irá assegurar que a sua composição seja controlada, reprodutível e até mesmo modulada.

O planejamento estatístico e a análise de superfície de resposta para o estudo da formação da rede de fibrina em diferentes condições experimentais mostrou-se uma valiosa estratégia. Os efeitos da razão soro/cálcio ($S/CaCl_2$) e da % de agonista em relação PRP (%A/PRP) e suas interações foram preditos com uma confiança estatística, requerendo um número mínimo de experimentos. Um modelo estatístico para a predição do raio das fibras foi gerado e agrupado em arquiteturas definidas na superfície de resposta e correlacionadas com a reologia dos *scaffolds* formados, a liberação dos fatores de crescimento, o tempo de formação do coágulo e a capacidade de sustentação do crescimento de células mesenquimais.

A incorporação do PRP em partículas de ácido hialurônico formadas pela reticulação com DVS mostraram a sua capacidade de influenciar na liberação dos FCs e no crescimento celular de células mesenquimais.

8.2 Sugestões para trabalhos futuros

- Estudo da preparação e modulação do plasma rico em plaquetas utilizando o ácido citrato dextrose (ACD-A) como anticoagulante;

- Modulação da preparação do L-PRP, ou plasma rico em plaquetas e em leucócitos.

- Correlação entre o estado de saúde dos doadores com os resultados obtidos na preparação e ativação do PRP.

- Aplicação do plasma rico em plaquetas em outros tipos de *scaffolds* para estudo da liberação dos fatores de crescimento e estudos de crescimento e diferenciação celular.

- Estudos em modelo animal da aplicação do P-PRP padronizado neste estudo.